Annual Report (2011)

No.23
The NOVARTIS Foundation (Japan)
for the Promotion of Science

平成23年度
財団年報 第23号

財団法人　ノバルティス科学振興財団

Contents

Introduction

"The Disaster in Eastern Japan"

Akimichi Kaneko, MD, PhD
Chairman of the Board of Trustees

This annual report includes research and meeting reports written by the 2010 grantees. Their tireless effort is the driving force to promote and to keep the high standard of the Japanese life science. I strongly believe that the aim of the Foundation is to help keeping their activity and we will do our best toward this goal. I sincerely appreciate the assistance and warm encouragement extended by the members of the Board of Trustees, the auditors, the Board of Councilors and the Selection Committee. The powerful support by the Novartis Pharma KK enabled us to sustain our activity without interruption.

In March this year, a huge scale earth quake accompanying a frightening tsunami hit Eastern Japan. In addition the complete damage and melt down of the nuclear reactors of the Fukushima First Nuclear Electric Plant heavily affected the life of victims and scared them by the unforeseen future when the damaged nuclear reactors could be put under control. I hereby extend my sincere sympathy to the victims of the present disaster and hope that everything will recover as soon as possible.

I learned that the land of the area has slid by several meters, but it may not be so surprising in billion-year-scales in which the Japanese islands drifted apart from the Eurasian Continent. During this drift many quakes must have occurred repeatedly. Unfortunately we are unable to predict exactly when such change will occur. The technology of earthquake prediction is still in immature stage.

There are quite a few scientists whose research facilities were damaged or who have lost their valuable materials by the quake. We, at the Foundation, wish to extend some assistance to suffered scientists. At the June meeting of the Board of Trustees we decided to reserve a part of our research grant of the coming year to scientists in Tohoku and Northern Kanto areas who are victims of the quake and tsunami. Our support is modest and late coming, but I strongly hope that it will help, at least partially, to reestablish their research activities.

はじめに　　「東日本大震災」

理事長　金 子 章 道

本年度もここに 2010 年度にノバルティス科学振興財団研究助成金を受けられた方々の研究報告を収録いたしました。受賞者の皆様の素晴らしい研究がまとめられたエッセイ集です。研究者お一人おひとりの努力の結晶は我が国の学術水準を発展させていく原動力です。こうした方々の研究に多少なりとお力添えをすることが本財団の事業の基本と考え、今後も努力を続けて行きたいと思っております。これらの優れた研究を選考していただいた選考委員の皆様をはじめ、財団の活動を支えて下さっている関係者の皆様に深く感謝いたします。とりわけノバルティスファーマ社の継続した強力な経済的支援に御礼申し上げたいと思います。

去る 3 月、東日本は未曾有の大震災と津波に襲われました。また津波の影響で引き起こされた東京電力福島第一原子力発電所の大事故は、その後も被災者の生活に計り知れない影響を及ぼしており、またその収束が見えない不安が被災地の方々を悩ませています。この地震では陸地が数メートルも移動したと聞きましたが、ずっと昔、日本列島がユーラシア大陸から離れて出来上がってきたことを考えると、陸地が移動することも、それに伴って大地震が起きることも、何億年というスケールからすれば驚くには値しないのでしょう。しかし、それが何時、どの程度の規模で起きるかを予知する技術は未熟です。このような大災害に遭遇された方々には心からご同情申し上げ、一日も早い復興を祈ります。

今回の大災害に直面して、財団として何が出来るかを考えてみました。震災によって研究設備が破損した方、貴重な資料や材料を失われた方、またご自身やご家族が被災された方々などがおられると思います。去る 6 月の理事会では、今年募集する研究助成金の一部を東北や北関東地方で研究室が被災された方に優先的に配分することを決議いたしました。ささやかな助成であり、また遅きに失した感もないわけではありませんが、この研究助成が研究室の再建に幾ばくかのお役にたてればと考えております。被災された研究者の皆様の研究が早急に復旧することを願っております。

II.

Reports from the Recipients of Novartis Research Grants

The roles of FoxO1 in the regulation of glucose and lipid metabolism via O-glycosylation of ChREBP

Yukari Kitamura
Institute for Molecular and Cellular Regulation, Gunma University
yukariam@showa.gunma-u.ac.jp

Abstract

We show that carbohydrate response element binding protein (ChREBP), a glucose-regulated transcription factor, is O-glycosylated by OGT, leading to increased ChREBP levels, owing to decreased ubiquitination. Conversely, expression of O-GlcNAcase (GCA) in hepatocytes decreases ChREBP O-glycosylation, thus reducing its protein levels. Moreover, ChREBP O-glycosylation is regulated by fasting (low) and re-feeding (high) in mouse liver. The nutritional regulation of ChREBP O-glycosylation is impaired in livers of high fat high sucrose diet fed mice. FoxO1, a downstream effector of insulin signaling, has been known to regulate glucose metabolism in liver. We show here that FoxO1 overexpression inhibits ChREBP O-glycosylation in hepatocytes, thus reducing ChREBP levels. Conversely, conditional FoxO1 knockout in liver results in increased levels of O-glycosylated ChREBP, even in the fasted state. Chromatin immunoprecipitation reveal that recruitment of ChREBP to the L-PK promoter is suppressed by FoxO1, and increased in liver-specific FoxO1 knockout mice in both fasted and fed conditions. Taken together, our results suggest that O-glycosylation is an important mechanism to regulate ChREBP function, and that FoxO1 is required for ChREBP O-glycosylation. We propose that FoxO1 is the shared signaling element linking glucose- and insulin-activated pathways to regulate hepatic glucose metabolism.

Keywords: ChREBP, FoxO1, O-glycosylation, Diabetes

Introduction

ChREBP is a major mediator of glucose action in the control of glycolysis and lipid synthesis in liver. ChREBP regulates the transcription of liver-pyruvate kinase (L-PK), one of the rate-limiting enzymes of glycolysis, and lipogenic genes, such as acetyl-CoA carboxylase (ACC) and fatty acid synthase (FAS). However, the molecular mechanism of ChREBP regulation has not been fully elucidated. Glucose taken into hepatocytes is mainly converted to pyruvate or glycogen to produce or store energy. However, excess glucose enters into hexosamine biosynthetic pathway (HBP), which produce UDP-N-acetylglucosamine (UDP-GlcNAc). By using UDP-GlcNAc as the donor substrate, O-GlcNAc transferase (OGT) catalyzes O-glycosylation modification of the proteins on Ser/Thr residues. It is known that hyperglycemia causes the increase in glucose flux into HBP and subsequent O-glycosylation of various proteins. It is suggested that the increase in O-glycosylation modification is associated with pathophysiology of diabetes. FoxO1 is a member of the forkhead box containing protein of the O subfamily, which regulates metabolism as well as cellular proliferation,

apoptosis, differentiation and stress resistance. FoxO1 transcriptional activity is regulated by insulin through phosphorylation by Akt and following nuclear exclusion. We previously reported that FoxO1 plays important roles in regulating glucose metabolism in liver through the regulation of gluconeogenic genes. We also previously showed that FoxO1 controls glycolytic (L-PK) and lipogenic (ACC) genes, two critical ChREBP targets.

Results

ChREBP protein level is regulated by nutrients via ubiquitination.

We found that the protein level but not mRNA level was significantly increased by high glucose in primary hepatocytes. Consistent with these results, ChREBP ubiquitination was decreased in high glucose compared to low glucose condition in MG132 treated hepatocytes. We also obtained similar observations in mouse liver. ChREBP ubiquitination was decreased by refeeding, and was dramatically decreased in the liver of HFHSD fed mice.

ChREBP is O-glycosylated by high glucose or refeeding in primary hepatocytes and mouse liver.

We found that high glucose significantly increased O-glycosylation of ChREBP in primary hepatocytes. DON, an inhibitor of GFAT (L-glutamine fructose-6-phosphate amino transferase), clearly inhibited O-glycosylation of ChREBP. In contrast, glucosamine treatment of the cells induced O-glycosylation of ChREBP even in low glucose condition. These results indicated that ChREBP is O-glycosylated by high glucose via hexosamine biosynthetic pathway (HBP) in hepatocytes. We also found that OGT interacts with ChREBP, and which was enhanced by HFHSD feeding.

ChREBP O-glycosylation and transcriptional activity are regulated by OGT and GCA.

When we transfected primary hepatocytes with OGT, ChREBP O-glycosylation was significantly increased in low glucose condition. Importantly, we observed that OGT was co-immunoprecipitated with ChREBP, and which was enhanced by high glucose. Conversely, when we knockdown OGT in primary hepatocytes using specific siRNA for OGT, ChREBP O-glycosylation was decreased in both high glucose and glucosamine treated conditions. Moreover, when we overexpressed GCA, ChREBP O-glycosylation was significantly decreased.

FoxO1 suppresses ChREBP O-glycosylation, decreases protein level and transcriptional activity of ChREBP.

When we overexpressed constitutively active FoxO1 mutant in primary hepatocytes, ChREBP target gene L-PK mRNA levels were significantly decreased, despite that ChREBP mRNA levels were not changed. FoxO1 expression significantly decreased O-glycosylation and protein levels of ChREBP. Conversely, when we knockdown FoxO1 by using specific siRNA for FoxO1 in primary hepatocytes, ChREBP O-glycosylation was increased. FoxO1-ADA expression enhanced ubiquitination of both endogenous and exogenously expressed ChREBP, which should account for the decrease in protein levels of ChREBP.

ChREBP O-glycosylation, protein level, and recruitment to the L-PK promoter were increased in the liver of FoxO1 knockout mice.

We generated liver specific FoxO1 knockout mice (L-FoxO1-KO) by crossing albumin-cre mice (reference) with FoxO1 flox mice and isolated livers from L-FoxO1-KO. In the liver of L-FoxO1-KO mice, ChREBP O-glycosylation and protein levels were significantly increased, and OGT interaction with ChREBP was enhanced. Consistent with the increase in ChREBP protein levels, ubiquitination of ChREBP was apparently decreased in the liver of L-FoxO1-KO mice.

Discussion & Conclusion

In this study, we shoed that O-glycosylation is an important mechanism to regulate ChREBP function, and that FoxO1 is required for ChREBP O-glycosylation. We propose that FoxO1 is the shared signaling element linking glucose- and insulin-activated pathways to regulate hepatic glucose metabolism. FoxO1 inhibition may increase glucose effectiveness.

References

1) Kitamura T, Kido Y, Nef S, Merenmies J, Parada LF, Accili D (2001) Preserved pancreatic beta-cell development and function in mice lacking the insulin receptor-related receptor. Mol Cell Biol 21: 5624-5630

2) Kitamura YI, Kitamura T, Kruse JP, et al. (2005) FoxO1 protects against pancreatic beta cell failure through NeuroD and MafA induction. Cell Metab 2: 153-163

The analysis of the functional linkage between genetically-disrupted cardiac transcriptional network and the onset of cardiomyopathy: Approach from the HOP gene mutation causing human dilated cardiomyopathy

Hiroyuki Morita
Department of Translational Research for Healthcare and Clinical Science,
University of Tokyo
hmrt-tky@umin.net

Abstract

HOP (Homeodomain-Only Protein) is a unique transcriptional regulator, which lacks DNA binding capacity but functions as the repressor of SRF-induced transcription. To identify the key molecule which could account for the functional consequences triggered by the HOP missense mutation identified previously in the patents with familial dilated cardiomyopathy, protein partner of HOP was screened using yeast 2-hybrid system. In this study, I could identify 14 proteins which can bind with HOP. Until now, however, any of these 14 partner proteins could not explain the drastic cardiac abnormality triggered by the HOP missense mutation. I will continue to examine in another experimental method the interaction of HOP with these partner proteins identified in this study.
Keywords: heart failure, cardiomyopathy, transcriptional regulator, protein-protein interaction

Introduction

HOP (Homeodomain-Only Protein) is a unique transcriptional regulator, which lacks DNA binding capacity but functions as the repressor of SRF-induced transcription [1, 2]. Previously, I identified a missense mutation of *HOP* in the patient with familial dilated cardiomyopathy (DCM) and heart failure. To elucidate the functional consequences of this *HOP* mutation, I created the transgenic mice overexpressing wild-type HOP and mutant HOP in the heart, and compared their phenotypes. Unlike mice overexpressing wild-type HOP, transgenic mice of mutant HOP could greatly recapitulate the human cardiac phenotype observed in the patient bearing *HOP* mutation. In the ANF-luciferase reporter assay, this mutated HOP was found to repress the SRF-induced transactivation in a gain-of-function manner, but the extent of which was not remarkable enough to account for the drastic cardiac abnormality caused by the *HOP* mutation in human and mice. Therefore, I hypothesized that the novel unknown partner of HOP should be the key molecule for modifying the molecular pathway triggered by HOP. By clarifying this partner (called as protein X), the drastic cardiac abnormality caused by a missense mutation of *HOP* can be well-explained. The aim of this study is to identify the novel partner of HOP and characterize the interaction between HOP and protein X.

Results

With the yeast 2-hybrid system (Matchmaker Gold Yeast Two-Hybrid System (Clontech)), the binding partners of HOP were screened. The full-length coding region of human *HOP* was inserted into the pGBKT7, which was used as the bait. Pretransformed Human Heart Matchmaker cDNA Library (Clontech) was used as the prey. Finally, 14 proteins were picked up as the candidate protein of HOP partner. Here, I describe ATPase Na/K β1 subunit, one of 14 proteins I identified in this study.

ATPase Na/K β1 subunit is a component of the transmembrane protein ATPase Na/K, which is well-known as the pharmacoceutical target of digitalis. Recently, this protein was demonstrated to be essential for maintaining the ventricular cardiomyocyte morphology and viability in the cardiac development [3].

With the immunoprecipitation experiments, binding of ATPase Na/K β1 subunit with HOP could be shown. However, ATPase Na/K β1 subunit could bind with mutant-type HOP as well as wild-type HOP, suggesting that the difference of the extent of binding with ATPase Na/K β1 subunit could not account for the consequences of the *HOP* mutation. The 13 other proteins are under investigation.

Discussion & Conclusion

In this study, the partner of transcriptional regulator HOP was screened using yeast 2-hybrid experiments. As a result, 14 candidate proteins were acquired. The purpose of this study was to identify the key molecule which could explain the drastic cardiac abnormality caused by the missense mutation of *HOP*. With the immunoprecipitation experiments, I could confirm the binding of HOP with ATPase Na/K β1 subunit, one of the 14 candidate proteins identified here, but the mutant-type HOP also could bind with this protein in the same manner. At least, from the viewpoint of the difference in binding affinity, this protein cannot explain the phenotypic change in the human and mouse bearing the mutant-type HOP. The 13 proteins else are under investigation. Also, as for the ATPase Na/K β1 subunit, I will perform the additional experiments on the downstream pathway followed by the binding with HOP.

So far, gene mutations of sarcomere proteins, Z-disc related proteins (muscle LIM protein, telethonin, α-actinin 2, cypher/ZASP), metavinculin, ion-cycling related proteins (phospholamban, K-ATP channel) were reported to be causative of the isolated DCM without extra-cardiac involvement [4]. However, few genetic mutations in transcriptional regulator have been reported to cause human isolated cardiomyopathy [5, 6]. Given that mutation in the structural or metabolic proteins is sufficient to cause inappropriate cardiac remodeling, it is surprising that defects in transcriptional regulation of these same proteins have not also been identified as primary causes of cardiomyopathy. Several possible explanations may account for this. Transcription factor gene mutations may be lethal or may at least substantially impair reproductive fitness so as to be rapidly lost. The consequences of transcription factor gene mutations may be so pleiotropic that these cause systemic rather than single-organ disease.

The abnormality in transcriptional regulators is related to the cardiac remodeling induced by pressure overload or reperfusion injury, therefore the identification of the pathways triggered by HOP could contribute to the clarification of the general mechanism how heart fails as well as the specific mechanism how *HOP* missense mutation causes severe dilated cardiomyopathy. After these pathways are clarified, the studies on the control of the cardiac remodeling through intervening HOP protein are warranted.

This study was performed with the aid of Research Grant of the NOVARTIS Foundation (Japan) for the Promotion of Science.

References

1) Chen F, Kook H, Milewski R, Gitler AD, Lu MM, Li J, Nazarian R, Schnepp R, Jen K, Biben C, Runke G, Mackay JP, Novotny J, Schwartz RJ, Harvey RP, Mullins MC, Epstein JA.
Hop is an unusual homeobox gene that modulates cardiac development.
Cell 2002;110(6):713-23.

2) Shin CH, Liu ZP, Passier R, Zhang CL, Wang DZ, Harris TM, Yamagishi H, Richardson JA, Childs G, Olson EN.
Modulation of cardiac growth and development by HOP, an unusual homeodomain protein.
Cell 2002;110(6):725-35.

3) Yuan S, Joseph EM.
The small heart mutation reveals novel roles of Na+/K+-ATPase in maintaining ventricular cardiomyocyte morphology and viability in zebrafish.}
Circ Res. 2004;95(6):595-603.

4) Morita H, Seidman J, Seidman CE.
Genetic causes of human heart failure.
J Clin Invest. 2005;115(3):518-26.

5) Schönberger J, Wang L, Shin JT, Kim SD, Depreux FF, Zhu H, Zon L, Pizard A, Kim JB, Macrae CA, Mungall AJ, Seidman JG, Seidman CE.
Mutation in the transcriptional coactivator EYA4 causes dilated cardiomyopathy and sensorineural hearing loss.
Nat Genet. 2005;37(4):418-22.

6) Moulik M, Vatta M, Witt SH, Arola AM, Murphy RT, McKenna WJ, Boriek AM, Oka K, Labeit S, Bowles NE, Arimura T, Kimura A, Towbin JA.
ANKRD1, the gene encoding cardiac ankyrin repeat protein, is a novel dilated cardiomyopathy gene.
J Am Coll Cardiol. 2009;54(4):325-33.

Elucidation of lipid chaperones, inflammation, and endoplasmic reticulum stress response in cardiovascular and metabolic diseases

Masato Furuhashi
Second Department of Internal Medicine, Sapporo Medical University School of Medicine
furuhasi@sapmed.ac.jp

Abstract

Increased adiposity is associated with a wide range of chronic metabolic disorders, including insulin resistance, type 2 diabetes, and cardiovascular disease. During the development of obesity, several inflammatory and stress responses occur in metabolically active tissues, leading to chronic, low grade inflammation which plays a central role in the inhibition of insulin action and disruption of systemic metabolic homeostasis. In recent years, organelle dysfunction emerged as a key mechanistic component in obesity and in the emergence of these metabolic abnormalities4. In this study, we focused on fatty acid-binding proteins (FABPs) and endoplasmic reticulum (ER) stress which can activate inflammatory responses and metabolic deterioration, resulting in the development of cardiovascular diseases.

***Keywords*:** Fatty acid-binding protein, endoplasmic reticulum stress, inflammation, insulin resistance, cardiovascular disease

Introduction

Obesity is characterized by an increase in adiposity, and it is well known that obesity is associated with several aspects of metabolic diseases, such as insulin resistance, type 2 diabetes, fatty liver disease, hypertension, dyslipidemia, and cardiovascular disease. In the adipose tissue, it has been suggested that the adipocyte and macrophage interact each other and regulate both metabolic and inflammatory responses. In these adipocyte and macrophages, several cytokines and lipids activate key regulators of metabolic and inflammatory signaling, which are c-Jun N-terminal kinase (JNK) and inhibitor of kappa kinase (IKK). Other intracellular stresses such as endoplasmic reticulum (ER) stress, oxidative stress, and some kinds of lipid chaperones, fatty acid-binding proteins (FABPs), can also activate JNK and IKK, resulting in enhanced inflammatory responses and metabolic deterioration.

FABPs are a family of about 14-15 kDa lipid chaperones that bind hydrophobic ligands such as long chain fatty acids and eicosanoids with high affinity. At least 9 FABPs have been already identified. Among them, aP2 (FABP4/A-FABP) and mal1 (FABP5/E-FABP) are expressed in both adipocytes and macrophages. We have demonstrated that both aP2 and mal1 play a significant role in many aspects of metabolic syndrome, and aP2/mal1-deficient mice protect form obesity, diabetes, hepatosteatosis, and atherosclerosis. Furthermore, we recently developed a specific inhibitor of aP2

and showed that it can treat diabetes and atherosclerosis in several animal models in a target specific manner. Interestingly, it has been shown that aP2 is secreted from adipocytes although there are no typical secretion signal peptides. Several clinical studies have demonstrated that serum aP2 levels are associated with obesity, type 2 diabetes, and risk for cardiovascular diseases. However, there is a lack of analysis in subjects without any medications. Furthermore, it is still unknown whether secreted aP2 might have a physiological function as an adipokine.

The endoplasmic reticulum (ER) is a vital organelle that serves as the quality control device for proteins and coordinates the synthesis, folding, and trafficking of proteins. The proper function of ER is critical for metabolism. ER stress and inappropriate adaptation through the unfolded protein response (UPR) is a feature of obesity, insulin resistance, and type 2 diabetes. The principal branches of UPR signaling are mediated through three molecules: inositol-requiring enzyme 1 (IRE1), PKR-like endoplasmic-reticulum kinase (PERK) and activating transcription factor 6 (ATF6). It has been indicated that ER stress is critical to the initiation and integration of pathways of inflammation and several diseases. However, the role of each canonical UPR sensor in metabolic regulation is not yet clearly understood.

Results

In FABP projects, we first investigated the detection of aP2 in conditioned medium (CM) from wild-type adipocytes. In the CM, aP2 and adiponectin as a control of secretary protein, but not actin as a non-secretary protein, were detected, suggesting that release of aP2 from adipocytes is not due to apoptosis or necrosis of cells. As another negative control, in aP2 deficient adipocytes, aP2 was not detected in cell lysates and CM.

We are now conducting an epidemiological cohort, the Tanno-Sobetsu Study, which has been continuing for more than 30 years. We measured aP2 concentration using ELISA kits in subjects without any medications. The concentration of aP2 was significantly higher in females than in males, which is similar to other adipokines, adiponectin and leptin. Serum levels of aP2 were positively correlated with HOMA-R, an index of insulin sensitivity, and adiposity such as body mass index (BMI) and waist circumference. Multiple regression analysis showed that aP2 was an independent predictor of insulin resistance independent of adiposity.

In ER stress projects, we examined the role of the PERK pathway in obesity and peripheral insulin sensitivity. Since PERK knockout mice are lethal, we used PERK heterozygous (*Perk*$^{+/-}$) mice. *Perk*$^{+/-}$ mice on a high fat diet had higher levels of glucose levels during glucose tolerance and insulin tolerance tests than did the controls, indicating that *Perk*$^{+/-}$ mice are more insulin resistant. Compromise of the PERK branch led to activation of JNK and inhibition of insulin receptor signaling.

Discussion & Conclusion

In FABP studies, we confirmed that aP2 is secreted from adipocytes although there are no secretary signal peptides. Non-classical pathway of secretion might be involved. Further investigations need to be done. It is still unknown whether circulating aP2 has a physiological function. In such a case, there might be receptors for aP2, developing for further studies. The small chemical molecules for blocking aP2 receptors might result in new treatments for obesity, diabetes, and atherosclerosis. We are now considering experiments of obesity and diabetes models using recombinant aP2 protein to elucidate whether aP2 has a physiological function in vivo.

In ER stress projects, our results indicate that roles of PERK and the consequent UPR activation in tissues are important for the development of insulin resistance and type 2 diabetes. To elucidate this regulation in each tissue under several conditions help us how to address these metabolic diseases for therapeutic purpose. Specific modulations of UPR branches would be a new therapeutic target for wide range of metabolic and cardiovascular diseases. Modulating ER function might be a paradigm-shifting approach for several diseases as a novel “organelle therapy”.

References

1) Maeda K, Cao H, Kono K, Gorgun CZ, Furuhashi M, Uysal K, Cao Q, Atsumi G, Malone H, Krishnan B, Minokoshi Y, Kahn BB, Parker RA, Hotamisligil GS. Adipocyte/macrophage fatty acid binding proteins control integrated metabolic responses in obesity and diabetes. *Cell Metab* 1: 107-119, 2005

2) Ozcan U, Yilmaz E, Ozcan L, Furuhashi M, Vaillancourt E, Smith RO, Gorgun CZ, Hotamisligil GS. Chemical chaperones reduce ER stress and restore glucose homeostasis in a mouse model of type 2 diabetes. *Science* 313: 1137-1140, 2006

3) Wellen KE, Fucho R, Gregor MF, Furuhashi M, Morgan C, Lindstad T, Vaillancourt E, Gorgun CZ, Saatcioglu F, Hotamisligil GS. Coordinated regulation of nutrient and inflammatory responses by STAMP2 is essential for metabolic homeostasis. *Cell* 129: 537-548, 2007

4) Furuhashi M, Tuncman G, Görgün CZ, Makowski L, Atsumi G, Vaillancourt E, Kono K, Babaev VR, Fazio S, Linton MF, Sulsky R, Robl JA, Parker RA, Hotamisligil GS. Treatment of diabetes and atherosclerosis by inhibiting fatty acid-binding protein aP2. *Nature* 447: 959-965, 2007

5) Furuhashi M, Fucho R, Görgün CZ, Tuncman G, Cao H, Hotamisligil GS. Adipocyte/ macrophage fatty acid-binding proteins contribute to metabolic deterioration through actions in both macrophages and adipocytes in mice. *J Clin Invest* 118: 2640-2650, 2008

6) Vallerie SN, Furuhashi M, Fucho R, Hotamisligil GS. A predominant role for parenchymal c-Jun Amino Terminal Kinase (JNK) in the regulation of systemic insulin sensitivity. *PLoS ONE* 3: e3151, 2008

7) Nakamura T, Furuhashi M, Li P, Cao H, Tuncman G, Sonenberg N, Gorgun CZ, Hotamisligil GS. Double-stranded RNA dependent protein kinase links pathogen sensing with stress and metabolic homeostasis. *Cell* 140: 338-348, 2010

Molecular mechanisms of host inflammatory responses mediated by Nod-like receptor NLRP3

Toshihiko Suzuki
Department of Molecular Bacteriology and Immunology
Graduate School of Medicine, University of the Ryukyus
t-suzuki@med.u-ryukyu.ac.jp

Abstract

Aeromonas are Gram-negative bacteria that cause serious infectious disease in humans. *Aeromonas* spp. have been shown to induce apoptosis in infected macrophages, yet the host responses triggered by macrophage death are largely unknown. Here, we demonstrate that the infection of mouse bone marrow derived macrophages with *A. hydrophila* or *A. veronii* triggers activation of caspase-1 with the ensuing release of IL-1β and pyroptosis. Our results indicated that multiple factors from both the bacteria and the host play a role in eliciting caspase-1 activation during infection with *Aeromonas*.
Keywords: caspase-1, inflammasome, infection

Introduction

The genus *Aeromonas* is responsible for a significant number of animal and human infections. *Aeromonas* are opportunistic human pathogens that cause intestinal infections, of which the most common is gastroenteritis with diarrhea. *Aeromonas* also cause extraintestinal infections, including wound, soft tissue, skin, and blood infections and septicemia. Recently, it has been reported that the infection with *A. hydrophila* and *A. veronii* biotype *sobria* (*A. veronii*) induces apoptosis in macrophages. While the cytotoxicity by the bacteria is thought to enable the bacteria to evade eradication and clearance by the macrophages, the host proinflammatory responses triggered by the death of the macrophages remain unknown. We focused the activation of caspase-1, a key molecule for processing pro-IL-1β and IL-18 to bioactive forms.

Results

We investigated the cell death of macrophages infected with *A. hydrophila* or *A. veronii*, and demonstrated that cell cells cause pyroptosis with caspase-1 activation and IL-1β release. Caspase-1 activation with the infection of *A. hydrophila* was dependent on inflammasome activation by NLRP3, one of the member of nucleotide-binding oligomerization domain (NOD)-like receptors (NLRs). Aerolysin, hemolysin and multifunctional repeat-in-toxin produced by *A. hydrophila* are required to elicit the NLRP3 inflammasome and necrotic cell death.

We also investigated the role of NLR inflammasome activation in macrophages during *A. veronii* infection and demonstrate that aerolysin and T3SS are required to elicit caspase-1 activation and the subsequent secretion of IL-1β and pyroptosis. Aerolysin triggers the activation of the NLRP3

inflammasome. By contrast, T3SS of A. veronii triggers both NLRP3 and NLRC4 inflammasome activation. Our data indicated that multiple factors from both the bacteria and the host are involved in caspase-1 activation during proinflammatory responses.

Discussion & Conclusion

We identified the essential bacterial and host factors for eliciting caspase-1 activation and the proinflammatory responses upon *Aeromonas* infection. Our data indicated that multiple factors from both the bacteria and the host are involved in caspase-1 activation during proinflammatory responses.

References

1) McCoy A, Koizumi Y, Higa N, Suzuki T. (2010) Differential regulation of caspase-1 activation via NLRP3/NLRC4 inflammasomes mediated by aerolysin and type III secretion system during *Aeromonas veronii* infection. **J Immunol** 185: 7077-7084.

2) McCoy A, Koizumi Y, Toma C, Higa N, Dixit V, Taniguchi S, Tschopp J, Suzuki T. (2010) Cytotoxins of the human pathogen *Aeromonas hydrophila* trigger, via the NLRP3 inflammasome, caspase-1 activation in macrophages. **Eur J Immunol** 40: 2797-2803.

Study of olfactory background canceling system that controls courtship behavior

Aki Ejima
Kyoto University
aki@cp.kyoto-u.ac.jp

Abstract

The excitatory feedback into the sensory neurons mediates the signal equilibrium between two pheromone pathways and contributes to background canceling.

Keywords: behavioral neurobiology

Introduction

In *Drosophila melanogaster*, *cis*-vaccenyl acetate (cVA), a product of the male ejaculatory bulb, works as a courtship inhibitory pheromone. Recently I found that a male was capable to detect as low cVA on a target fly as one thousandth of its own and exhibited a reduced level of courtship. But the mechanisms that allows a male to detect such a tiny amount of cVA without being distracted by his own cVA was largely unknown.

Results

In order to examine how pheromonal information is processed in the olfactory system, we performed physiological analysis using an activity-sensitive fluorescent markers, synaptopHluorin (spH) and GCaMP in two groups of pheromone odorant receptor neurons (ORNs), one expressing OR47b which respond to fly odors and the other expressing cVA-responsive OR65a.

The "naked brain" expressing the markers showed that both Or65a and Or47b ORNs received cholinergic excitatory input to their presynaptic terminals. Blocking expression of the acetylcholine receptor in either Or65a or Or47b ORNs diminished cVA-responsive courtship suppression, suggesting that lateral feedback modification of ORNs is critical for pheromone coding. Intriguingly, however, co-suppression of the excitatory feedback in both ORNs rescued the cVA-response defect, indicating that the behavioral output is determined by the signal equilibrium between the Or65a courtship inhibitory pathway and the Or47b courtship stimulatory pathway.

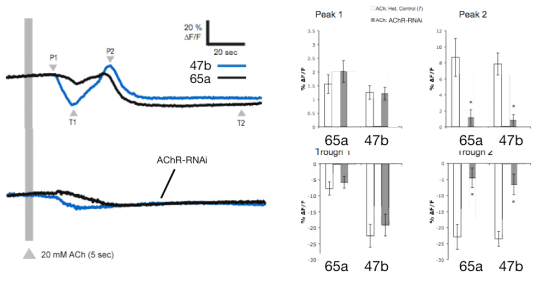

Both Or47b and Or65a receive ACh excitatory input at their presynaptic terminal.

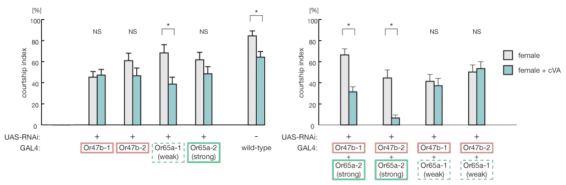

Blocking AChR diminishes cVA responsive courtship suppression.

It was also found that prolonged exposure

to purified cVA caused an enhanced level of subsequent courtship activity, indicating that the basal balance between the two groups of ORNs is maintained at neutral level and this adjusting mechanism contributes to the background-noise canceling mechanism that allows a male to ignore his own smell and lead to an appropriate courtship decision.

Discussion & Conclusion

In this study, the neural-activity imaging and behavioral analysis revealed the role of acetylcholine input at the ORN presynaptic terminals for pheromone coding and behavior control in *Drosophila melanogaster*. It was found that the basal activity levels of two pheromone pathways are maintained by the homeostatic control to adjust constant background activities, which allows a male to detect novel stimuli and lead to appropriate behavior decision-making. Further analysis would uncover the detailed physiological mechanism that underlies the lateral interaction of the multiple ORN groups.

Molecular Basis for microtubule plus-end tracking protein CLASP2

Ikuko Hayashi
Department of Supramolecular Biology, Graduate School of Nanobioscience,
Yokohama City University, Japan
ihay@tsurumi.yokohama-cu.ac.jp

Abstract

Crystal structures of CLASP2 microtubule-binding domains

Keywords: Crystallography, microtubule, cell migration

Introduction

Microtubule (MT) is essential for many cellular functions, such as cell polarity, cell division and cell migration. The dynamic behavior of MTs is highly regulated by MT-associated proteins (MAPs): they stabilize or destabilize MT structure, which leads to MT two alternating phases of growing or shortening, called dynamic instability. CLASPs are a member of a conserved class of MAPs which specifically bind to MT plus-ends to stabilize MT filament. We determined the crystal structures of CLASP2 MT binding domains and showed that they possess known MT-associated TOG domains. Furthermore, our biochemical analyses showed CLASP2 cooperatively promotes MT assembly with another MT plus-end associated protein EB1 *in vitro*.

Results

1. Crystal structures of MT-binding domains in CLASP2

We expressed, purified and crystallized the MT binding domains of CLASP2 using bacterial expression system. Crystal structures of two CLASP2 MT-binding domains were determined by selenomethionine multiwavelength anomalous diffraction method (Fig. 1). These domains both comprise six HEAT-repeat helices stacked side by side, belonging to the MT-binding TOG domains

Fig. 1 Crystal structures of TOG domains.
CLASP2 possesses two TOG domains with six HEAT-repeat modules seen in XMAP215. Trptophan and basic residues essential for MT recognition are shown.

(a) CLASP2 N-terminal TOG (b) CLASP2 C-terminal TOG (c) XMAP215 TOG

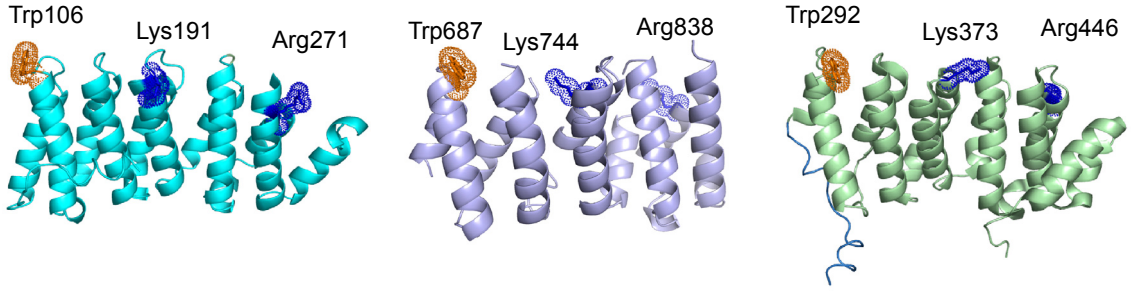

found in MT stabilizing factor XMAP215. The Trp and basic residues identified as MT-interacting elements in XMAP215 TOG domains are also conserved in the ternary structure of CLASP2 MT-binding domains, indicating that CLASP2 has a similar mechanism to stabilize MTs. We mutated conserved residues in CLASP2 TOG domains and found that the mutations cause the defect in TOG's binding to MTs.

2. CLASP2 and EB1 cooperatively promote MT assembly *in vitro*

Although CLASP family proteins are conserved throughout the eukaryotes, there are significant differences between the species. Human CLASPs are monomeric, on the other hand yeast CLASP homologue (Cls1p) dimeric; CLASPs associates with the plus-end MAP EB1, whereas Cls1p does not. EB1 binding to CLASPs Ser-rich region leads to the specific localization of CLASPs to MT plus-ends (ref. 1). By the use of isothermal titration calorimetry, we determined the Kd value for CLASP2 and EB1 binding ($3x10^{-6}$ M). MT polymerization effects of EB1 and CLASP2 were examined by light scattering analyses. CLASP2 increases the turbidity of MTs by itself, and the cooperative MT stabilization effect between CLASP2 and EB1 is observed.

3. GCC185 associates with C-terminal domain of CLASP2

C terminus of CLASP2 is shown to interact with trans-Golgi network (TGN) protein GCC185 (ref. 2). The interaction is essential for Golgi-derived MT growth in a migrating cell. By yeast two-hybrid assay using C terminal region of CLASP2 as a bait, we identified approximately 100 a.a. CLASP2 binding region in GCC185.

With fluorescent microscopic technique, we examined if the region affects the localization of CLASPs in the cell. This GCC185 fragment removed CLASPs from the Golgi apparatus, revealing the dominant-negative effects (Fig. 2). Mass spectroscopy and gel filtration analyses showed that this GCC185 mutant forms a dimer. Now we are investigating the structural analyses of GCC185 and CLASP2 complex by x-ray crystallography.

Fig. 2 Overexpression of dominant-negative GCC185 mutant causes mislocalization of CLASPs.
(left) Overexpression of GCC185 mutant in Hela cells. GFP labeled GCC185 localizes to the Golgi.
(middle) CLASPs do not localize to the Golgi because of dominant-negative GCC185. Asterisks show CLASP localization at MT plus-ends.
(right) Merged image

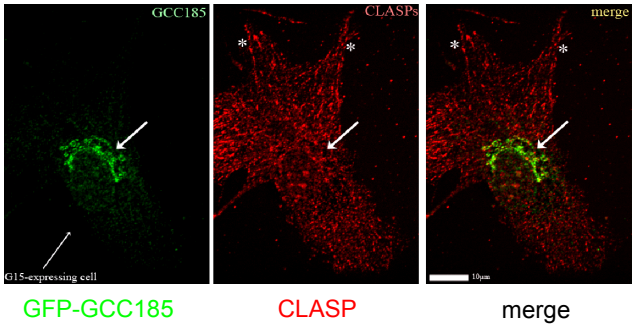

Discussion & Conclusion

Multiplicity of the MT-binding domains gives a wide variety of MT dynamics. Here we showed that CLASPs MT-binding domains possess TOG-domain fold – one of the typical MT-binding

domains seen in XMAP215. CLASPs' MT-binding ability is also regulated by EB1 binding sites. The region possesses serine/arginine-rich stretches that can affect CLASPs' MT-lattice binding as well as EB1 binding. Although CLASPs are shown to be one of the members of XMAP215/Dis1 family proteins, MT-recognition depends not only on the divergence of TOG domain characters but also on the franking region of TOGs. The serine/arginine-rich region can be phosphorylated by GSK3β, which is critical to the localization of CLASPs in the cell (ref. 3). GSK3β is not active at the cell periphery, where non-phosphorylated CLASPs can localize at MTs. The effect of GSK3β phosphorylation is now examined *in vitro* to see how the interactions between CLASP2 and MTs/EB1 can be affected. We further investigated CLASPs C-terminal domain's interaction with GCC185. CLASPs C-terminal domain is responsible for cellular localization such as Golgi, cell cortex and kinetochore by interacting with its binding partners. We believe that CLASP association with GCC185 will shed light on the structural basis of CLASP2 recognition, eventually explain the cellular localization mechanisms between CLASPs and its binders.

References

1) Mimori-Kiyosue Y et al. (2005) CLASP1 and CLASP2 bind to EB1 and regulate microtubule plus-end dynamics at the cell cortex. *J Cell Biol*, **168**, 141-53.

2) Efimov A et al. (2007) Asymmetric CLASP-dependent nucleation of noncentrosomal microtubules at the trans-Golgi network. *Dev Cell* **12**, 917-30.

3) Kumar P et al. (2009) GSK3beta phosphorylation modulates CLASP-microtubule association and lamella microtubule attachment. *J Cell Biol* **184**, 895-908.

Engineered Biosynthesis of Steroidal Antibiotics

Ikuro Abe
The University of Tokyo
abei@mol.f.u-tokyo.ac.jp

Abstract

Oxidosqualene:protostadienol cyclase (OSPC) from the fungus *Aspergillus fumigatus*, catalyzes the cyclization of (3*S*)-2,3-oxidosqualene into protosta-17(20)*Z*,24-dien-3b-ol which is the precursor of the steroidal antibiotic helvolic acid. To shed light on the structure-function relationship between OSPC and oxidosqualene:lanosterol cyclase (OSLC), we constructed an OSPC mutant in which the C-terminal residues ^{702}APPGGMR^{708} were replaced with ^{702}NKSCAIS^{708}, as in human OSLC. As a result, the mutant no longer produced the protostadienol, but instead efficiently produced a 1:1 mixture of lanosterol and parkeol. This is the first report of the functional conversion of OSPC into OSLC, which resulted in a 14-fold decrease in the V_{max}/K_M value, whereas the binding affinity for the substrate did not change significantly. Homology modeling suggested that stabilization of the C-20 protosteryl cation by the active-site Phe701 through cation–π interactions is important for the product outcome between protostadienol and lanosterol.

keywords: oxidosqualne cyclase; lanosterol synthase; protostadienol synthase; steroidal antibiotics; helvolic acid

Introduction

Oxidosqualene cyclases (OSCs) are pivotal enzymes in the biosynthesis of sterols and triterpenes [1-4]. Oxidosqualene:lanosterol cyclase (OSLC) catalyzes the cyclization of (3*S*)-2,3-oxidosqualene into lanosterol, which is the key step in the biosynthesis of sterols in animals and fungi (Fig. 1). The formation of lanosterol is initiated by the oxirane ring opening of oxidosqualene folded in the *chair-boat-chair* conformation; the sequential ring forming reaction first produces the tetracyclic protosteryl C-20 cation, which then undergoes backbone rearrangement (H-17a→20, H-13a→17a, CH_3-14b→13b, CH_3-8a→14a) followed by removal of H-9 to generate the D^8 double bond of lanosterol. On the other hand, oxidosqualene:protostadienol cyclase (OSPC) (AfuOSC3 or *Afu4g14770*) from the fungus *Aspergillus fumigatus* is a recently reported novel OSC which is involved in the biosynthesis of the fusidane-type steroidal antibiotic helvolic acid [5,6]. OSPC is an *M*r 83,086 membrane bound protein with 735 amino acids, sharing 40% amino acid identity with human OSLC. A recombinant OSPC heterologously expressed in an OSLC-deficient mutant GIL77 strain of *Saccharomyces cerevisiae* catalyzed the cyclization of (3*S*)-2,3-oxidosqualene into a 3:1 mixture of protosta-17(20)*Z*,24-dien-3b-ol and (20*R*)-protosta-13(17),24-dien-3b-ol (Fig. 1) [5]. In this case, the cyclization of (3*S*)-2,3-oxidosqualene proceeds *without* the backbone rearrangement, and the C-20 protosteryl cation immediately undergoes proton elimination from H-17a or H-13a to form a double-bond between C-17/C-20 or C-13/C-17, respectively.

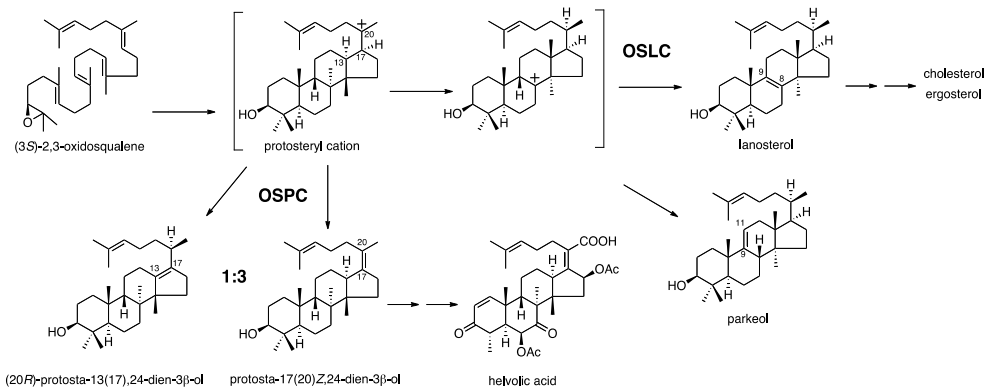

Fig. 1. Proposed mechanism of cyclization of (3*S*)-2,3-oxidosqualene into lanosterol by OSLC and protosta-17(20)*Z*,24-dien-3b-ol and (20*R*)-protosta-13(17),24-dien-3b-ol by OSPC.

To clarify the structure-function relationship between OSLC and OSPC, and to understand the intimate structural details that govern the stabilization of the C-20 protosteryl cation and the backbone rearrangement reactions, we constructed a series of *A. fumigatus* OSPC mutants and investigated the effects of the mutagenesis on the enzyme activity. Here we report the functional conversion of *A. fumigatus* OSPC into OSLC by replacing the C-terminal residues ^{702}APPGGMR^{708}, located just downstream of the active-site Phe701, with ^{702}NKSCAIS^{708}, as in human OSLC (Fig. 2). The active-site Phe701 is considered to be important for stabilization of the positive charges at the C-20 protosteryl cation through cation-p interactions, which would be crucial for the formation of lanosterol *via* the backbone rearrangement reaction [7]. The results suggested that the swapping of the residues neighboring the active-site Phe701 caused changes in the position of Phe701, thereby affecting the cation-p interactions and the stabilization of the C-20 cation, which led to the production of lanosterol by the OSPC mutant.

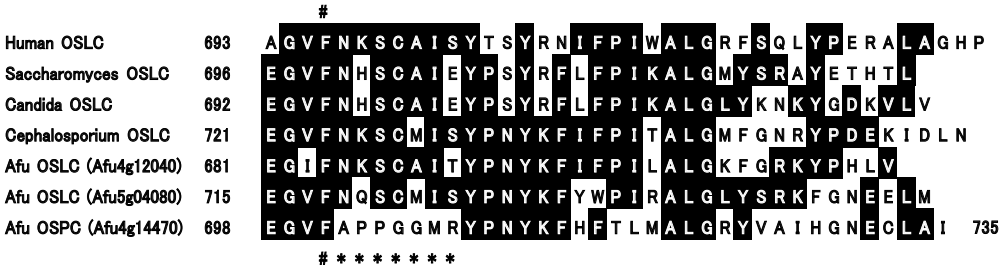

Fig. 2. Comparison of the amino acid sequences of the C-terminal regions of the *A. fumigatus* OSPC and the OSLCs from a mammal, yeast and fungi: Human, *Homo sapiens*; Saccharomyces, *Saccharomyces cerevisiae*; Candida, *Candida albicans*; Cephalosporium, *Cephalosporium caerulens*; Afu, *Aspergillus fumigatus*. The active-site Phe701 (numbering in *A. fumigatus* OSPC) is marked with #. The residues ^{702}APPGGMR^{708} are marked with *.

Results

A comparison of the primary sequences of the *A. fumigatus* OSPC and OSLC enzymes from a mammal, yeast and fungi revealed that the moderately conserved C-terminal residues of human OSLC, ^{697}NKSCAIS^{703}, located just downstream of the active-site Phe696 (numbering in human OSLC), are characteristically replaced with ^{702}APPGGMR^{708} in *A. fumigatus* OSPC (Fig. 2) [5]. In the X-ray crystal structure of human OSLC, the active-site Phe696 (which corresponds to Phe701 in *A. fumigatus* OSPC) is located near the C-13/C-20 of the bound lanosterol. This Phe residue is

considered to be important for stabilization of the positive charges at the C-13 anti-Markovnikov tricyclic cation and also at the C-20 tetracyclic protosteryl cation through cation-p interactions, thereby guiding the stereochemical course of the enzyme reaction [7]. Indeed, the F696T mutant of *S. cerevisiae* OSLC (ERG7) (numbering in human OSLC) was recently shown to produce a truncated rearrangement product, protosta-13(17),24-dien-3b-ol, which was formed by hydride shift from C-17 to C-20 followed by proton elimination of H-13a [8,9]. We therefore surmised that the residues located around Phe701 might be participating in the fate of the C-20 cation, and the difference between OSLC around this region might be responsible for the different product outcomes between the two enzymes. Thus, we first constructed a mutant of *A. fumigatus* OSPC in which the residues ^{702}APPGGMR^{708} were replaced with ^{702}NKSCAIS^{708}, as in human OSLC, and investigated the effects of the mutagenesis on the enzyme activity.

As in the case of the wild-type *A. fumigatus* OSPC, the gene encoding the mutant enzyme was cloned into the yeast expression vector pESC(Ura) and heterologously expressed in the OSLC-deficient sterol auxotrophic yeast mutant strain GIL77 (*erg7*, *ura3-167*, *hem3-6*, *gal2*) under the control of the *GAL10* promoter [5]. After induction, the transformed cells were harvested and the recombinant membrane-bound enzyme was solubilized with Triton X-100 and partially purified by hydroxylapatite column chromatography as described previously [10].

An *in vitro* enzyme assay revealed that the *A. fumigatus* OSPC mutant in which the residues ^{702}APPGGMR^{708} were replaced with the conserved ^{702}NKSCAIS^{708} sequence no longer produced protostadienols, but instead efficiently produced a 1:1 mixture of lanosterol and parkeol (Fig. 3). Indeed, the mutant complemented the *erg7* deficiency of the yeast GIL77 strain, since the transformed cells could grow on media lacking ergosterol, in sharp contrast to the wild-type OSPC.

The steady-state kinetic analysis revealed that the mutant had an apparent K_M = 16.5 μM, V_{max} = 0.32 μM min^{-1}, and V_{max}/K_M value of 0.019 min^{-1}, which are comparable to the values of the wild-type OSPC, which showed an apparent K_M = 14.4 μM, V_{max} = 4.08 μM min^{-1}, and V_{max}/K_M value of 0.283 min^{-1}. Thus, the swapping of the residues resulted in a 14-fold decrease in the V_{max}/K_M value whereas the binding affinity for the substrate did not change significantly.

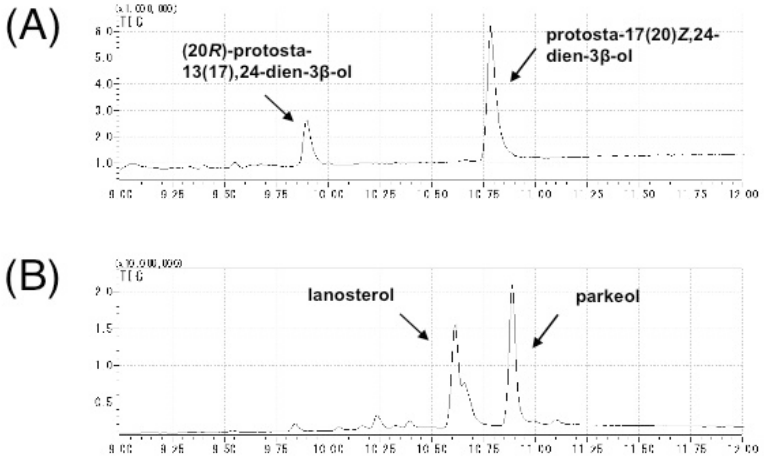

Fig. 3. GC-MS trace of the enzyme reaction products of (A) the wild-type *A. fumigatus* OSPC and (B) the OSPC mutant in which the residues ^{702}APPGGMR^{708} were replaced with the conserved ^{702}NKSCAIS^{708}.

Discussion & Conclusion

This is the first demonstration of the functional conversion of OSPC into OSLC and the formation of lanosterol by the OSPC mutant. Here the proposed mechanism of (3*S*)-2,3-oxidosqualene cyclization to parkeol is essentially the same as that for lanosterol; the only difference is the final proton elimination from H-11 to produce the double-bond between C-9/C-11 of parkeol, whereas proton elimination from H-9 generates the double-bond between C-8/C-9 of lanosterol (Fig. 1).

To further evaluate the importance of the conserved residues, we also created a set of four point mutations (A702N, P703K/P704S, G705C, and M707I) in *A. fumigatus* OSPC. However, none of the three mutants (A702N, G705C, and M707I) affected the enzyme reaction product pattern while the P703K/P704S mutant lost its activity, which clearly demonstrated that a single amino acid substitution is not sufficient for the functional conversion of OSPC into OSLC.

It was thus confirmed that these residues located just downstream of Phe696 of human OSLC play important roles for the formation of lanosterol *via* the stabilization of the C-20 protosteryl cation and the backbone rearrangement reaction. Presumably, the swapping of the residues neighboring the active-site Phe701 caused changes in the position of Phe701, thereby affecting the cation-p interactions and the stabilization of the tetracyclic C-20 cation, which led to the formation of lanosterol and parkeol by the OSPC mutant. Indeed, a homology model based on the human OSLC crystal structure [7] suggested that in *A. fumigatus* OSPC, the active-site Phe701 is located a bit farther from the presumed C-20 cationic center of the protosteryl cation as compared with that in human OSLC. This increased distance would reduce both the cation-p interactions and the stabilization of the C-20 cation, and hence would interrupt the backbone rearrangement, resulting in termination of the enzyme reaction by proton elimination of H-17a or H-13a to produce a 3:1 mixture of protosta-17(20)*Z*,24-dien-3b-ol and (20*R*)-protosta-13(17),24-dien-3b-ol (Fig. 1). Alternatively, an activated water molecule might be located in a cavity formed between the C-20 cation and Phe701, and abstract a proton from C-17 or C-13 to terminate the reaction at the protosteryl cation stage. The relocation of the Phe701 residue in the mutant might have prevented the water molecule from entering this cavity, thus precluding the early termination of the reaction to produce lanosterol and parkeol.

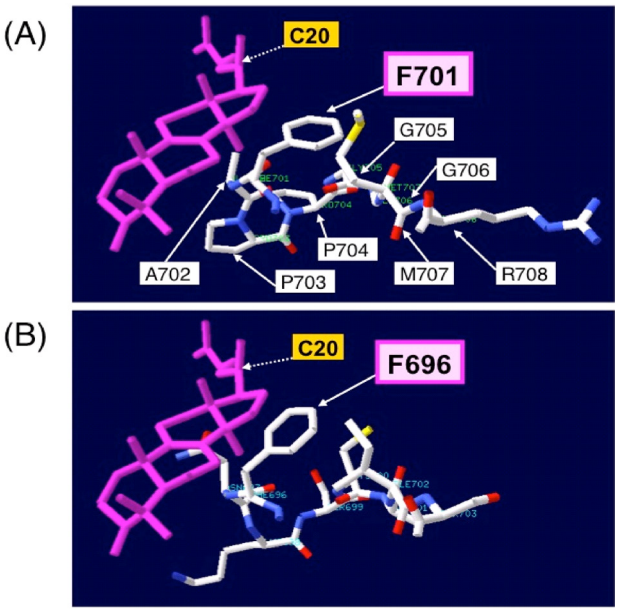

Fig. 4. (A) A homology model of *A. fumigatus* OSPC complexed with lanosterol. (B) The X-ray crystal structure of human OSLC complexed with lanosterol. Only the active-site Phe701 and the residues ^{702}APPGGMR^{708} (numbering in *A. fumigatus* OSPC) are indicated. Lanosterol is shown in magenta and the position of the C-20 indicated.

In conclusion, this is the first report of the functional conversion of OSPC to OSLC

by changing the conserved C-terminal residues ^{702}APPGGMR^{708} into ^{702}NKSCAIS^{708}. The results suggested that stabilization of the C-20 protosteryl cation by the active-site Phe701 through cation-π interactions is important for the product outcome between protostadienol and lanosterol. To further clarify the structural details of the enzyme reactions, crystallization trials of both the wild-type and mutant *A. fumigatus* OSPCs are now in progress in our laboratories.

References

1) I. Abe, M. Rohmer, G.D. Prestwich, Enzymatic cyclization of squalene and oxidosqualene to sterols and triterpenes, Chem. Rev. 93 (1993) 2189-2206.

2) I. Abe, Enzymatic synthesis of cyclic triterpenes, Nat. Prod. Rep. 24 (2007) 1311-1331.

3) K.U. Wendt, G.E. Schulz, E.J. Corey, D.R. Liu, Enzyme mechanisms for polycyclic triterpene formation, Angew. Chem. Int. Ed. 39 (2000) 2812-2833.

4) T. Kushiro, Y. Ebizuka, Triterpene, in: L.N. Mander, H.-w. Liu (Eds.), Comprehensive Natural Products II: Chemistry and Biology, Vol. 1, Elsevier, Oxford, 2009, in press.

5) H. Mitsuguchi, Y. Seshime, I. Fujii, M. Shibuya, Y. Ebizuka, T. Kushiro, Biosynthesis of steroidal antibiotic fusidanes: functional analysis of oxidosqualene cyclase and subsequent tailoring enzymes from *Aspergillus fumigatus*, J. Am. Chem. Soc. 131 (2009) 6402-6411.

6) S. Lodeiro, Q. Xiong, W.K. Wilson, Y. Ivanova, M.L. Smith, G.S. May, S.P.T. Matsuda, Protostadienol biosynthesis and metabolism in the pathogenic fungus *Aspergillus fumigatus*, Org. Lett. 11 (2009) 1241-1244.

7) R. Thoma, T. Schulz-Gasch, B. D'Arcy, J. Benz, J. Aebi, H. Dehmlow, M. Hennig, M. Stihle, A. Ruf, Insight into steroid scaffold formation from the structure of human oxidosqualene cyclase, Nature 432 (2004) 118-122.

8) T.-K. Wu, H.-Y. Wen, C.-H. Chang, Y.-T. Liu, Protein plasticity: a single amino acid substitution in the *Saccharomyces cerevisiae* oxidosqualene-lanosterol cyclase generates protosta-13(17),24-dien-3b-ol, a rearrangement product, Org. Lett. 10 (2008) 2529-2532.

9) T.-K. Wu, C.-H. Chang, Y.-T. Liu, T.-T. Wang, *Saccharomyces cerevisiae* oxidosqualene-lanosterol cyclase: a chemistry-biology interdisciplinary study of the protein's structure-function-reaction mechanism relationships, Chem. Rec. 8 (2008) 302-325.

10) I. Abe, M. Bai, X.-y. Xiao, G.D. Prestwich, Affinity labeling of vertebrate oxidosqualne cyclases with a tritiated suicide substrate, Biochem. Biophys. Res. Commun. 187 (1992) 32-38.

Physiological function of the active zone protein CAST/ELKS family

Ohtsuka Toshihisa
Department of Biochemistry, Interdisciplinary Graduate School of Medicine and Engineering, University of Yamanashi
tohtsuka@yamanashi.ac.jp

Abstract

To explore the physiological roles of the CAST/ELKS family, we have tried to produce the double KO mice.

Keywords: Active Zone, CAST, ELKS

Introduction

Our higher brain functions such as learning and memory, emotion, and consciousness rely on the complicated neural network in the brain. The fundamental unit of this network is called “synapse”, which is composed of the three parts: the presynaptic terminal, synaptic cleft, and postsynaptic compartment. In the presynaptic nerve terminals, a specialized structure, active zone, plays a pivotal role in neurotransmitter release and possibly in synaptic plasticity. We have recently isolated and characterized the active zone-specific protein, named CAST (cytomatrix at active zone -associated structural protein) and its family member ELKS. While CAST is mainly expressed in the brain, ELKS is ubiquitously expressed in the body. And, unfortunately, the KO mice for ELKS was embryonic lethal. To overcome this difficulty, we attempted to produce the double KO mice and examine the effect on synaptic structure and function.

Results

Because we have already obtained flox-ELKS hetero mice, we first produced the homozygotes for flox-ELKS. Then, we cross-bred these mice with transgenic mice containing flipase: flipase is an enzyme, which can delete the neomycin site. While we maintain these conditional ELKS mice, we obtained transgenic mice expressing Cre recombinase, which can be driven by CaMKII. Our conditional ELKS was bred with CaMKII-cre mice, and we analyzed if ELKS is specifically deleted in the brain. CaMKKII-cre has been known to be expressed in the fore brain. Thus, we prepared the homogenates of various brain regions such as olfactory bulb, cortex, hippocampus, and cerebellum. Western blot analysis using the anti-ELKS antibody showed that ELKS was specifically deleted in the forebrain containing olfactory bulb, cortex and hippocampus, whereas its expression was intact in the cerebellum. The expression of CAST was unchanged throughout the brain.

Discussion & Conclusion

The presynaptic active zone is believed to play a crucial role in the docking, priming, and fusion if synaptic vesicles upon elevation of intracellular concentration of Ca ion. However, especially in mammals, its physiological role or significance of the active zone is still obscure in the whole anima level. CAST and ELKS forms a complex with the other active zone proteins including Bassoon, Piccolo, RIM1, and Munc13-1. Accumulating evidence suggest that there were no changes in the structure of the active zone in the KO mice for Bassoon, Piccolo, RIM1, and Munc13-1, although severe impairments were observed. Therefore, using the conditional KO mice for ELKS produced in this project, we will be able to produce the double KO for CAST and ELKS, and reveal the physiological role of the CAST/ELKS family in the establishment and maintenance of the active zone, which will definitely shed new light on the role of active zone in our higher brain function and neuronal disorders such as autism, schizophrenia, and Parkinson diseases.

The role of Sox17 in gastrointestinal tumorigenesis

Masanobu Oshima
Cancer Research Institute, Kanazawa University
oshimam@kenroku.kanazawa-u.ac.jp

Abstract

Sox17 belongs to SRY transcription family members, and plays an important role in definitive endoderm development. It has been shown that Sox17 functions as a tumor suppressor through repression of canonical Wnt signaling. We have investigated expression of Sox17 in gastric and intestinal tumors using mouse models. Importantly, Sox17 expression is induced in the Wnt-activated tumor epithelial cells at early stage of tumorigenesis. However, Sox17 expression was significantly suppressed in human gastric cancer tissues. Consistently, in the malignant mouse intestinal adenocarcinomas, Sox17 expression was rarely detected. These results suggest that Sox17 plays a protective role against malignant progression at early stage of tumorigenesis, and that downregulation of tumor suppressor Sox17 contributes to malignant progression.

Keywords: Sox17, Wnt, gastric tumor, intestinal tumor

Introduction

Sox17 is a member of SRY family transcription factors. Disruption of Sox17 gene in mice resulted in lethal at the early embryogenesis by impaired definitive endoderm formation[1]. On the other hand, functions of Sox17 in adult tissues have not been understood yet. In human colon cancer tissues, Sox17 is widely downregulated by DNA methylation[2]. Moreover, transfection of Sox17 in colon cancer cells resulted in suppression of colony formation[2]. These results suggest that Sox17 functions as tumor suppressor in colon cancer development. However, molecular mechanisms of Sox17 in cancer development have not been elucidated.

Canonical Wnt signaling is important for maintenance of gastrointestinal epithelial stem cells. Constitutive activation of Wnt pathway by genetic or epigenetic alterations causes tumor development in the gastrointestinal tract. We have constructed genetically engineered mouse models, *Gan* mice and $Apc^{\Delta 716}$ mice, in which Wnt signaling is activated by *Wnt1* gene expression[3] or *Apc* gene mutation[4], respectively. *Gan* mice develop gastric tumors, while $Apc^{\Delta 716}$ mice develop intestinal polyps. Moreover, we previously constructed $Apc^{\Delta 716}$ *Smad4* compound mutants that develop malignant adenocarcinomas in the intestine by mutations in both *Apc* and *Smad4* genes simultaneously[5]. Here, we have investigated expression of Sox17 during gastrointestinal tumorigenesis using these mouse models. Importantly, we found that Sox17 is induced at the early stage of tumorigenesis as a Wnt target gene, but downregulated in the malignant progressed tumors.

Results

We previously examined gene expression profile in *Gan* mouse tumors by microarray analyses[6]. Expression of Sox family member genes were extracted from the data set and compared with that of normal gastric mucosa of the wild-type mice. Notably, Sox17 as well as Sox2, Sox4, Sox7, and Sox9 showed elevated expression in gastric tumors[7] (Fig. 1A). We thus examined expression of Sox17 in the primary cultured gastric tumor cells derived from *Gan* mice. In the primary culture system, undifferentiated epithelial cells formed spheroid structure (Fig. 1B), whereas surrounding monolayer cells showed differentiated morphology. We confirmed that active form of β-catenin is accumulated in the spheroid-forming epithelial cells but not in the surrounding monolayer cells, indicating Wnt activation only in the spheroid cells. Importantly, Sox17 expression was detected only in the nuclei of spheroid-forming cells (Fig. 1B, *right*). These results strongly suggest that Sox17 is induced as one of the Wnt target genes in the gastric tumor cells.

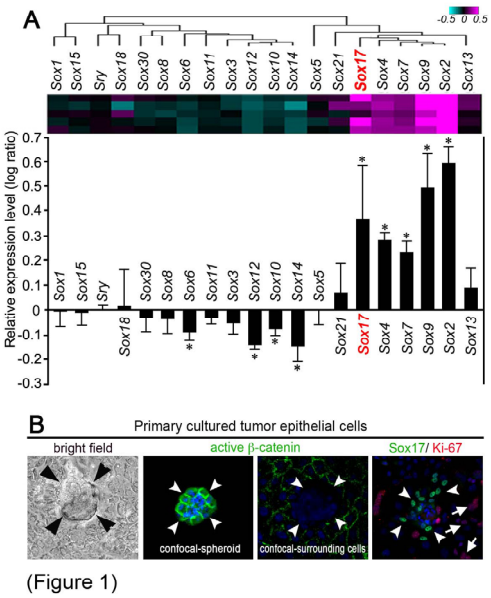

(Figure 1)

On the other hand, it has been suggested that Sox17 functions as a tumor suppressor in human colon cancer development through Wnt suppression. We thus examined expression profiles of Sox family members in human gastric cancers using public database. Interestingly, the mean expression level of Sox17 was significantly decreased in malignant gastric cancer, although Sox4 and Sox9 are still elevated (Fig. 2A). These results suggest that Sox17 is induced at early stage of tumorigenesis, but downregulated during malignant progression. We thus examined Sox17 expression in mouse benign and malignant intestinal tumors developed in *Apc*$^{\Delta 716}$ and *Apc*$^{\Delta 716}$ *Smad4* compound mice, respectively (Fig. 2B). In the *Apc*$^{\Delta 716}$ mice, strong Sox17 expression was detected in the adenoma tumor cells but not in the normal cells. In contrast, Sox17 expression was no longer detected in the invasive malignant adenocarcinoma of the *Apc*$^{\Delta 716}$ *Smad4* mouse intestines[7]. These results support the idea that Sox17 is upregulated at early stage but downregulated at the progression stage of gastrointestinal tumorigenesis.

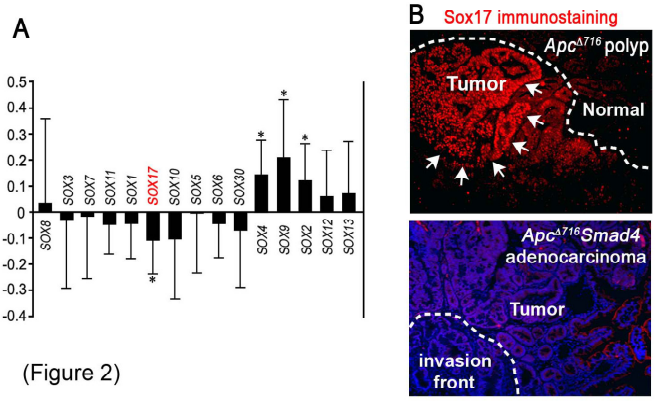

(Figure 2)

Discussion & Conclusion

It has been suggested that Sox17 represses Wnt signaling activity through unknown mechanism. Accordingly, suppression of Sox17 expression in tumors may cause Wnt activation, which contributes to malignant progression. However, our present results indicate that Sox17 expression is induced by Wnt activation in the gastrointestinal tumor cells at early stage. These results, taken together, indicate that Wnt activation triggers tumor development in the gastrointestinal tract, and that Wnt activation at the same time induces Sox17 expression, which partially represses Wnt activation level. Accordingly, it is possible that Sox17 plays a protective role against malignant progression by regulation of Wnt activation level at the early stage of tumorigenesis. When Sox17 expression is suppressed possibly by DNA methylation, Wnt activation level in tumor cells is increased, resulting in malignant progression. It is therefore possible that Sox17 is a negative regulator of Wnt signaling pathway.

References

1) Kanai-Azuma M, Kanai Y, Gad JM, et al. Depletion of definitive gut endoderm in *Sox17*-null mutant mice. Development, 129: 2367-2379, 2002.

2) Zhang W, Glockner SC, Guo M, et al. Epigenetic inactivation of the canonical Wnt antagonist SRY-box containing gene 17 in colorectal cancer. Cancer Res 68: 2764-2772, 2008.

3) Oshima H, Matsunaga A, Fujimura T, et al. Carcinogenesis in mouse stomach by simultaneous activation of the Wnt signaling and prostaglandin E_2 pathway. Gastroenterology 31: 1086-1095, 2006.

4) Oshima M, Oshima H, Kitagawa K, et al. Loss of *Apc* heterozygosity and abnormal tissue building in nascent intestinal polyps in mice carrying a truncated *Apc* gene. Proc Natl Acad Sci USA 92: 4482-4486, 1995.

5) Kitamura T, Kometani K, Hashida H, et al. SMAD4-deficient intestinal tumors recruit CCR1+ myeloid cells that promote invasion. Nat Genet, 39: 467-475, 2007.

6) Itadani H, Oshima H, Oshima M, Kotani H. Mouse gastric tumor models with prostaglandin E2 pathway activation show similar gene expression profiles to intestinal-type gastric cancer. BMC Genomics, 10: 615, 2009.

7) Du YC, Oshima H, Oguma K, et al. Induction and down-regulation of Sox17 and its possible roles during the course of gastrointestinal tumorigenesis. Gastroenterology, 137: 1346-1357, 2009.

4D imaging analysis of insulin exocytosis

Mica Ohara-Imaizumi
Department of Biochemistry, Kyorin University School of Medicine
mimaizu@ks.kyorin-u.ac.jp

Abstract

A variant of the *CDKAL1* gene was reported to be associated with type 2 diabetes. To determine the role of CDKAL1 in β-cells, we studied insulin release profiles in *CDKAL1* gene knockout (KO) mice using 4D-total internal reflection fluorescence (TIRF) microscopy. 4D-TIRF imaging of *CDKAL1* KO β-cells showed that the number of fusion events during first-phase insulin release was reduced with delayed and slow cytosolic Ca^{2+} increase. The responsiveness of K_{ATP} channels to glucose was blunted in KO cells. In addition, glucose-induced ATP generation was impaired. Although CDKAL1 is homologous to CDK5RAP1, there was no difference in CDK5 activity between WT and KO islets. Thus, CDKAL1 controls first-phase insulin exocytosis in β-cells by facilitating ATP generation, K_{ATP} channel responsiveness and subsequent Ca^{2+} channels activity through pathways other than CDK5-mediated regulation.

Keywords: TIRF microscopy, CDKAL1, insulin, pancreatic β cells, exocytosis, type 2 diabetes

Introduction

Recent genome-wide association studies (GWAS) have identified *CDKAL1* (cyclin-dependent kinase 5 regulatory subunit associated protein 1-like 1) as a susceptibility gene for type 2 diabetes, which has been replicated in several populations (Zeggini et al. 2007; Steinthorsdottir et al. 2007; Saxena et al. 2007; Scott et al. 2007). The *CDKAL1* gene is located on chromosome 6p22.3 and encodes a 65-kDa protein (CDKAL1). Although the function of CDKAL1 is still unclear, CDKAL1 is similar to cyclin-dependent kinase 5 regulatory subunit-associated protein 1 (CDK5RAP1) which inhibits cyclin-dependent kinase 5 (CDK5) activity by binding to the CDK5 activator p35 (Ching et al. 2002).

Recently, Groenewoud et al. (2008) and Stancakova et al. (2008) reported that a *CDKAL1* variant (rs7754840) decreased first-phase insulin secretion but not second-phase insulin secretion during hyperglycaemic clamps and intravenous glucose tolerance tests, respectively. Furthermore, the gene variants were not associated with the insulin sensitivity index, suggesting that *CDKAL1* variants influence the risk of type 2 diabetes by impairing first-phase insulin secretion. However, the molecular mechanisms through which CDKAL1 modulates insulin release in pancreatic β cells are unknown. To understand the role of CDKAL1 in β cells, we studied the phenotype of mice deficient in CDKAL1 expression established using a gene-trap technique (*CDKAL1* KO mice).

Results

4D-TIRF imaging of *CDKAL1* KO β cells showed that the number of fusion events during first-phase insulin release was reduced. However, there was no significant difference in the number of fusion events during second-phase release or high K^+-induced release between WT and KO cells. CDKAL1 deletion resulted in a delayed and slow increase in cytosolic free Ca^{2+} concentration during high glucose stimulation. Patch-clamp experiments revealed that the responsiveness of ATP-sensitive K^+ (K_{ATP}) channels to glucose was blunted in KO cells. In addition, glucose-induced ATP generation was impaired. Although CDKAL1 is homologous to cyclin-dependent kinase 5 (CDK5) regulatory subunit-associated protein 1, there was no difference in the kinase activity of CDK5 between WT and *CDKAL1* KO islets.

Discussion & Conclusion

In this study, we found that pancreatic β cells from mice null for *CDKAL1*, which was identified as a susceptibility gene for type 2 diabetes in humans, have a reduced first-phase insulin release *in vitro*. Our results indicate that CDKAL1 controls first-phase insulin exocytosis in β cells by facilitating ATP generation, K_{ATP} channel responsiveness and the subsequent activity of Ca^{2+} channels through pathways other than CDK5-mediated regulation. Defects in the process by decreased CDKAL1 expression levels may confer an increased risk of diabetes.

References

1) Ohara-Imaizumi M. , Yoshida M . Aoyagi K, Saito T , Okamura T , Takenaka H , Akimoto Y , Nakamichi Y, Takanashi-Yanobu R , Nishiwaki C, Kawakami H , Kato N , Hisanaga S , Kakei M , and Nagamatsu S (2010) Deletion of CDKAL1 Affects First-phase Glucose-stimulated Insulin Exocytosis **PLoS ONE** 5, e15553

2) Aoyagi K, Ohara-Imaizumi M, Nishiwaki C, Nakamichi Y, Nagamatsu S. (2010) Insulin/phosphatidylinositol 3-kinase pathway accelerates the glucose-induced first phase insulin secretion through TrpV2 recruitment in pancreatic beta-cells. **Biochem J.** 432, 375-386

Mechanism for development and homeostatic maintenance of human dendritic cell subsets

Nobuyuki Onai
Department of Biodefense Research, Medical Research Institute,
Tokyo Medical and Dental University
onai.bre@mri.tmd.ac.jp

Abstract

In the mice, we isolated mouse common dendritic cell progenitor (CDP), which gave rise to only DC subsets but not other lineage *in vivo*. Thus, mouse DC subsets were derived from CDP in the bone marrow. While the origin and developmental pathway of human DC subsets are completely unknown. In this study, we try to isolate human CDP counterpart using the humanized mice. After reconstitution of human hematopoiesis in the mouse, we found $lin^-CD34^+CD34^+Flt3^+M\text{-}CSFR^+$ cells, which are quite similar cell surface maker expression with mouse CDP. Interestingly, these cells gave rise to only conventional DC *in vitro*. Thus, humanized mice system is very useful to identified human DC progenitors.

Keywords: Humanized mice, progenitor, dendritic cell, Flt3, M-CSF receptor

Introduction

In the mouse lymphoid organ, resident dendritic cell (DC) sub-divided into two subsets such as plasmacytoid DC (pDC) and conventional DC (cDC)[1]. It has not been clear whether these two DC subsets are derived from common progenitor or different progenitors. We have identified mouse common DC progenitor (CDP) from bone marrow based on the expression of Flt3 and M-CSF receptor, which are important cytokine receptor for DC development. CDP gave rise to pDC and cDC but not other lineage cells, both *in vitro* as single cell level and *in vivo* as population level[2]. Quantitative RT-PCR analysis revealed that CDP highly expressed DC development affiliated genes, which have been shown by us previously[3]. Thus, based on these results, we conclude that mouse pDC and cDC are mainly derived from CDP in the bone marrow[2]. While the origin, DC progenitors, and developmental pathway of human DC subset are not clear. Because it is very difficult to collect human sample for using experiments. Most of studies about human DC subsets have been done by using pDC and cDC directly isolated from peripheral blood, or *ex vivo* culture system using $CD34^+$ cells. To solve this problem, we used humanized mice system, which are reconstituted human hematopoiesis by transplanting $CD34^+$ human stem cell fraction into sub-lethally irradiated immunodeficiency mice (NOG mice). Using these humanized mice, we try to identified the mouse CDP counterpart in the humanized mice, and clarify human DC developmental pathway.

Results

1) For generating humanized mice, human $CD34^+$ cells are isolated from cord blood derived from healthy. The lineage negative cell fractions are purified from cord blood using combination of PE-Cy5-lebaed lineage antibodies staining and Cy5 micro-beads, and AutoMACS. After pre-enrichment of lineage negative cells, $CD34^+CD3^-lin^-$ cells are highly purified using cell sorter.
2) $1x10^5$ cells of $CD34^+CD3^-lin^-$ cells are transplanted into sub-lethally irradiated NOG mice intravenously. These transplanted mice are maintained SPF conditions.
3) 8 weeks after transplantation, 20~25% of human $CD45^+$ cells were detected in peripheral blood of transplanted mice (data not shown). These human $CD45^+$ cells are include $CD19^+$ B cells, $CD33^+$ myeloid cells, gp-41^+ erythroid cells, and some $CD3^+$ T cells (data not shown).
4) The human pDC ($CD123^+CD11c^-$) and cDC ($CD123^+CD11c^-$) subsets are detected in PB of humanized mice.
5) In the bone marrow of humanized mice, over 75% of cells expressed human CD45, suggest that very nice reconstitution is established in humanized mice.
   In lineage negative fraction, $CD34^+CD38^{int}$ and $CD34^+CD38^+$ cells, which are long-term hematopoietic stem cells, and multi-potent progenitor cells, respectively. In the MPP cell fraction, we found $Flt3^+$M-$CSFR^+$ cells which are quite similar cell surface maker expression with murine CDP(Fig.A)

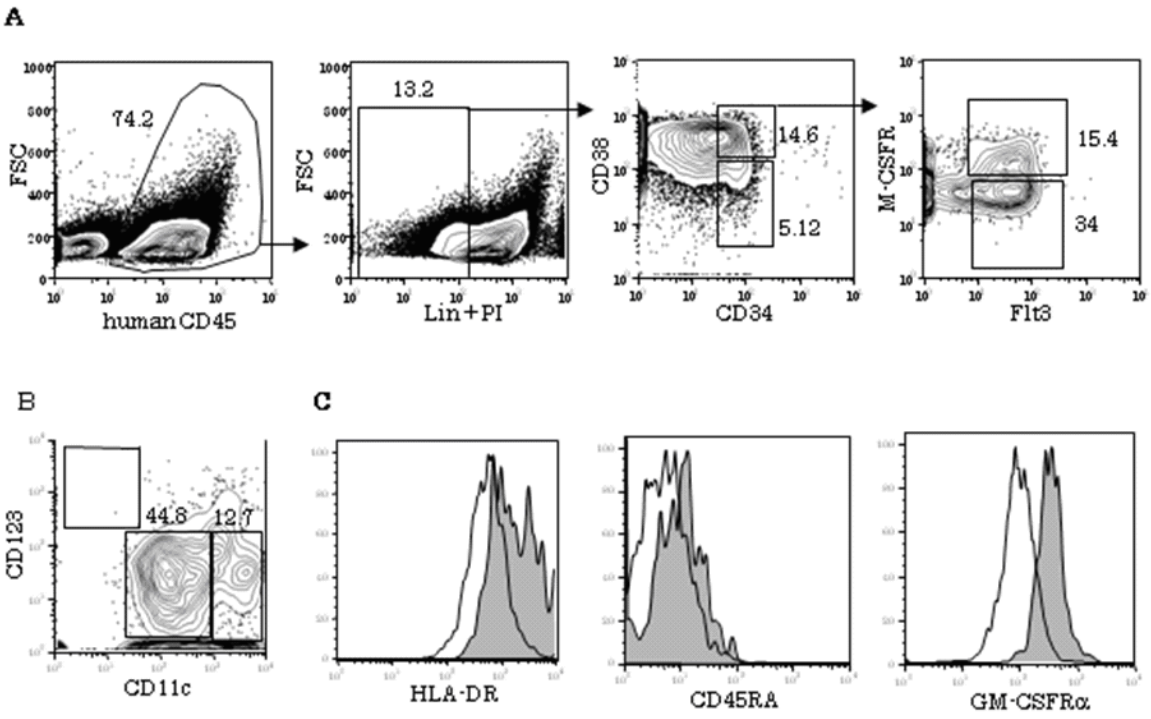

Figure Identification of human DC progenitor in bone marrow of humanized mice.
A) Lin^- cells from $CD45^+$ human cells, are divided by CD34 and CD38.
   $Lin^-CD34^+CD38^+$ cells faction contained $Flt3^+$M-$CSFR^+$, and Flt3+M-$CSFR^-$ cells factions.
B) Sorted $Flt3^+$M-$CSFR^+$ cells are co-cultured with mouse stromal cells Ac-6 + human Flt3-ligand for 12 days.
   These cells differentiate into $CD11c^+CD123^-$ cDCs.
C) $CD11c^{hight}CD123^-$ cDCs and $CD11c^{int}CD123^-$ cDCs are expressed cDC makers, HLA-DR and GM-CSFRα.

6) lin-$CD34^+CD38^+Flt3^+$M-$CSFR^+$ cells are sort out, and cultured in mouse stromal cells :Flt3-ligand for 12 days. These cells gave rise to only cDC ($CD123^+CD11c^-$) but not pDC ($CD123^+CD11c^-$). In cDC cells derived from these cell, included two cDC fraction, $CD11c^{high}$ and $CD11c^{int}$ (Fig. B). $CD11c^{high}$ cells are mature DC, since these cells showed higher expression of cDC maker such as HLA-DR and GM-CSFRα than those in CD11cint cells (Fig.C). Thus, human lin-$CD34^+CD38^+Flt3^+$M-$CSFR^+$ cells gave rise to cDC, but not pDC *in vitro*.

Discussion & Conclusion

In this study, we established humanized mice which are transplanted human $CD34^+$ stem cell fraction from cord blood into immunodeficiency NOG mice, and try to identify human DC progenitor cells in the bone marrow. 8 weeks after transplantation, we detected very nice reconstitution of human hematopoiesis in PB and bone marrow. In the PB, $CD19^+$ B cells, $CD33^+$ myeloid cells, gp-41^+ erythroid cells, pDC ($CD123^+CD11c^-$), cDC ($CD123^+CD11c^-$) subsets and some $CD3^+$ T cells are detected in the mice. These results indicated that human hematopoiesis is reconstituted in the NOG mice, and humanized mice are optimal system for human hematopoiesis *in vivo*. Furthermore, we detected $lin^-CD34^+CD38^+Flt3^+$M-$CSFR^+$ cells, which are similar, cell surface maker expression with murine CDP. These cells gave rise to only cDC but not pDC *in vitro*. These results are different with murine CDP, since murine CDP gave rise to both pDC and cDC *in vitro* as well as *in vivo*. To identify human common DC progenitor , it would be better combined staining other cell surface maker such as CD123 (IL3 receptor) and CD116 (GM-CSFRα), since both cytokines are important human DC development. Now we are preparing the manuscript of these results[4].

References

1) Shortman, K., and S.H. Naik. Steady-state and inflammation dendritic cell development. *Nat. Rev. Immunol.*7:19-30, 2007.

2) Onai, N., Obata-Onai, A., Schmid, M.A., Ohteki, T., Jarrossay, D., and Manz, M.G. Identification of clonogenic common $Flt3^+$M-$CSFR^+$ plasmacytoid and conventional dendritic cell progenitors in mouse bone marrow. *Nat. Immunol.*, 8, 1207-1216, 2007.

3) Onai, N., Obata-Onai, A., Tussiwand, R., Lanzavecchia, A., and Manz, M.G. Activation of the Flt3 signal transduction cascade rescues and enhances type I interferon-producing and dendritic cell development. *J. Exp. Med.*, 203, 227-238, 2006.

4) Onai, N., Kurabayashi, K., Hosoi, M., and Ohteki, T. Perspective isolation of human DC progenitor using humanized mice. (in preparation).

Research of tumorigenesis and invasion/metastasis mediated by small GTPase Ral

Hisanori Horiuchi
Institute of Development, Aging and Cancer, Tohoku University
horiuchi@idac.tohoku.ac.jp

Abstract

Reduced expression of RalGAPα2 promoted the invasion and metastasis of urothelial cancer.

A gelsolin family protein, Fli-I promoted formin-induced actin assembly in collaboration with RhoA.

Keywords: Bladder cancer, Ral, GAP, actin, rho, mDia1, Fli-I

Introduction

Ral small GTPase plays a critical role in the invasion and metastasis of cancer. Pal is activated by Ral guanine nucleotide exchange factors (GEFs) and inactivated by Ral GTPase-activating proteins (GAPs), heterodimers of a catalytic α1 or α2 subunit and a common β subunit.

Actin reorganization is important tumor invasion and metastasis, where small GTPase Rho and its effector formin, such as mDia1 and DAAM1, play critical roles.

Results

We found that Ral is highly activated in invasive urothelial cancer cells due to reduced expression of the RalGAPα2 subunit. We are extensively investigating the role of RalGAP as a tumor progression suppressor.

We identified a gelsolin family protein, Fli-I as a binding partner of Daam1 and showed its function in the formin-induced actin assembly regulated by RhoA.

Discussion & Conclusion

RalGAPα2 might play an important role in the invasion and metastasis of urothelial cancer.

A gelsolin family protein, Fli-I plays a critical role in formin-induced actin assembly.

References

T. Higashi, T. Ikeda, T. Murakami, R. Shirakawa, M. Kawato, K. Okawa, M. Furuse, T. Kimura, T. Kita, H. Horiuchi* (2010) Flightless-I (Fli-I) regulates the actin assembly activity of Diaphanous-related formins (DRFs), Daam1 and mDia1, in cooperation with active Rho GTPase. *J Biol Chem.* 285, 16231-16238

Hepatic fatty acid profile relates to inflammation and fibrosis in nonalcoholic steatohepatitis

Tsuguhito Ota
Frontier Science Organization, Kanazawa University
tota@staff.kanazawa-u.ac.jp

Abstract

To delineate the hepatic fatty acid (FA) compositions which are specific to NASH and simple steatosis, we examined the profile of long chain FAs in the liver of NAFLD in mice by gas chromatography. We found that normal liver, simple steatosis and NASH showed significant differences in FA content and composition in the liver of mice. Importantly, these changes in hepatic FA profiles are associated with the progression of NAFLD/NASH and whole-body insulin resistance.

Keywords: NASH, NAFLD, fatty acid, insulin resistance

Introduction

Insulin resistance is crucially involved in the development of nonalcoholic steatohepatitis (NASH). We have demonstrated that insulin resistance accelerates the pathology of NASH in genetically and diet-induced obese rodents (Gastroenterology 132:282, 2007; Hepatology 46:1392,2007). These studies clearly showed that fatty acid (FA)-induced insulin resistance leads to the progression of hepatic inflammation and fibrosis. In the present study, we clarified the profile of long chain FAs in the liver of nonalcoholic fatty liver disease (NAFLD) and examined the association between insulin sensitivity, histological features, and FA profiles in the liver of NAFLD mice.

Results

NAFLD was divided into simple steatosis (SS) and steatohepatitis (SH). We used the liver of genetically (ob/ob) and high fat (HF) diet-induced obese (DIO) mice as an SS model. As an SH model, the liver from methionine choline deficient and HF (MCF) diet-induced NASH, and cholesterol and HF (CL+HF) diet-induced NASH mice were studied. Normal liver (NL) from C57Bl/6 wild type mice used as controls. FAs were extracted from liver tissue by a modification of the method of Folch, and their content per mg of wet liver tissue was determined by gas chromatography.

The content of most fatty acids were significantly higher in the SS and SH than in the NL mice. Because the content of C16:0 was highest in the liver of all the groups, we compared the ratio of each FA to C16:0 between NL, SS, and SH. The ratio of C18:0/C16:0 was higher in the order of SH, SS, and NL groups ($P<0.05$, $n=8$) and this ratio was associated with increased insulin resistance assessed by HOMA-R. In addition, C18:2/C16:0 was markedly higher in the liver of SH than that of SS

(Fig.1). In contrast, C18:1/C16:0 was decreased in the order of SH, SS, and NL groups. The ratio of C18:1/C16:0 was decreased in SH group with hepatocellular ballooning and advanced inflammation and fibrosis. These histological changes were associated with decreased mRNA expression of fibrogenesis (TGF-b, type 1 collagen) and TNF-a. The C16:1/C16:0 was similar between NL, SS, and SH groups.

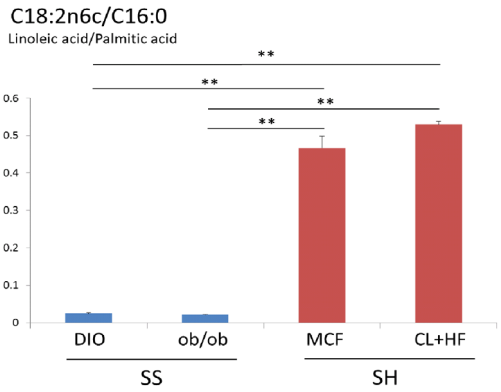

Fig.1

Discussion & Conclusion

The NL, SS, and NASH had markedly different FA content and composition in the liver of mice. These changes in hepatic FA profiles were associated with the progression of NAFLD/NASH and whole-body insulin resistance. We plan clarify the hepatic FA profile in the patients with liver biopsy-proven 80 NAFLD including 50 with SS and 30 with SH. By comparing the results between human and animal studies, we will delineate the hepatic FA compositions specific to NASH and SS.

References

1) Ota T, Takamura T, Kurita S, Matsuzawa N, Kita Y, Uno M, Akahori H, Misu H, Sakurai M, Zen Y, Nakanuma Y, Kaneko S: Insulin resistance accelerates a dietary rat model of nonalcoholic steatohepatitis. *Gastroenterology* 132:282-293, 2007

2) Matsuzawa N, Takamura T, Kurita S, Misu H, Ota T, Ando H, Yokoyama M, Honda M, Zen Y, Nakanuma Y, Miyamoto K, Kaneko S: Lipid-induced oxidative stress causes steatohepatitis in mice fed an atherogenic diet. *Hepatology* 46:1392-1403, 2007

Analysis of the role of CD317/tetherin, inhibitor of virus budding, in the whole body

Shoichiro Miyatake
Tokyo Metropolitan Institute of Medical Science
Miyatake-si@igakuken.or.jp

Abstract

CD317/tetherin deficient mouse was established. pDCs derived from CD317/tetherin deficient mice produced elevated level of typeI IFN upon stimulation, suggesting that CD317/tetherin transmits suppressive signal on typeI IFN induction. CD317/tetherin is involved in the antigen presentation activity of both MHC I and MHC II restricted antigens.

Keywords: CD317, tetherin, cytokine, dendritic cell

Introduction

CD317/tetherin is specifically expressed on mouse plasmacytoid dendritic cells (pDC) but not on other hematopoietic cells during the homeostatic state, therefore CD317/tetherin is used as a specific marker for mouse pDC. In addition CD317/tetherin is induced on various cell types by typeI or typeII IFN. Ab against CD317/tetherin suppressed typeI IFN production of the activated pDC, suggesting the presence of ligands for CD317/tetherin and their role in typeI IFN production. CD317/tetherin inhibits virus release from cells by tethering viruses such as HIV or Ebola virus on the plasma membrane when the viruses bud from cells. Most of its effects on viruses were revealed by the experiments utilizing human cell lines. To elucidate the role of this molecule in the whole body and in immune responses against pathogens or cancer cells, a mouse carrying the CD317/tetherin gene flanked by loxP recognition elements for Cre recombinase (floxed allele) was created.

Results

Germline disruption of CD317/tetherin gene did not affect mouse development. CD317/tetherin deficient mice (-/-) appeared normal at birth, developed as well as their control littermates and were fertile.

The number of pDC isolated from -/-

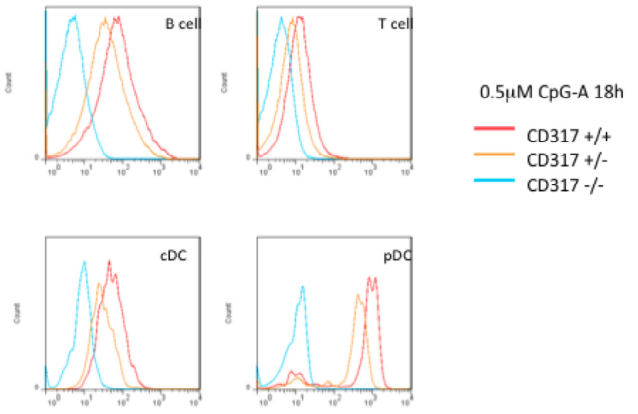

Figure
CD317/tetherin was not detected on various cells derived from -/- mice. Spleen cells prepared from litter control(+/+), +/- or -/- mouse were stimulated with 0.5 M CpG-A for 18h. CD317/tetherin expression on B cells, T cells, cDC and pDC were analyzed by flow cytometry. CD317/tetherin was not detected on cells derived from -/- mouse. The CD317/tetherin expression (Mean Fluorescence Intensity) of cells derived from +/- mouse was less than half of that of litter control.

mice was comparable to that of the litter control. CD317/tetherin was not detected on the pDC of -/- mouse identified by the expression of B220 and CD11c (Figure). The expression level of CD317/tetherin on pDC of heterozygous (+/-) mice was less than half of that of the litter control.

pDCs derived from -/- or litter control mice were stimulated with TLR9 ligand CpG or H1N1 influenza virus (PR8). The level of typeI IFN produced by pDC derived from -/- mice was more elevated than that from the litter control. As expected, when pDCs were stimulated by CpG or influenza virus in the presence of anti-CD317/tetherin Ab, typeI IFN production by pDC of the litter control but not -/- mice was suppressed.

Conventional DC (cDC) was prepared from -/- or litter control mice as Ag presenting cells. CD4+ T cells from OT-2 mice or CD8+ T cells from OT-1 mice were prepared for responder T cells. As antigen OVA protein or antigenic peptide derived from OVA was used. The Ag presentation activity to either OT-1 or OT-2 T cells was reduced when cDC was derived from -/- mice.

Discussion & Conclusion

Since CD317/tetherin disrupted mice were born without defects, grow healthy and fertile, CD317/tetherin is not required for normal development and reproduction. CD317/tetherin deficient pDC produced elevated level of typeI IFN compared to wild type pDC, suggesting that CD317/tetherin delivers some signal that suppresses typeI IFN production of pDC. pDCs used in this experiment were enriched but not nearly 100% pure, thus the possibility of the requirement of any ligand molecules expressed on other cell types for this suppressive effect was not eliminated. There are no putative signaling motifs in the cytoplasmic region of CD317/tetherin, and the signaling pathways that CD317/tetherin may utilize are totally unknown.

CD317/tetherin contributes to the Ag presentation activity of cDC. Both MHC II restricted Ag presentation and MHC I restricted cross presentation activity were affected by the absence of CD317/tetherin. CD317/tetherin is present not only on the cell surface but also in the endosome. One possible site of its action is Ag uptake and processing in lysosomes. Since crosspresentation was affected, critical machinery for the crosspresentation, retrotranslocon might be affected by CD317/tetherin.

Driving mechanisms for axon guidance: studies on asymmetric membrane dynamics in the growth cone

Hiroyuki Kamiguchi
RIKEN Brain Science Institute
Kamiguchi@brain.riken.jp

Abstract

An extending axon in the developing nervous system is tipped by a growth cone, a highly motile structure that can translate extracellular guidance information into directed migration along the correct path. In this project, I found that guidance cues repel growth cones via clathrin-mediated endocytosis. Also, an intracellular signal transduction cascade has been identified that links guidance cues to clathrin-mediated endocytosis: influx of calcium ions from the extracellular space followed by calcineurin activation. These results demonstrate for the first time that repulsive axon guidance is driven by polarized membrane trafficking in the growth cone.

Keywords: Axon; Growth cone; Guidance; Calcium; Calcineurin; Clathrin; Endocytosis

Introduction

The formation of functional neuronal circuits relies on the spatial accuracy of axon extension. The tip of each extending axon, a growth cone, recognizes molecular "guidance cues" in its microenvironment and navigates the axon along the correct path. When a growth cone migrates in a guidance cue gradient, the cue binds its receptor preferentially on the side of the growth cone facing higher concentrations of the cue. This asymmetric receptor occupancy polarizes the growth cone for turning either toward increasing concentrations of the cue (attraction) or away from the cue (repulsion), via intracellular generation of Ca^{2+} signals. Ca^{2+} release from the endoplasmic reticulum mediates growth cone turning toward the side with elevated Ca^{2+}, whereas Ca^{2+} influx across the plasma membrane mediates repulsive turning if unaccompanied by secondary Ca^{2+} release from the endoplasmic reticulum (Ooashi et al., 2005; Tojima et al., 2009; Akiyama et al., 2009; Tojima et al., 2011). We have previously reported that attractive Ca^{2+} signals cause growth cone turning by facilitating centrifugal transport of membrane vesicles and exocytosis ensuing in the growth cone periphery (Tojima et al., 2007; Akiyama and Kamiguchi 2010). However, signaling and driving mechanisms underlying repulsive axon guidance have remained unclear. Here I report how repulsive Ca^{2+} signals mediate growth cone turning.

Results

Dissociated cultures of dorsal root ganglion neurons derived from chicken embryos were used in this study. Clathrin-mediated endocytosis in live growth cones was visualized by total internal reflection fluorescence imaging of clathrin and dynamin. When repulsive Ca^{2+} signals were

generated by UV-induced photolysis of caged Ca^{2+} on one side of the growth cone, the formation of clathrin-coated pits was facilitated only on the side with elevated Ca^{2+}. Similarly, directional application of repulsive guidance cues such as Semaphorin 3A caused asymmetric facilitation of clathrin-mediated endocytosis. Such Ca^{2+}-elicited facilitation of clathrin-mediated endocytosis required the activity of calcineurin that can dephosphorylate and activate endocytic-adaptor proteins. In contrast, attractive Ca^{2+} signals did not influence the frequency of clathrin-mediated endocytosis. Pharmacological or genetic Inhibition of clathrin-mediated endocytosis abolished growth cone repulsion, but not attraction, induced by Ca^{2+} or extracellular physiological cues. Intriguingly, growth cone repulsion by Semaphorin 3A or myelin-associated glycoprotein was converted to attraction after inhibition of clathrin-mediated endocytosis, and this attraction was blocked by tetanus neurotoxin that blocks vesicle-associated membrane protein 2 (VAMP2)-dependent exocytosis. This result suggests that guidance cues can evoke both endocytosis and exocytosis, the balance of which determines the turning direction. Furthermore, we showed that asymmetric perturbation of the balance of endocytosis and exocytosis in the growth cone was sufficient to initiate its turning toward the side with less endocytosis or more exocytosis.

To gain insight into mechanisms of how asymmetric endocytosis drives growth cone turning, we estimated the area of plasma membrane that was removed asymmetrically from the growth cone surface in response to Semaphorin 3A gradients. The number of newly formed clathrin-coated pits in these growth cones after Semaphorin 3A application was $0.78 \pm 0.11/\mu m^2$/min on near sides and 0.38 ± 0.06 /μm^2/min on far sides (mean ± SEM; n = 7 growth cones). Assuming the diameter of clathrin-coated pits to be 120 nm, the difference in the area of membrane removal between the near and far sides would be 0.018 μm^2 per 1-μm^2 growth cone area (1.8%) every minute, therefore the cumulative difference during the course of growth cone turning (40 min) would correspond to 72%. This estimation suggests that clathrin-mediated endocytosis can generate a substantial asymmetry in membrane removal across the growth cone during repulsive guidance.

Discussion & Conclusion

In conclusion, the present and previous (Tojima et al., 2007) studies demonstrate that growth cone repulsion and attraction involve preferential removal and addition of plasma membrane components of the growth cone on the side with elevated Ca^{2+}, respectively, and that the balance between these counteractive events may determine the directional polarity of axon guidance (Itofusa and Kamiguchi 2011).

References

1) Akiyama H, Kamiguchi H: *J Biol Chem* 285: 41740-41748, 2010
2) Akiyama H, Matsu-ura T, Mikoshiba K, Kamiguchi H: *Sci Signal* 2: ra34, 2009
3) Itofusa R, Kamiguchi H: *Mol Cell Neurosci* (in press)
4) Ooashi N, Futatsugi A, Yoshihara F, Mikoshiba K, Kamiguchi H: *J Cell Biol* 170: 1159-1167, 2005

5) Tojima T, Itofusa R, Kamiguchi H: *Neuron* 66: 370-377, 2010
6) Tojima T, Itofusa R, Kamiguchi H: *J Neurosci* 29: 7886-7897, 2009
7) Tojima T, Hines JH, Henley JR, Kamiguchi H: *Nat Rev Neurosci* 12: 191-203, 2011

Mechanism of pathogenesis by human T-cell leukemia virus type 1

Masao Matsuoka
Institute for Virus Research, Kyoto University
mmatsuok@virus.kyoto-u.ac.jp

Abstract

Human T-cell leukemia virus type 1 (HTLV-1) causes adult T-cell leukemia (ATL) and HTLV-1 associated myelopathy (HAM). The *HTLV-1 bZIP factor* (*HBZ*) gene, which is encoded by the minus strand of the provirus, is expressed in all ATL cases and promotes proliferation of ATL cells. Recently, we have reported that HBZ expression causes T-cell lymphomas and inflammatory diseases, which are very similar to HTLV-1 infection. In HBZ expressing transgenic mice, and HTLV-1 carriers, regulatory T cells increase. As a mechanism, we found that HBZ enhanced TGF-b signaling via interaction with Smad2/3 and p300. This activity of HBZ enhanced transcription of Foxp3 gene, which accounts for increased regulatory T cells in HBZ expressing cells. ATL patients and HTLV-1 infected individuals succumb to opportunistic infections due to impaired cell-mediated immunity. However, the mechanism of immunodeficiency remains to be solved. We found that HBZ-transgenic mice were susceptible to herpes simplex type 2 (HSV-2) and Listeria infection. Production of interferon-g (IFN-g) was hindered in CD4+ T cells. HBZ interacted with NFAT and c-Jun, and inhibited DNA binding of these transcription factors to the promoter region of the IFN-g gene. HBZ mediated inhibition of IFN-g is a possible mechanism of immunodeficiency caused by HTLV-1 infection. Thus, HBZ plays an important role in pathogenesis by HTLV-1.

Keywords: HTLV-1, ATL, HBZ, Foxp3, regulatory T cell

Introduction

Human T-cell leukemia virus type 1 (HTLV-1) is a causal agent of adult T-cell leukemia (ATL) and inflammatory diseases including HTLV-1 associated myelopathy (HAM).[1] HTLV-1 causes ATL after a long latent period. HTLV-1 has regulatory genes (tax and rex) and accessory genes (p12, p13, p30, and HBZ). After discovery of HTLV-1, many studies suggest that Tax plays critical roles in pathogenesis of HTLV-1. However, we found that Tax expression was not detected in about 60% of ATL cases.[2] We identified three mechanisms to inactivate Tax expression in vivo: 1) nonsense mutation, deletion and insertion of tax gene, 2) DNA methylation of 5' long terminal repeat (LTR) and 3) deletion of 5'LTR. However, HTLV-1 bZIP factor (HBZ) gene remains intact in all ATL cases, indicating the importance of HBZ gene in ATL cells. We have reported that the HBZ gene is expressed in all ATL cases, and HBZ promotes proliferation of ATL cells.[3] Recently, we have reported that transgenic expression of HBZ causes T-cell lymphomas and inflammatory diseases in the mice.[4] These data show that HBZ is a responsible gene for pathogenesis by HTLV-1. In HBZ-

transgenic (HBZ-Tg) mice, the number of regulatory T cells increases. We found that HBZ enhanced transcription of Foxp3 gene in T cells, resulting in increased regulatory T cells. However, precise mechanism remains unsolved.

ATL and HTLV-1 carriers frequently succumb to opportunistic infections caused by fungus, virus and bacteria. In these patients, cell mediated immunity is impaired. However, its mechanism remains unknown. HBZ is expressed in all ATL cases and HTLV-1 carriers, indicating the association with immunodeficiency caused by HTLV-1. We used HBZ-Tg mice that express sHBZ in CD4 T cells and studied well-established infection models of two pathogens. The first model involves intravaginal viral infection with herpes simplex virus type-2 (HSV-2). Interferon-γ(IFN-γ production by CD4 T cells is critical for the exclusion of HSV-2 from the host. The other model involves infection with the Gram-positive intracellular bacterium, *Listeria monocytogenes* (LM), which is known as an opportunistic pathogen. In LM infection, CD4 T cells play pivotal roles in the acquired immune response by producing IFN-γ and inducing the activation of macrophages, which eliminate LM by phagocytosis and subsequent bactericidal activity.

Results

1) Effect of HBZ on TGF-b signaling

Vector expressing HBZ was transfected into HepG2 cells and then transfected cells were treated with TGF-β. HBZ enhanced TGF-β signaling (Figure 1). Physiological level of HBZ could rescue the repressed TGF-b responses by Tax.

2) Mechanism how HBZ enhances TGF-b signaling.

We checked binding of HBZ with Smad proteins using immunoprecipitation assay, and found that HBZ physically interacted with Smad2/3 (Figure 2), and colocalized with Smad3 protein in the nucleus.

3) Detailed interaction between Smad and p300

HBZ enhanced TGF-β signaling through its N-terminal LXXLL motif, while C-terminal MH2 domain of Smad3 was essential for interacting with HBZ. HBZ protein enhances TGF-β signaling in a p300 dependent manner. HBZ formed a ternary complex with Smad3 and p300 (Figure 3), and enhanced Smad3-p300 interaction.

4) Effects of HBZ enhanced TGF-b signaling

By expression HBZ in naïve T cells, HBZ enhanced the transcription of *PDGFB*, *SOX4*, CTGF, *FOXP3*, *RUNX1*, *TSC22D1* genes and suppressed the *ID2* gene expression; such effects were similar to those by TGF-β. HBZ enhanced Foxp3 expression in mouse and human naïve T cells (Figure 4). HBZ activated *Foxp3* enhancer activity through its Smad binding site. HBZ was recruited to the *Foxp3* enhancer through forming a complex with Smad3 and p300.

5) Susceptibility of HBZ-Tg mice to HSV-2

In the primary infection assay, we found no significant difference in the viral titers between non-Tg and HBZ-Tg mice at day 2 after inoculation, when innate immunity is responsible for the host

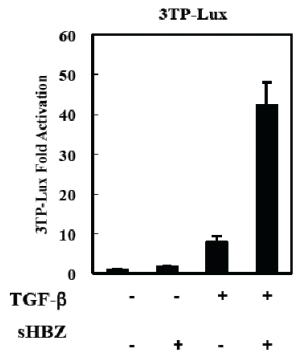

Figure 1. Enhancement of TGF-β signaling by HBZ

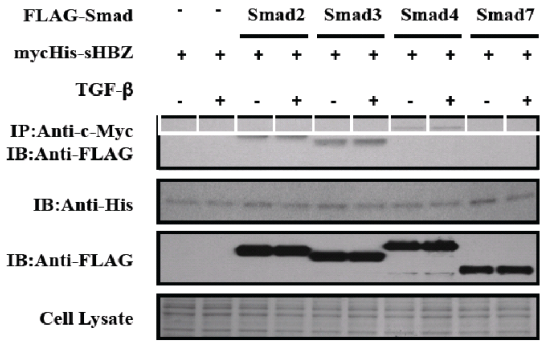

Figure 2. Interaction of HBZ with Smad proteins

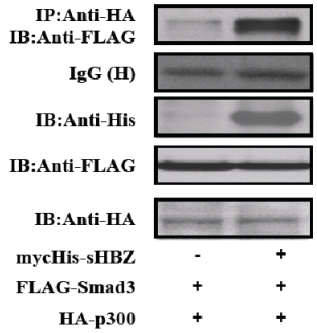

Figure 3. Ternary complex formation of HBZ, Smad3, and p300

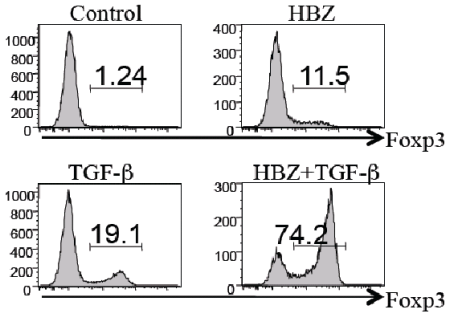

Figure 4. Enhanced expression of Foxp3 by HBZ

defense. In contrast, at day 6 post-infection, when acquired immunity becomes important, HBZ-Tg mice showed significantly higher viral titers of HSV-2 than non-Tg mice. In CD4+ T cells of HBZ-Tg mice, productions of IFN-γ, TNF-α, and IL-2 were suppressed.

6) Susceptibility of HBZ-Tg to Listreria infection

The number of LM recovered from HBZ-Tg spleen on day 2 was comparable to that from non-Tg mice, yet the bacterial burden in HBZ-Tg mice at day 5 was higher than that in non-Tg mice, suggesting a reduced protection in HBZ-Tg mice against LM, especially when acquired immunity is being established.

7) Mechanism of HBZ mediated suppression on IFN-g production

We found that HBZ suppressed transcription from the promoter of IFN-γ. Deletion and mutation analyses of the promoter showed that NFAT and AP-1 binding sites were responsible for suppressive effects of HBZ. HBZ can interact with NFAT and c-Jun. Chromatin immunoprecipitation assay revealed that HBZ inhibited DNA binding of NFAT and c-Jun to the promoter of IFN-γ gene.

Discussion & Conclusion

FoxP3 was detected in two thirds of ATL cases, and FoxP3+ regulatory T cells were increased in HTLV-1 infected individuals. These reports suggest that ATL is a leukemia of regulatory T cells, and HTLV-1 infects regulatory T cells. We have reported that HBZ expression induces transcription of Foxp3 gene, indicating that HBZ plays a central role in phenotype of regulatory T cells in ATL

cells. This study revealed the detailed mechanism how HBZ induces transcription of Foxp3 gene. HBZ can bind to Smad2/3 and p300, resulting in activation of TGF-β signaling. Transcriptions of other cellular genes activated by TGF-β were also enhanced by HBZ expression.

Previous studies have reported that Tax suppresses TGF-β signaling. In contrast, this study showed that HBZ enhanced TGF-β signaling. This study showed that enhancing activity by HBZ was predominant to suppressive effects by Tax.

It is well known that ATL patients are complicated with opportunistic infections like AIDS patients. One possible reason is increased regulatory T cells. This study first reported that HBZ was implicated in immunodeficiency caused by HTLV-1. HBZ directly interacts with NFAT and c-Jun, and hinders DNA binding of these transcription factors.

As shown in this study, HBZ has pleiotropic functions for pathogenesis by HTLV-1. Further studies will disclose detailed mechanism of HBZ mediated pathogenesis.

References

1) Matsuoka M, Jeang KT. Human T-cell leukaemia virus type 1 (HTLV-1) infectivity and cellular transformation. *Nat Rev Cancer*. 2007;7(4):270-280.
2) Takeda S, Maeda M, Morikawa S, et al. Genetic and epigenetic inactivation of tax gene in adult T-cell leukemia cells. *Int J Cancer*. 2004;109(4):559-567.
3) Satou Y, Yasunaga J, Yoshida M, Matsuoka M. HTLV-I basic leucine zipper factor gene mRNA supports proliferation of adult T cell leukemia cells. *Proc Natl Acad Sci U S A*. 2006;103(3):720-725.
4) Satou Y, Yasunaga J, Zhao T, et al. HTLV-1 bZIP Factor Induces T-Cell Lymphoma and Systemic Inflammation In Vivo. *PLoS Pathog*. 2011;7(2):e1001274.

Development of chemical fragmentation method for glycan sequencing

Shunji Natsuka
Niigata University
natsuka@bio.sc.niigata-u.ac.jp

Abstract

Micro-heterogeneity is a fundamental character of glycans. The structural variation mainly bears on non-reducing ends of the glycans. In vertebrates, *N*-acetyllactosamine structure and its relatives with various modifications are responsible to the variation of the non-reducing ends. We developed analytical method for the non-reducing end units. Acetyl residue on *N*-acetylglucosamine was removed under alkaline condition, and then non-reducing end units were torn by deamination reaction with nitrite. The newly appeared reducing end, which was 2,5-anhydromannose converted from *N*-acetylglucosamine, was tagged with 2-aminopyridine to become fluorescent. The pyridylamino (PA-) glycans derived from non-reducing ends were separated and analyzed with size-fractionation and reversed phase HPLCs. We optimized and fixed the reaction conditions for the preparation steps of the PA-non-reducing end units.

Keywords: Carbohydrate sequence, Nitrous deamination, HPLC mapping

Introduction

Development of the sequencing techniques (i.e. the Edman method for protein and the Sanger method for DNA) has expanded the research of these biomolecules. Although the importance of the glycan molecules is pointed out, a general spread of the glycan research is relatively small as compared with that of protein or DNA. The major cause of that is in the absence of a sequencing technique of the glycans. In this research, I built a new glycan-analytical method which combined glycan-fragmentation and sensitive separation. This method can expect to develop into the sequencing technique of the glycans.

Sample (PA-glycan mixture, etc.)
↓ deacetylation
100 μl of 1 M NaOH, 90°C, 15 h
↓ purification by GL-Pak Carbograph
↓ lyophilization
↓ deamination
8 μl of 0.2 M $NaNO_2$, 2 μl of AcOH, on ice, 60 min
↓ pyridylamination
coupling: 10 μl of PA reagent, room temp., 30 min
reduction: 70 μl of reduction reagent, 60°C, 30 min
↓ co-evaporation with toluene/methanol, 60°C, 10 min, 5 times
↓ purification by GL-Pak Carbograph
↓ lyophilization
Pyridylaminated fragments
↓ 1st HPLC: Size-Fractionation HPLC
Column: TSKgel Amide-80, 0.46 x 7.5 cm
Solvent: 50 mM $HCOONH_4$, pH4.4 – CH_3CN
Flow rate: 0.5 ml / min
↓ 2nd HPLC: Reversed phase HPLC
Column: TSKgel ODS-80Ts, 0.46 x 15 cm
Solvent: 50 mM AcOTEA, pH6.0 – n-BuOH
Flow rate: 1.0 ml / min

Scheme. Fixed condition of the analytical method for glycans

Results

The acetyl groups on pyridylaminated glycans were removed by heating under strong basic condition, and then the glycans were cleaved at the reducting end of amino sugars by nitrite deamination. As a strong base, sodium hydroxide, potassium hydroxide, and hydrazine were examined under several conditions. The condition of deamination reaction was examined with various times and temperatures. From results of those experiments, optimum condition was fixed as followed: de-acetylation with1M NaOH at 90ºC for 15 h, and deamination with 0.2 M $NaNO_2$ on ice for 60 min. The amino sugars at the cleaving site were converted into 2,5-anhydro sugars. Pyridylamino residue was tagged to the 2,5-anhydro sugar for fluorescence-labeling of generated fragments. An aldehyde of 2,5-anhydro sugar is more reactive than the aldehyde of common sugars, which is hemiacetal. Thus, authentic condition (1) for pyridylamination was not suitable for this case, and I re-examined the pyridylamination condition. As a result, optimum condition was fixed as followed: tagging reaction with PA-reagent at room temperature for 30 min, and reduction reaction at 60 ºC for 30 min.

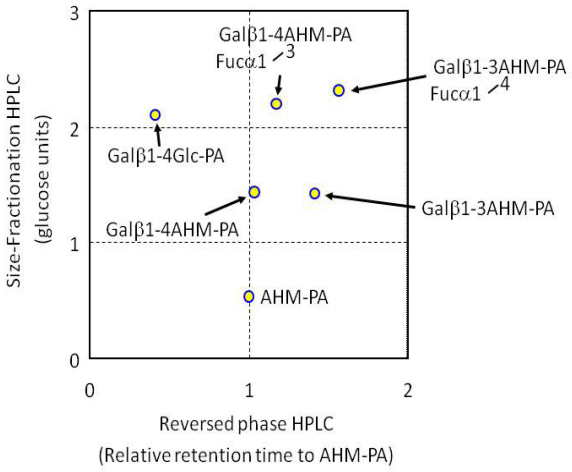

Figure. Example of two-dimensional HPLC map of glycan fragments.

The labeled fragments were separated by two modes of HPLCs, and analyzed by two dimensional HPLC map method. The conditions of the HPLCs were fixed, and two dimensional HPLC map of the fragments was made.

Discussion & Conclusion

The conditions of de-*N*-acetylation and nitrite deamination were set up for glycan fragmentation. The optimization of the reaction for fluorescence tagging of the fragment was carried out. From those experiments, the conditions for the fragmentation of glycans and the fluorescence labeling were fixed. Moreover, the system for analysis of the prepared fragments with two-dimensional HPLC mapping was established. From now on, the development to a glycan sequencer is aimed by using this technique. On the other hand, this technique has a possibility of becoming a new method of screening glycan biomarkesr.

References

1) Shunji Natsuka, Sumihiro Hase. Analysis of *N*- and *O*-glycans by pyridylamination. In *Method in Molecular Biology*, *Vol. 76: Glycoanalysis Protocols* (Hounsell,E.F. ed) Humana Press Inc. pp101-113 (1998).

2) Sumihiro Hase, Shunji Natsuka, Hisashi Oku, Tokuji Ikenaka. Identification method for twelve oligomannose-type sugar chains thought to be processing intermediates of glycoproteins. *Analytical Biochemistry*, **167**, (2) 321-326 (1987).

Development of the direct arylation of C-H bonds in nitrogen heteroaromatics

Mamoru Tobisu
Graduate School of Engineering, Osaka University
tobisu@chem.eng.osaka-u.ac.jp

Abstract

We previously reported nickel-catalyzed direct C-2 arylation of pyridine and related N-heteroaromatics using arylzinc reagents. Based on this reaction, C-4 and C-9 arylation of acridine ring system is developed using rhodium and nickel catalysts, respectively.

Keywords: Acridine, Arylation, Zinc, Rhodium, Nickel

Introduction

Electron-deficient heteroaromatics, such as pyridines and quinolines, are privileged scaffolds that occupy a central role in many bioactive or medicinally relevant compounds. Therefore, brilliant methods for their expeditious functionalization are strongly demanded. In this context, arylation reactions, which can directly transform the C-H bonds in pyridines to C-C bonds should represent an efficient and environmentally-friendly method. However, such reactions have not been accomplished, although success has been met for both electron-rich heteroaromatics, such as pyrroles and thiophenes and ones with relatively acidic C-H bonds, such as azoles.

Results

We have previously established a powerful C-H arylation methodology by employing the combination of a nickel-based catalyst and arylzinc reagents (eq 1). This is the first general catalytic method for the regioselective C-H arylation of electron-deficient heteroaromatics. A variety of aryl groups can be introduced into the 2-position of pyridine derivatives.

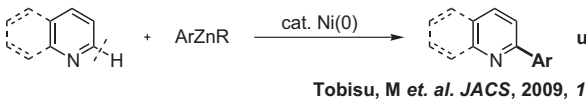

Tobisu, M *et. al. JACS*, 2009, *131*, 12070.

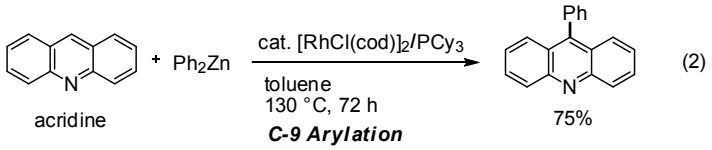

In this study, we applied this catalytic arylation to acridine ring system, in which no hydrogen is present at the 2-position, thus alternation of the regioselectivity is expected. After extensive screening of the catalyst and conditions, we found that arylation

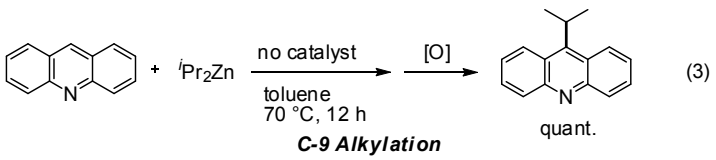

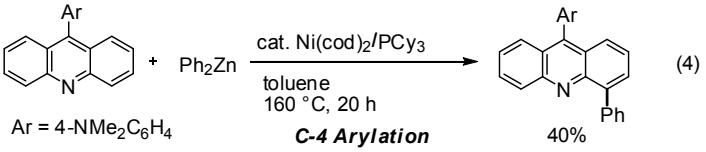

took place at the 9 position exclusively when $[RhCl(cod)]_2$ was used as a catalyst precursor and PCy_3 as a supporting ligand (eq 2). $Cu(OTf)_2$, $FeCl_3$, and $InCl_3$ also exhibited catalytic activity for this C-9 arylation of acridine, although the yields were decreased compared to the rhodium-based catalyst. The quality of the zinc reagents proved to affect the efficiency significantly. When diphenyl zinc prepared from PhMgBr and $ZnCl_2$ was used directly, the yield was dramatically decreased. The use of Mg salt-free zinc reagent is essential.

We next examined the possibility of installing an alkyl substituent onto acridine by using dialkylzinc reagents. Among the zinc reagents examined (Me_2Zn, Et_2Zn, $^iPr_2Zn$), only $^iPr_2Zn$ afforded the expected alkylated product. Interestingly, the addition of $^iPr_2Zn$ proceeded in the absence of any transition-metal catalysts to initially form dearomatized dihydroacridine, which was then converted into an aromatized product by the treatment with suitable oxidizing agents (eq 3).

On the other hand, when acridine was treated with diphenylzinc in the presence of a nickel catalyst, a mixture of C-4 and C-9 arylation product was obtained. By using 9-substituted acridine, C-4 arylation product was selectively synthesized through the nickel-catalyzed reaction (eq 4). Although the yield was modest, the reaction was quite clean and the corresponding amount of the starting material was recovered. Further study is on going to improve the yield of this intriguing C-4 arylation of acridine.

Discussion & Conclusion

Three methods for the regioselective functionalization of acridine have been developed. 1) C-9 arylation by rhodium catalysis, 2) C-9 alkylation without transition metal catalysts, and 3) C-4 arylation by nickel catalysis. By properly choosing the catalyst and conditions, we can directly functionalize the C-H bonds in acridine in a regioselective manner. Most of the reported methods for the direct arylation of heteroaromatics depends on either nucleophilic or acidic reactivity, which limits the applicable substrates to five-membered heterocycles. By contrast, our protocol utilizes the electrophilic reactivity of heterocycles, thus 6-membered substrates, such as pyridines and related heteroarenes are applicable. In the first two reactions (rhodium and no catalyst), the reaction occurs at the most electrophilic C-9 position, exemplifying our reaction design concept. On the other hand, the last reaction catalyzed by nickel delivered C-4 arylated products. This type of selectivity cannot be explained by nucleophilic or electrophilic reactivity. Further study toward the elucidation of the mechanism of this C4-selectivity and synthetic application is currently underway.

References

Nickel-Catalyzed Reaction of Arylzinc Reagents with N-Aromatic Heterocycles: A Straightforward Approach to C-H Bond Arylation of Electron-Deficient Heteroaromatic Compounds
M. Tobisu, I.Hyodo, N. Chatani
J. Am. Chem. Soc. **131**, 12070-12071 (2009).

Self-Defence Mechanism for Natural Toxin-Containing Species

Keiichi Konoki
Graduate School of Agricultural Science, Tohoku University
konoki@biochem.tohoku.ac.jp

Abstract

OABP2 might play a role in self-defense of the sponge *Halichondria okadai*.

Keywords: okadaic acid, secondary metabolite, binding protein, self-defense

Introduction

Physiological roles of secondary metabolites in secondary metabolite-producing or -accumulating species have not been investigated in detail. Okadaic acid (OA)-binding proteins OABP1 and OABP2 were isolated from the sponge *Halichondria okadai* where OA was originally isolated. Since OABP2 is not homologous to protein phosphatase 2A, the physiological target for OA in mammals, it might be an important substance that helps us understand self-defense of the sponge.

Results

1. **Cloning and expression of OABP1**
   Prior to this study, the cDNA cloning of OABP1 was performed in spite of being incomplete. In this study, we determined the complete cDNA sequence. We subcloned it into bacterial expression vector and expressed as a fusion protein. The recombinant protein was subjected to binding assay and the dissociation constant K_d for OA was determined.
2. **Immunocytochemistry of the sponge *Halichondria okadai***
   The sponge *Halichondria okadai* was thought to possess OABP2 for reducing self-intoxication. We attempted to elucidate localization of OABP2 in the sponge, though we faced a technical problem to perform.
3. **Sponge cell culture**
   The fresh sponge specimen was cut into small pieces and suspended in sterilized seawater. The sponge cells were dissociated and successfully kept for a long period. The sponge DNA was extracted and OABP2 DNA was amplified by PCR. We thus concluded that OABP2 is the sponge protein.
4. **Variation of OA and OABP2 contents in the sponge**
   In order to obtain a clue as for the function of OABP2, the sponge specimen was collected in several places from Japan. OA content was measured with LC-MS/MS (MRM) and OABP2 content was measured with Western blotting or ELISA using antibody.

Discussion & Conclusion

1. The physical distance between OABP1/OABP2 and OA in the sponge tissue might be important for self-defense of the sponge *Halichondria okadai*. Further studies should be continued to elucidate localization of OA, OABP1 and OABP2.
2. Molecular biological experiments let us conclude that OABP2 would be the sponge protein.
3. Statistical analysis would be required, though all these results indicated that OABP2 plays a role in self-defense of the sponge.

References

Keiichi Konoki, Kaori Saito, Hiroki Matsuura, Naoyuki Sugiyama, Yuko Cho, Mari Yotsu-Yamashita, and Kazuo Tachibana. Binding of diarrheic shellfish poisoning toxins to okadaic acid binding proteins purified from the sponge *Halichondria okadai*. *Bioorg. Med. Chem.* **2010**, *18*, 7607-7610.

Palladium-Catalyzed Enantioselective Synthesis of Highly Substituted Epoxides

Hideki Yorimitsu
Kyoto University
yori@kuchem.kyoto-u.ac.jp

Abstract

Epoxides and aziridines are among the most synthetically useful intermediates and are found in many biologically intriguing compounds. We found a conceptually new approach to these strained heterocycles. Treatment of tertiary allylic alcohols with aryl halides under palladium catalysis resulted in arylative cyclization to form the corresponding epoxides. When we employed enantiomerically enriched allylic alcohol bearing a bulky *t*-butyl group and a small methyl group at the oxygenated carbon, the reaction proceeded with exclusive diastereoselectivity as well as perfect chirality transfer. Similar transformations were applicable to the synthesis of aziridines and methylenecyclopropanes, starting from allylic amines and propargyl-substituted malonate esters, respectively.

Keywords: Epoxides, Aziridines, Methylenecyclopropanes

Introduction

Epoxides are synthetically useful intermediates and are found in many natural products and biologically active compounds. A number of methods for the preparation of epoxides have been reported so far, such as epoxidation of olefins, reaction of carbonyl compounds with sulfur ylides, and ring closure of *vic*-halohydrins.[1)] However, novel synthetic methods for the construction of epoxides have been still required because of their synthetic importance in organic chemistry.

Recently, Wolfe reported that palladium-catalyzed carboetherification/arylation reactions of alkenes with aryl bromides have provided a very efficient way to construct multisubstituted five-membered heterocycles.[2)] However, his method is limited to the synthesis of unstrained medium-sized rings. We serendipitously found that Wolfe's carboetherification is applicable to more rigid three-membered ring construction, which is a new synthetic strategy for the preparation of epoxides. Here we report palladium-catalyzed reactions of readily accessible tertiary allyl alcohols with aryl halides. We also disclose herein that similar transformations were applicable to the synthesis of aziridines and methylenecyclopropanes, starting from allylic amines and propargyl-substituted malonate esters, respectively.

Results

1) Synthesis of Epoxides by Palladium-Catalyzed Reactions of Tertiary Allyl Alcohols with Aryl Halides[3)]

Treatment of enantiomerically enriched tertiary allyl alcohol bearing a *t*-butyl and a methyl group at the oxygenated carbon with 1-bromonaphthalene in the presence of sodium *t*-butoxide under palladium/SPhos catalysis resulted in diastereoselective arylative cyclization to provide the corresponding chiral epoxide (Figure 1). Based on our results and Wolfe's report,[2)] we assume the reaction mechanism as follows. Oxidative addition and subsequent ligand exchange between the palladium intermediate and allyl alcohol in the presence of the base provide arylpalladium alkoxide. Intramolecular oxypalladation then takes place to generate (2,3-epoxyalkyl)palladium intermediate. Finally, reductive elimination gives the desired product and regenerates Pd(0). The diastereoselectivity would be determined in the oxypalladation step. The intermediate in the catalytic cycle is more favorable than the intermediate off the catalytic cycle because, in the former, the larger *t*-butyl group is located at the pseudoequatorial position, thus minimizing the steric repulsion from the vinylic proton or the ligand L (SPhos) that coordinates to the palladium center.

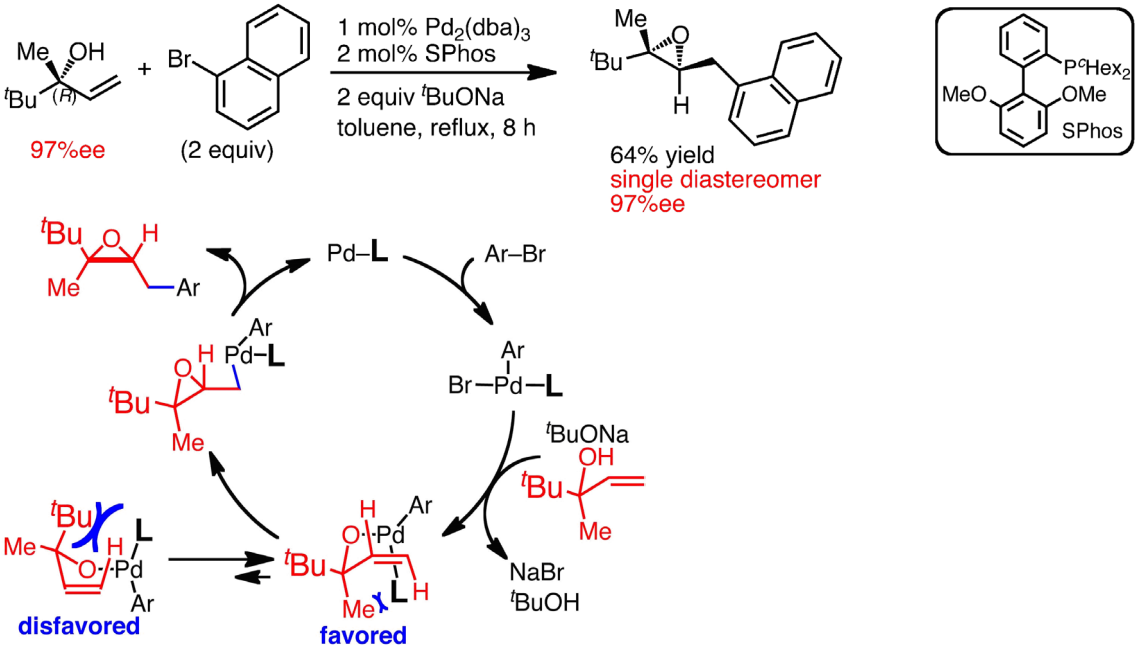

Figure 1. Synthesis of Optically Enriched Epoxide and Plausible Mechanism.

2) Synthesis of Aziridines by Palladium-Catalyzed Reactions of Allylamines with Aryl and Alkenyl Halides[4)]

The new epoxidation reaction could be extended to carboamination for the synthesis of aziridines, especially when the aziridination employed *N*-allylanilines as substrates (Figure 2). The arylative aziridination of *N*- allylanilines that have a phenyl and a methyl group at the allylic position proceeded in a diastereoselective fashion. Interestingly, the sense of the diastereoselectivity is opposite to that of the epoxidation reaction. The steric repulsion between the phenyl group on the nitrogen and the pseudoequatorial substituent can account for the stereochemical reversal.

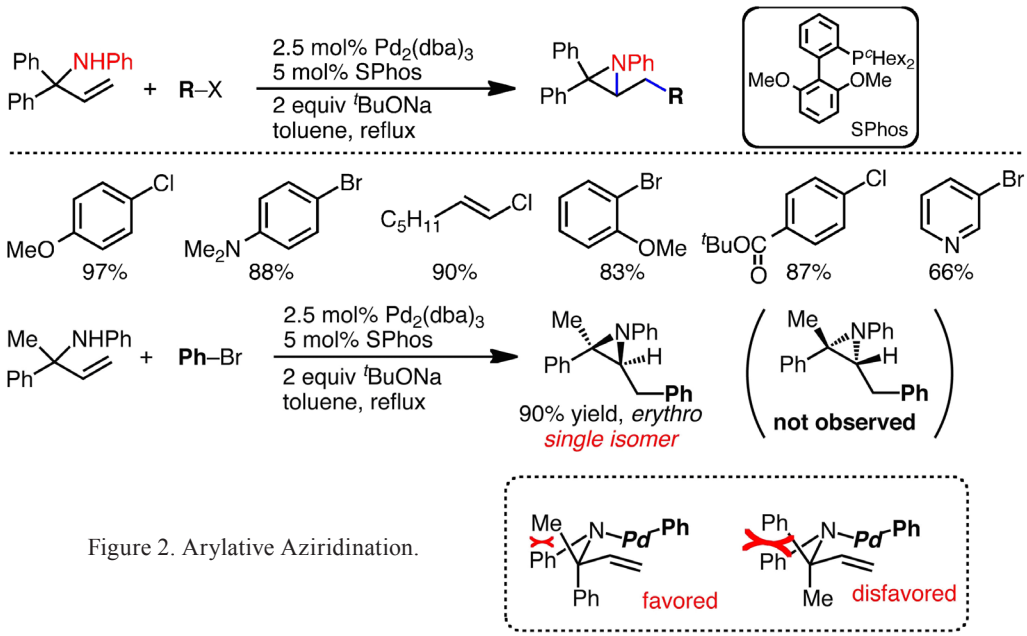

Figure 2. Arylative Aziridination.

3) Palladium-Catalyzed Arylative Cyclization of N-Allylacetamides with Aryl Halides Yielding Benzyl-Substituted Oxazolines[5)]

The reactions of *N*-allylacetamides, instead of *N*-arylallylamines, with aryl halides under conditions similar to the aziridination reaction resulted in the formation of five-membered oxazolines without providing the corresponding aziridines (Figure 3). The nucleophilicity of the nitrogen atom decreases, leading to the facile formation of the unstrained 5-membered ring.

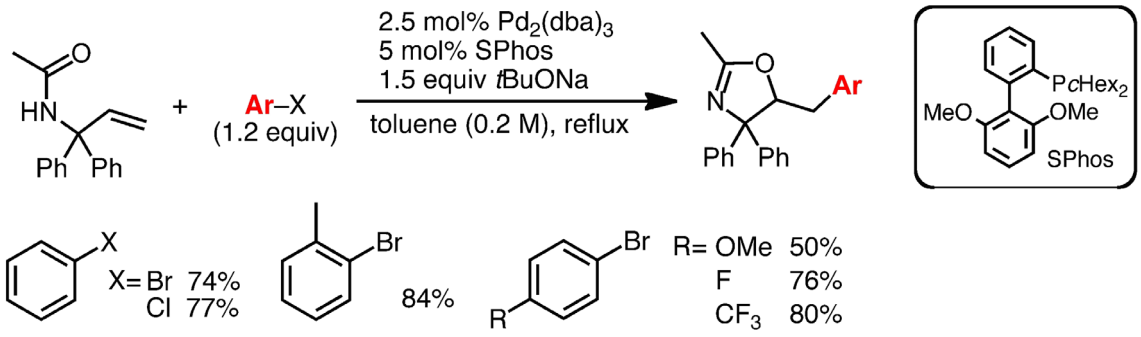

Figure 3. Synthesis of Oxazolines.

4) Synthesis of Methylenecyclopropanes by Palladium-Catalyzed Reaction of Propargyl-Substituted Malonate Esters with Aryl Halides[6)]

Palladium-catalyzed arylative cyclization of propargyl-substituted malonate esters with aryl halides proved to offer a stereoselective approach to methylenecyclopropanes. The reaction proceeds by an *anti*-carbopalladation pathway, which guarantees the exclusive stereocontrol of the resulting double bond (Figure 4). The highly strained as well as densely substituted skeletons

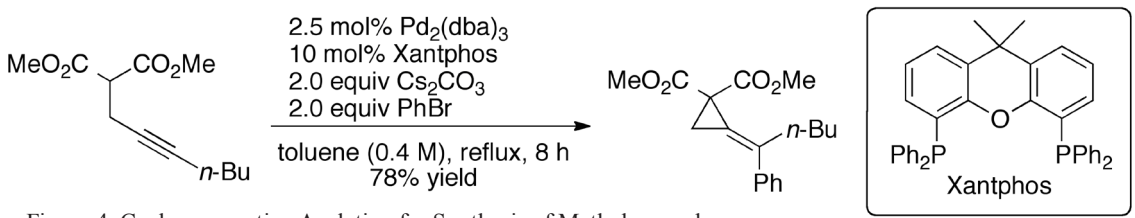

Figure 4. Cyclopropanative Arylation for Synthesis of Methylenecyclopropanes.

of the products facilitate further versatile transformations with the aid of Lewis acids. For instance, Lewis acid-mediated ring-opening etherification proceeded with perfect retention of the configuration of the double bond, thereby being useful as a new stereo- and regioselective approach to tetrasubstituted alkenes. (Figure 5).

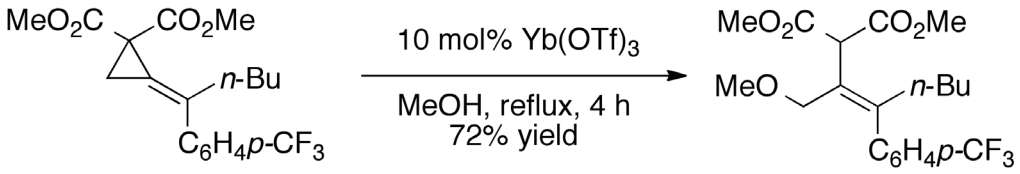

Figure 5. Ring-opening Reaction of Methylenecyclopropane.

5) NHC-Cu-Catalyzed Allenyl Transfer Reactions from 2,3-Alkadien-1-ols to Imines via Cleavage of C–C Bonds: Application to Synthesis of 3-Pyrrolines[7)]

Serendipitously, we found that treatment of a 2,3-butadien-1-ol derivative with imine in the presence of a catalytic amount of a copper-NHC complex and sodium *t*-butoxide resulted in allenyl group transfer and that, after the product was treated in hot aqueous ethanol, cyclization took place to yield 3-pyrrolines (Figure 6).

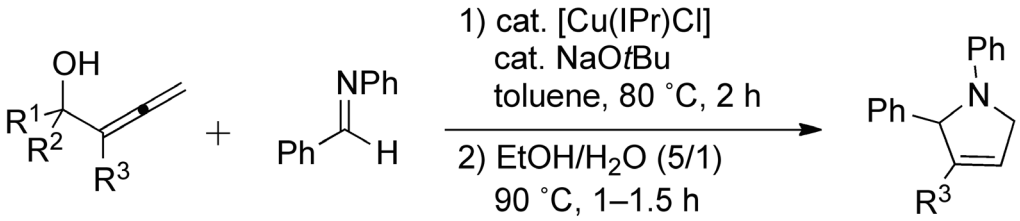

Figure 6. Synthesis of 3-Pyrrolines by Allenyl Transfer/Cyclization

Discussion & Conclusion

Epoxides, aziridines, and methylenecyclopropanes are extremely important classes of cyclic compounds, especially as versatile synthetic intermediates, in organic synthesis. Although numerous methods for the preparation of these strained rings have been reported so far, novel approaches have been still urgently required.

Our approach to the strained rings is uniquely characterized by the followings.

(1) Tertiary allyl alcohols and *N*-allylanilines are readily available, and their enantiomerically pure forms are also available by the conventional asymmetric synthesis if required. The arylative cyclization rapidly increases molecular complexity from readily available compounds, providing a diverse range of substituted three-membered heterocycles in short steps. The reactions can provide strained heterocycles that are otherwise difficult to synthesize, which contributes to further sophistication of synthetic organic chemistry.

(2) For the last five years, palladium-catalyzed intramolecular carboetherification and carboamination reactions have been rapidly emerging as powerful tools for the construction of five-membered heterocycles. On the other hand, one had thought it impossible to synthesize

epoxides and aziridines by palladium-catalyzed cyclization of allyl alcohols and amines because of the high strain energy arising. We found that the combination of sodium *t*-butoxide and the bulky biphenyl-based phosphine ligand is uniquely effective for the synthesis of epoxides and aziridines. The reactions have made a quantum leap in the field of small-ring construction.

(3) Methylenecyclopropanes (MCPs) are very useful building blocks and also found in many bioactive compounds. However, the conventional syntheses of multisubstituted MCPs are usually achieved by multi-step preparations, which require preformation of cyclopropane derivatives or allenes. These methods often encountered difficulty of controlling the stereochemistry of the carbon-carbon double bond of MCPs. Our protocol to MCPs is highly selective and thus unique and efficient. The highly strained as well as densely substituted skeletons of the products facilitate further versatile transformations, which underscores the importance of the products as synthetic intermediates.

(4) 3-Pyrrolines are prominent structural motifs in natural products, and straightforward methods for their preparation are to be explored. Our copper-catalyzed protocol is not only useful but also mechanistically interesting because development of efficient methods for transition-metal-catalyzed selective cleavage of C—C bonds and their application have been a challenging subject of modern organic synthesis.

References

1) (a) Sello, G.; Fumagalli, T.; Orsini, F. *Curr. Org. Synth.* **2006**, *3*, 457–476. (b) Wong, O. A.; Shi, Y. *Chem. Rev.* **2008**, *108*, 3958–3987. (c) Yang, D. *Acc. Chem. Res.* **2004**, *37*, 497–505. (d) Aggarwal, V. K.; Winn, C. L. Acc. Chem. Res. **2004**, *37*, 611–620.

2) Wolfe, J. P. *Synlett* **2008**, 2913–2937.

3) Hayashi, S.; Yorimitsu, H.; Oshima, K. *J. Am. Chem. Soc.* **2009**, *131*, 2052–2053.

4) Hayashi, S.; Yorimitsu, H.; Oshima, K. *Angew. Chem. Int. Ed.* **2009**, *48*, 7224–7226.

5) Fujino, D.; Hayashi, S.; Yorimitsu, H.; Oshima, K. *Chem. Commun.* **2009**, 5754–5756.

6) Fujino, D.; Yorimitsu, H.; Oshima, K. *Submitted.*

7) Sai, M.; Yorimitsu, H.; Oshima, K. *Angew. Chem. Int. Ed.* **2011**, *50*, 3294–3298.

Generation of a new common marmoset glioma model

Tomotoshi Marumoto
Division of Molecular and Clinical Genetics, Medical Institute of Bioregulation,
Kyushu University
marumoto@sentan.med.kyushu-u.ac.jp

Abstract

Glioblastoma (GBM) is the most malignant form of glioma in adults. Patients with GBM die within a year from the time of diagnosis. Therefore it is important to find a new strategy of treatment for this severe disease. To develop a novel strategy of treatment, appropriate animal models are needed to test the efficacy of new approaches. The Common Marmoset (CM, callithrix jacchus), a New World primate, is considered one of the most useful experimental animals for medical research because CM is similar to human especially in immune systems. In this study we have attempted to generate a new CM glioma model using Cre controlled lentiviral vectors.

Keywords: Cancer, Glioma, Animal model, Lentiviral Vector

Introduction

Gliomas are the most common central nervous system tumor in adults. They are histologically classified as astrocytomas, oligodendrogliomas and oligoastrocytomas. According to their degree of malignancey, they are graded on the World Health Organization (WHO) grading system (Furnari FB et al., , *et al.* Genes Dev *21*, 2683-2710, 2007). The most malignant GradeIV gliomas are called glioblastoma (GBM) which exhibits advanced features of malignancy, including necrosis, vascular proliferation and pleomorphism. Patients with GBMs generally die within a year from the time of diagnosis due to their strong resistance to conventional therapies including surgery, chemotherapy and irradiation. Although, until recently, chemotherapy for GBMs did not substantially improve outcomes when added to the other treatment methods, a randomized clinical trial showed that combined therapy of chemotherapy using temozolomide and radiation was superior to radiation alone (Stupp R *et al.* N England J of Med 352, 987-996, 2005). The median survivial of the patients who received this combination treatment was 14.6 months. This is 2.5 months superior compared to a median survival time of the patients who received radiation alone. Combination therapy using temozolomide and radiation is now widely used all over the world, however patients and physicians certainly need more effective drug for GBMs. To find the new strategy of treatment for GBMs, understanding of molecular mechanisms related to the initiation and progression of GBMs and the presence of animal models being able to test the new strategy of treatment are still of importance. In this study we have tried to generate a novel Common Marmoset (CM, callithrix jacchus) glioma model using Cre controlled lentiviral vectors.

Results

Recently we have generated a novel mouse glioma model using Cre controlled lentiviral vectors (Marumoto *et al.* Nat Med 15, 110-116. 2009). This model can induce oncogenic events in a cell type and region specific manner in adult GFAP-Cre mice. The induction of H-Ras in GFAP+ cells in the hippocampus or subventricular zone in GFAP+/p53+/- mouse brains resulted in the generation of GBM like tumors.

To establish the technology to induce oncogenic events in a cell type and region specific manner in adult CM brains, we constructed pToDi lentiviral vectors (pToDi LV, Fig.1) and Cre recombinase expressing lentiviral vectors under the control of GFAP (GFAP Cre-LV), and planned to inject both vectors into the hippocampus and subventricular zone of adult CM. As shown in Fig.1, pToDi LVs are capable of expressing shRNAs targeting tumor suppressors and oncogenes in the presence of Cre recombinase.

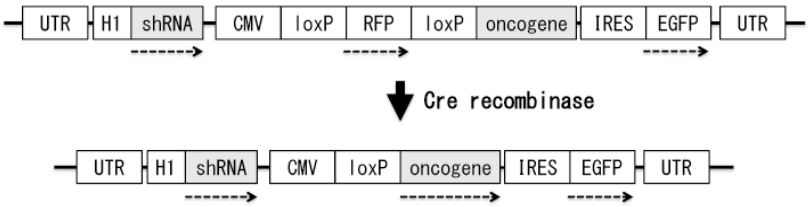

Fig.1 Cre controlled lentiviral vector, pToDi: In the presence of Cre, the stuffer sequence, RFP, would be cut out and the oncogene would be expressed. ShRNA targeting for tumor suppressorswould also be expressed under the control of H1 promoter.

We found that all the GFAP-Cre mice injected with pToDi LVs into the hippocampus showed the formation of GBM-like tumors (data not shown).

Next we are planning to generate a new CM GBM model by injecting both pToDi LVs and GFAP-Cre LVs in adult CM.

Discussion & Conclusion

To generate CM GBM model by injecting both pToDi LVs and GFAP-Cre LVs into the brains of adult CM, we plan to express H-RasV12 which is an activated form of H-Ras and inhibit p53 tumor suppressor by shRNA (Fig. 2). Injection of these vectors will probably induce GBM formation in adult CM. If this approach could not

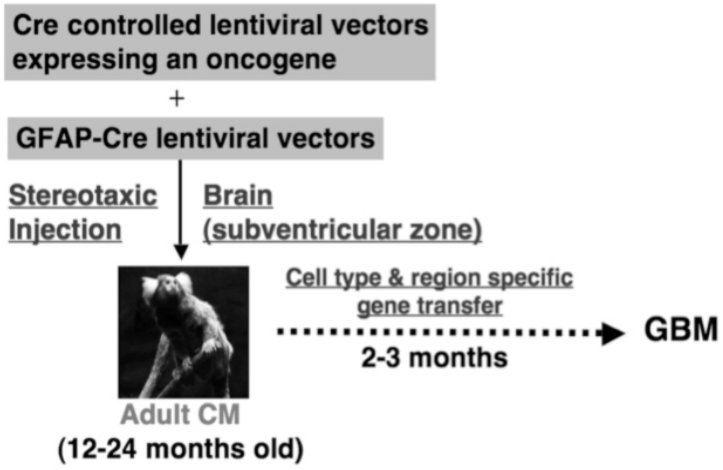

Fig.2 Novel common marmoset GBM model: Injection of both Cre controlled lentiviral vectors expressing oncogenes and Cre expressing lentiviral vectors under the control of GFAP promoter into the brain of adult CM can induce oncogenic events in a cell type and region specific manner.

induce GBM formation, we would test other combinations. For example, activation of EGFR and inactivation of p53 or p16.

If the tumor arose, we would perform pathological analyses and try to generate CM CBM cell line in culture to characterize them.

References

1) Furnari, F.B., Fenton, T., Bachoo, R.M., Mukasa, A., Stommel, J.M., Stegh, A., Hahn, W.C., Ligon, K.L., Louis, D.N., Brennan, C., *et al.* Malignant astrocytic glioma: genetics, biology, and paths to treatment. Genes Dev 21: 2683-2710, 2007

2) Stupp R, Mason WP, van den Bent MJ, Weller M, Fisher B, Taphoorn MJ, Belanger K, Brandes AA, Marosi C, Bogdahn U, Curschmann J, Janzer RC, Ludwin SK, Gorlia T, Allgeier A, Lacombe D, Cairncross JG, Eisenhauer E, Mirimanoff RO; European Organisation for Research and Treatment of Cancer Brain Tumor and Radiotherapy Groups; National Cancer Institute of Canada Clinical Trials Group. Radiotherapy plus concomitant and adjuvant temozolomide for glioblastoma. N Engl J Med. 10;352(10):987-96, 2005

3) Marumoto T, Tashiro A, Friedmann-Morvinski D, Scadeng M, Soda Y, Gage FH, Verma IM. Development of a novel mouse glioma model using lentiviral vectors. Nat Med. 2009 Jan;15(1):110-6.

Revealing olfactory processing algorithm by the study of insects

Makoto Mizunami
Hokkaido University
mizunami@sci.hokudai.ac.jp

Abstract

Representation of odors in the primary olfactory center was studied by using calcium-imaging techniques in the American cockroach. Presentations of each of 20 different kinds of odors to an antenna induced each specific pattern of activities in a group of 45 glomeruli in the antennal lobe. We found no evidence of "odotopic map", i.e., no specific relationship between the chemical properties of odorant molecules and the location of responded glomeruli. Response to a mixture of some of these odors often deviated from linear summation of responses to components, indicating non-linear interaction among glomeruli. The results provide solid basis for further examining olfactory processing algorithm in the primary olfactory center.

Keywords: Calcium imaging, odor representation, primary olfactory center, non-linear summation, cockroach

Introduction

Cockroaches have been used as model animals to study neural mechanisms of olfaction and olfactory learning (1,2,3). We have recently established neuroanatomical map of glomeruli in the antennal lobe, primary olfactory center, of the cockroach, *Periplaneta Americana* (1): Cockroaches possess about 206 glomeruli in the antennal lobe, which could be divided into ten clusters. In each glomerulus, axon terminals of a specific type of olfactory receptor neurons on the antennae make synaptic connections with dendrites of a few interneurons. In this study, I examined responses of about 45 glomeruli in the frontal surface of the antennal lobe to 20 kinds of odors by using calcium-imaging techniques.

Results

By loading the antennal lobe with a calcium-sensitive dye (calcium green AM) and by using optical recording techniques, we measured responses of neurons in the antennal lobe to 20 different kinds of odors presented to an antenna: Responses of neurons to an odor could be optically measured by accompanying changes of calcium concentration in the neurons. Several lines of evidence suggested that the recorded optical signals reflect, in large part, activities of axon terminals of receptor neurons. Odors were selected on the basis of the results of previous studies on olfactory receptor neurons (3). These included 1-butanol, 1-pentanol, 1-hexanol, 1-octanol, trans-2-hexen-1-ol, 2-pentanol, 2-hexanol, 2-octanol, hexanon, cineol, menthol, linalool, geraniol, citral and eugenol. After recording, the antennal lobe was stained with a dye (neutral red) to facilitate matching of the

neural activity with neuroanatomical map of glomeruli (Fig. 1A).

We observed that presentation of an odor induced responses in a specific set of glomeruli, and each glomerulus responded to a specific set of odors, indicating overlapping, combinatory code of odors in an array of glomeruli (Fig. 1B). We observed no specific relationship between chemical structures of odorant molecules and locations of responded glomeruli in the antennal lobe, indicating no “odotopic map” in the antennal lobe of the cockroach.

We also compared the response to a mixture of odors and the responses to its components. In some cases, responses to a mixture of odors roughly matched to a linear summation of responses to components. In many other cases, however, response to a mixture of odors markedly differed from a linear summation of responses to components, indicating non-linear, inhibitory interactions among glomeruli in the antennal lobe.

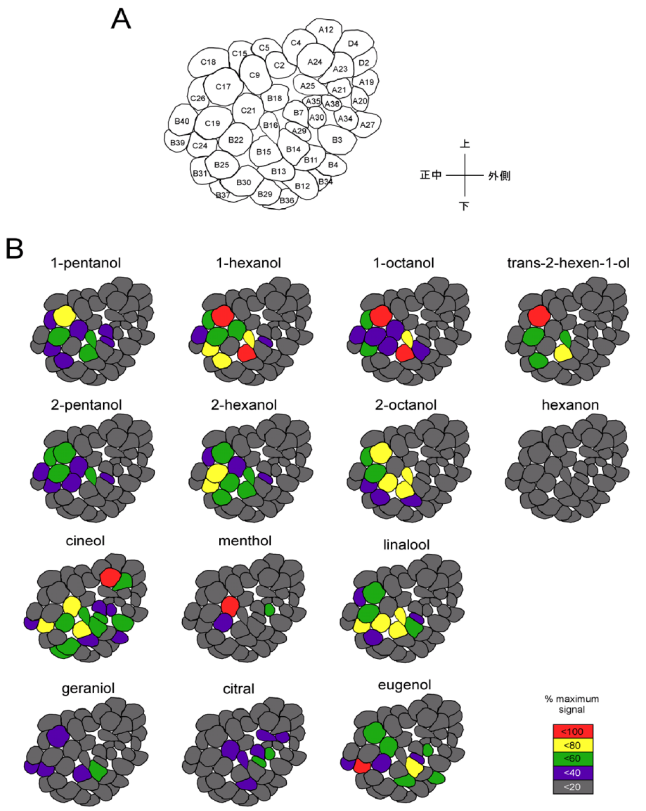

Figure 1.
A: Morphologically identified 45 glomeruli at the frontal surface of the antennal lobe of the cockroach.
B: Representation of odors in an array of 45 glomeruli in the antennal lobe of the cockroach. The intensity of response to an odor is shown with a color code. There is a highly overlapping representation of odors in an array of glomeruli.

Discussion & Conclusion

We observed a highly overlapping, combinatory code of odors in an array of glomeruli in the primary olfactory center of cockroaches. Similar observations have been made in the olfactory bulb in mammals and the antennal lobe of honey bees and fruit-flies, suggesting a common feature among olfactory systems in vertebrates and invertebrates. A characteristic feature of odor representation in the cockroach antennal lobe is that there is no obvious spatial arrangement regarding the chemical features of the odorant molecules. This is in contrast to that some of previous studies in mammalian olfactory bulb and insect antennal lobe emphasized the presence of “odotopic map” (4). Our findings provide a solid basis for further examining the odor processing in the antennal lobe in the cockroach.

We found nonlinear summation effect in the response to a mixture of odors, indicating non-linear, inhibitory interaction among glomeruli. Such interaction is likely to be mediated by GABA-ergic local interneurons that connect among glomeruli (3). Future study using a specific antagonist of GABA receptors will help to clarify neural mechanisms of odor processing in the antennal lobe of the cockroach.

References

1) Watanabe H, Nishino H, Nishikawa M, Mizunami M, Yokohari F. (2010) Complete mapping of glomeruli based on sensory nerve branching pattern in the primary olfactory center of the cockroach *Periplaneta americana*. J. Comp. Neurol. 518: 3907-3930.

2) Sakura M, Okada R, Mizunami M. (2002) Olfactory discrimination of structurally similar alcohols by cockroaches. J. Comp. Physiol. A. 188: 787-797.

3) Boeckh J, Ernst K-D. (1987) Contribution of single unit analysis in insects to an understanding of olfactory function. J. Comp. Physiol., 161: 549-565.

4) Christensen TA, White J. (2000) Representation of Olfactory Information in the Brain, eds. Finger TE, Silver WL, Restrepo D. (Wiley-Liss), pp. 202-232.

Human RNA dependent RNA polymerase and cancer stem cell

Kenkichi Masutomi
National Cancer Center Research Institute, Division of Cancer Stem Cell
kmasutom@ncc.go.jp

Abstract

A complex of hTERT, BRG1 and the nucleolar GTP-binding proteins GNL3L and nucleostemin regulates tumor initiating cell behavior.

Keywords: Telomerase, cancer stem cell, RMRP, RdRP

Introduction

Accumulating evidence indicates that the human telomerase catalytic subunit (*hTERT*) contributes to stem cell turnover and the transformation of human cells through both telomere-dependent and telomere-independent mechanisms. Constitutive expression of hTERT not only stabilizes telomere length and facilitates cell immortalization but also increases tumor susceptibility and alters stem cell cycling *in vivo* even when telomere lengths are not limiting.

Results

We show that hTERT forms a protein complex with the SWI/SNF component BRG1 and the nucleolar GTP-binding proteins, nucleostemin (NS) or GNL3L. Although overexpression or suppression of GNL3L or NS did not affect telomerase activity or telomere length, cells that constitutively express NS/GNL3L exhibit increased hTERT expression. Moreover, cells that constitutively express elevated levels of hTERT, BRG1 and NS/GNL3L exhibit increased CD133 and CD44 expression and enhanced tumorigenicity at limiting cell numbers. These phenotypes were dependent on the expression of hTERT and BRG1 and NS immunoprecipitated RMRP. These observations indicate that a complex composed of hTERT, BRG1 and NS or GNL3L participates in the regulation of tumor initiating cell phenotypes and imply potential link between cancer stem cell and RNA dependent RNA polymerase (RdRP).

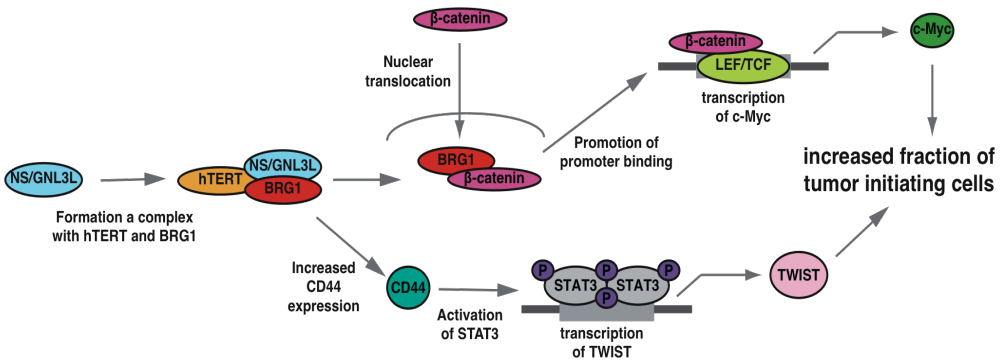

Discussion & Conclusion

These observations demonstrate that a complex composed of hTERT, BRG1 and the nucleolar GTP binding proteins NS and GNL3L regulates pathways implicated in the regulation of tumor initiating cells. Overexpression of NS and GNL3L leads to altered tumor initiating cell phenotypes in a manner that is dependent on hTERT but does not depend on either of the two non-coding RNAs associated with hTERT, *hTERC* and *RMRP*. These observations indicate that hTERT exists at least three complexes: one composed of hTERT and *hTERC* that is involved in telomere maintenance, a RNA-dependent RNA polymerase composed of hTERT and *RMRP*, and a third complex composed of BRG1 and NS/GNL3L that regulates Wnt/β-catenin signaling in both normal stem cells and glioblastoma derived tumor initiating cells.

References

Maida et al., “An RNA-dependent RNA polymerase formed by TERT and the RMRP RNA”; Nature 2009

Okamoto et al., “Induction of tumor initiating cells of defined genetic composition by a complex composed of nucleostemin, hTERT and BRG1” ; revised manuscript under peer review

Pattern formation played by growth factors signaling in the mammalian embryo

Isao Matsuo
Osaka Medical Center and Research Institute for Maternal and Child Health
Osaka Prefectural Hospital Organization
imatsuo@mch.pref.osaka.jp

Abstract

Heparan sulfate (HS) proteoglycans modulate the activity of multiple growth factors on the cell surface and extracellular matrix. However, it remains unclear how the HS chains control the movement and reception of growth factors into targeted receiving cells during mammalian morphogenetic processes. In order to clarify the short-range spreading mechanism of FGF-signaling activation by HS chains during mouse extraembryonic ectoderm (ExE) development, several chemical reagents, which were previously proposed to specifically inhibit the movement processes of HS chains; planar transcytosis, cyotoneme (filopodia), proteolytic and heparanase cleavages were exploited. FGF-signaling activity was affected by inhibitors for serine protease but neither for actin filaments, heparanase, metalloproteinase, nor other proteases in the ExE. These findings suggest that FGF-signaling activation is likely to be mediated by serine protease-dependent processes. To verify the specificity of roles of serine protease inhibitors on activation of FGF signaling, expression of other FGF targets and non-FGF targets were also analyzed. These above studies together suggest that the proteolytic cleavage of HS proteoglycans through the secreted serine protease can contribute to proper FGF-signaling activation, including the spread of FGF signaling during mammalian ExE development.

Keywords: *Ext2*, Heparan sulfate, FGF signaling, Protease inhibitors

Introduction

The stability, movement and reception of growth factors have been suggested to be controlled by HS proteoglycans (Haecker et al., 2005; Bishop et al., 2007; Yan and Lin, 2009). In other words, HS proteoglycans modulate the activity of signaling factors by controlling extracellular stabilization, movement and retention both on the cell surface and on the ECM during development and growth. HS proteoglycans are formed by HS-chains and core proteins via a multi-step process in the Golgi apparatus (Haecker et al., 2005; Yan and Lin, 2009). However, it remains poorly understood how HS chains control the movement and reception of growth factors into targeted receiving cells during mammalian morphogenetic processes. In order to clarify the short-range spreading mechanism of FGF-signaling activation by HS chains, we have exploited several chemical reagents which were previously proposed to specifically inhibit the following movement processes of HS chains (Haecker et al., 2005; Yan and Lin, 2009): planar transcytosis, cyotoneme (filopodia), proteolytic and heparanase cleavages (Fig.1).

Results

Since the above mechanisms of planar transcytosis and cytoneme are required for the actin cytoskeleton (Fig.1; model I), wild-type E6.5 embryos were treated with cytochalasin D, and then dp-Erk expression was examined to determine whether it is actin-dependent or not.

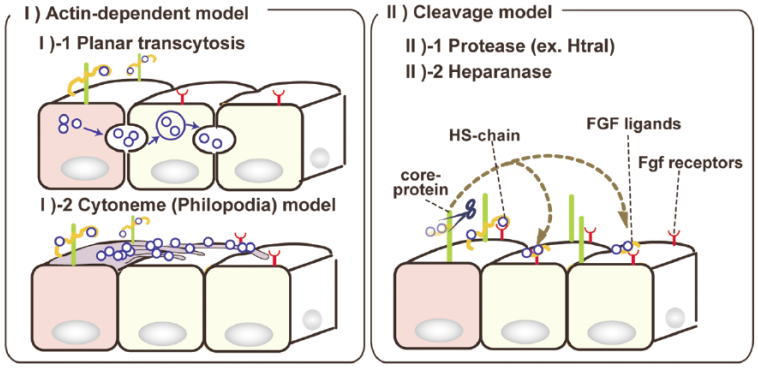

Fig.1: Schematic models illustrate the role of HS chains in the movement or transport of FGF ligands.

Although F-actin staining clearly showed that cytochalasin D abolished the actin cytoskeleton, under this condition dp-Erk expression of the ExE was unchanged. These findings indicate that FGF-signaling activity was not affected by actin filaments, suggesting that FGF-signaling activation is likely to be mediated by actin-independent processes. Next, to determine whether proteolytic or heparanase cleavages can mediate activation of FGF signaling (Fig.1; model II), embryos were incubated with two serine proteinase inhibitors benzamide and phenylmethanesulfonyl fluoride (PMSF) (Fig.1; model II-1), and a heparanase inhibitor, OGT2115 (Fig.1; model II-2). The results showed that dp-Erk expression was completely lost in the ExE of the embryos treated with serine proteinase inhibitors. However, dp-Erk expression was unaffected by the heparanase inhibitor. These findings suggest that the proteolytic cleavage of HS proteoglycans through the secreted serine protease but not heparanase is involved in FGF-signaling activation via HS chains in the ExE. Additionally, the matrix metalloproteinase inhibitor, G6001, which broadly inhibits ECM-localized proteinase activity, did not reduce dp-Erk expression. Moreover, other four protease inhibitors, i.e. E-64 and Chymostatin, which are specific for a cysteine protease, Pepstatin A, which is specific for an aspartic protease, Calpain inhibitor I, which is specific for Calpain and Cathepsin, did not reduce the dp-Erk expression at all. These results confirm that proteolytic release of ECM-associated proteoglycans and other proteases with the exception of a serine protease may not primarily participate in activation of FGF signaling via HS chains.

To further verify the specificity of roles of serine protease inhibitors on activation of FGF signaling, we have examined the expression of other FGF targets, *Cdx2* and *Dusp6/Mkp3,* and expression of non-FGF targets, phosphorylation of Smad2 and Smad1/5/8 for Nodal and BMP signaling, respectively. Consequently, after incubation with the serine protease inhibitor, both *Cdx2* and *Dusp6/Mkp3* expression were significantly reduced while the expressions of non-FGF targets, pSmad2 and pSmad1/5/8, were unaffected. These findings together suggest that the proteolytic cleavage of HS proteoglycans through the secreted serine protease can contribute to proper FGF-signaling activation, including the spread of short-range FGF signaling during ExE development.

Discussion & Conclusion

The present experiments are in good agreement with previous models in which the following proposals were made to explain the modulation of the activity of multiple growth factors by HS chains (Haecker et al., 2005; Bishop et al., 2007; Yan and Lin, 2009): HS chains mediate the movement of growth factors through diffusion or transport, via transcellular transport of vesicles, filopodial processes (cytoneme), sheddases (proteolytic release), endoglycosidase (heparanase) and so on. Our expression analyses of FGF targets with the serine proteinase inhibitors suggest that cell surface-tethered HS chains can spread out FGF ligands to adjacent HS-deficient cells within a short distance partly through proteolytic cleavage. It was previously thought that the complex of HS chains and FGF ligands could be transported across longer-range distances after having been cleaved by sheddases or endoglycosidase (Yan and Lin, 2009). However, it is noteworthy that the spreading of FGF signaling is likely to be limited to much shorter distances in the early mouse embryo than previously proposed (Hou et al., 2007).

References

1) Bishop, J.R., Schuksz, M., Esko, J.D. (2007). Heparan sulphate proteoglycans fine-tune mammalian physiology. Nature *446*, 1030-1037.

2) Haecker, U., Nybakken, K., and Perrimon, N. (2005). Heparan sulphate proteoglycans: the sweet side of development. Nature Rev. Mol. Cell. Biol. *6*, 530-541.

3) Hou, S., Maccarana, M., Min, T.H., Strate, I., and Pera, E.M. (2007). The secreted serine protease xHtrA1 stimulates long-range FGF signaling in the early Xenopus embryo. Dev. Cell *13*, 226-241.

4) Yan, D. and Lin, X. (2009). Shaping morphogen gradients by proteoglycans. Cold Spring Harb. Perspect. Biol. *1*, a002493.

Inhibition of USAG-1, a BMP antagonist, ameliorates hereditary kidney disease of glomerular basement membrane

Motoko Yanagita
Hakubi Project, Kyoto University Graduate School of Medicine
motoy@kuhp.kyoto-u.ac.jp

Abstract

The glomerular basement membrane (GBM) is a key component of the filtering unit in the kidney. Mutations involving COL4A3/4/5 affect the assembly of GBM, and cause Alport syndrome, a progressive hereditary kidney disease with no definitive therapy.

Previously, we demonstrated that the BMP antagonist USAG-1 negatively regulates the reno-protective action of bone morphogenetic protein7 (BMP7) in tubular injury during acute renal failure. This study demonstrates that genetic ablation of USAG-1 led to significant attenuation of disease progression and to preservation of renal function in *COL4A3*$^{-/-}$ mice, a model for human Alport syndrome. The pathogenetic role of USAG-1 might involve crosstalk between kidney tubules and glomerulus, since USAG-1 and BMP7 colocalized in the macula densa in the distal tubules, lying in direct contact with glomerular mesangial cells, where BMP7 attenuated and USAG-1 enhanced the expression of MMP-12 that degrade GBM. We propose that the inhibition of USAG-1 may be developed as a novel therapeutic approach for the treatment of this hereditary disease.

Keywords: Chronic Kidney Disease, USAG-1, BMP7, BMP antagonist, prognosis

Introduction

The renal glomerular basement membrane (GBM) contributes importantly to maintenance of the structural integrity of the glomerular capillaries. Type IV collagen is the major component of the GBM and its mutations have been linked to the genetic disorder Alport syndrome, a progressive hereditary kidney disease associated with sensoryneural deafness. With a genetic frequency of about 1 in 5000 people, it counts among the more prevalent of known genetic disorders. The disease is caused by the mutations in any one of the genes encoding the α3, α4, and α5 chains of type IV collagen (*COL4A3*, *COL4A4* and *COL4A5*), and a mutation affecting one of these chains forming the α3/α4/α5(IV) collagen network can alter or abolish the GBM expression not only of the corresponding chain but also of the other two chains. The GBM in Alport syndrome instead retains the fetal α1/α1/α2(IV) collagen network, which confers an increased susceptibility to proteolytic enzyme, leading to progressive destruction of the GBM with subsequent hematuria and proteinuria, glomerulosclerosis, and ultimately end-stage renal disease. The current therapy is limited to dialysis and transplantation, with a higher risk of anti-glomerular basement membrane disease in the transplanted organs due to immune reaction against the type IV collagen chains.

BMP7 is a promising candidate to treat Alport syndrome. BMP7 belongs to the transforming

growth factor-β (TGF-β superfamily and the kidney is the major site of BMP7 expression during both embryogenesis and postnatal developmen. Pharmacological doses of BMP7 can repair damaged renal tubules and preserve renal function in several models of renal diseases, including the Col4A3 knockout model of Alport syndrome. However, the exact role of endogenous BMP7 and its mechanism of action remain unclear. In addition, the administration of recombinant BMP7, whose target cells are widely expressed throughout the body, might also produce some undesired extrarenal effect.

The local activity of endogenous BMPs is controlled by certain classes of binding molecules that act as positive or negative regulators of BMP signaling activity. BMP antagonists function through direct association with BMP, thus inhibiting the binding of BMP to its receptors, and defining the boundaries of BMP activity.

The product of *uterine sensitization-associated gene-1* (USAG-1) acts as a kidney-specific BMP antagonist, and USAG-1 binds to and inhibits the biological activity of BMP7. USAG-1 is expressed in distal tubules, and colocalizes with BMP7 in distal convoluted tubules and connecting tubules. Furthermore, *USAG-1*$^{-/-}$ mice are resistant to tubular injury such as acute renal failure and interstitial fibrosis, and USAG-1 is the central negative regulator of BMP function in the adult kidney. Because in adults the expression of USAG-1 is confined to the kidneys, targeting the activity of this protein might yield safer and more kidney-specific therapies than the administration of BMP7. For this, it will be important to first elucidate the role of USAG-1 in the pathology of progressive glomerular injury.

Results

COL4A3$^{-/-}$ mice, a mouse model of human Alport syndrome, develop progressive glomerulonephritis associated with tubulointerstitial fibrosis leading to renal failure. To test the role of USAG-1 in the progression of end-stage renal disease originated from glomerular injury, mice deficient in both *COL4A3* gene and *USAG-1* gene were generated (*USAG-1*$^{-/-}$*:COL4A3*$^{-/-}$ mice). A histological examination of the kidneys from *USAG-1*$^{+/+}$*:COL4A3*$^{-/-}$ mice revealed segmental sclerosis and intraglomerular hemorrhage at 6 weeks of age, while these changes were almost completely absent in *USAG-1*$^{-/-}$*:COL4A3*$^{-/-}$ mice. At 10 weeks of age, *USAG-1*$^{+/+}$*:COL4A3*$^{-/-}$ mice demonstrated glomerulosclerosis associated with inflammatory cell infiltration, interstitial fibrosis, tubular atrophy and cast formation, while these changes were significantly decreased in *USAG-1*$^{-/-}$*:COL4A3*$^{-/-}$ mice. In addition, *USAG-1*$^{-/-}$*:COL4A3*$^{-/-}$ mice showed less albuminuria and preserved renal function in comparison to that of *USAG-1*$^{+/+}$*:COL4A3*$^{-/-}$ mice, consistent with the results of renal histology. Furthermore, upon aging beyond 13 weeks, *USAG-1*$^{-/-}$*:COL4A3*$^{-/-}$ mice showed less mortality than *USAG-1*$^{+/+}$*:COL4A3*$^{-/-}$ mice. Renal expression of inflammatory cytokines as well as MMPs, GBM-degrading enzyme which play key roles in progression of Alport syndrome, was significantly reduced in *USAG-1*$^{-/-}$*:COL4A3*$^{-/-}$ mice.

Deficiency of USAG-1 significantly attenuated glomerular pathology in the *COL4A3*$^{-/-}$ mouse

model of Alport syndrome, in spite of the absence of USAG-1 expression in glomeruli. Instead, both BMP7 and USAG-1 is expressed in the part of the distal tubule which came in contact with its own glomerulus, the macula densa. To investigate potential mechanisms that are responsible for the beneficial effect of USAG-1 deficiency in Alport syndrome, the effect of BMP7 and USAG-1 in cultured mesangial cells was examined. The administration of BMP7 suppressed TGF-β-induced MMP-12 up-regulation in mesangial cells, and simultaneous administration of USAG-1 antagonized the suppressive effect of BMP7. These results indicate that USAG-1 secreted from macula densa might enhance MMP-12 expression in the glomeruli by suppressing the inhibitory effect of BMP7 and exacerbate glomerular disease progression in Alport syndrome (Figure).

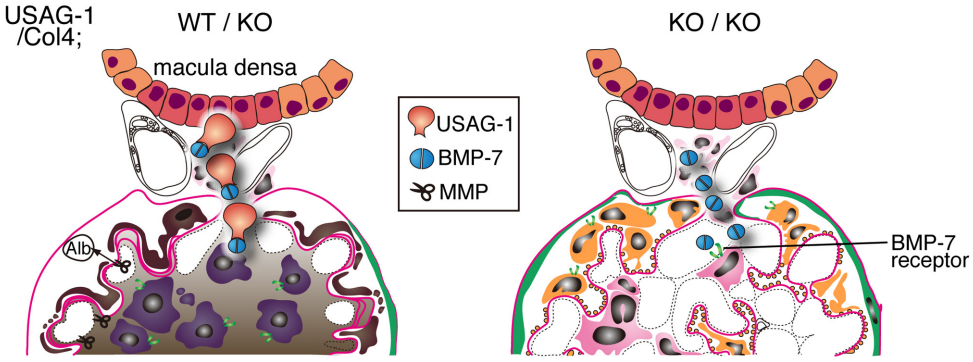

Hypothetical model for involvement of USAG-1 secreted from distal tubules in the pathogenesis of glomerular damage in Alport syndrome.

Discussion & Conclusion

At present there is no definitive therapy to prevent or slow renal disease progression in Alport syndrome. Several studies using a mouse model of Alport syndrome have provided potential therapies, such as MMP inhibitor, angiotensin-converting enzyme inhibitor, statins, transplantation of bone-marrow derived stem cells, and total body irradiation. The results of the present study support the notion that therapeutic trials to inhibit the function of USAG-1 may become a novel therapeutic approach for Alport syndrome either alone or in combination with other approaches. A therapeutic trial targeting USAG-1 is promising because it is expected to be effective in both glomerular and tubular injuries, and is more kidney-specific and has fewer extra-renal effects, because the expression of USAG-1 is confined to the kidney.

References

1) Mari Tanaka, Misako Asada, Atsuko Y Higashi, Jin Nakamura, Akiko Oguchi, Mayumi Tomita, Sachiko Yamada, Nariaki Asada, Masayuki Takase, Tomohiko Okuda, Hiroshi Kawachi, Aris N. Economides, Elizabeth Robertson, Satoru Takahashi, Takeshi Sakurai, Roel Goldschmeding, Eri Muso, Atsushi Fukatsu, Toru Kita, and Motoko Yanagita
Loss of the BMP antagonist, USAG-1 ameliorates disease in a mouse model of progressive hereditary kidney disease Alport syndrome
J Clin Invest. 120 (3):768-77, 2010

2) Motoko Yanagita
BMP antagonists in kidney diseases
Curr Opin Invest Drugs. 11(3):315-22, 2010.

3) Atsuko Y. Higashi, Tomokatsu Ikawa, Masamichi Muramatsu, Aris N. Economides, Akira Niwa, Tomohiko Okuda, Andrew J. Murphy, Jose Rojas, Toshio Heike, Tatsutoshi Nakahata, Hiroshi Kawamoto, Toru Kita, and Motoko Yanagita
Direct hematological toxicity and illegitimate chromosomal recombination caused by the systemic activation of $CreER^{T2}$
Journal of Immunology 182 (9):5633-40, 2009.

4) New horizons at the caudal embryos: coordinated urogenital/reproductive organ formation by growth factor signaling.
Kentaro Suzuki, Aris Economides, Motoko Yanagita, Daniel Graf, Gen Yamada.
Curr Opin Genet Dev. 19(5):491-6, 2009

5) Motoko Yanagita
BMP modulators regulate the function of BMP during body patterning and disease progression
Biofactors 35(2):113-9, 2009.

Molecular analysis of social behavior using a humanoid model mouse of autism

Toru Takumi
Hiroshima University
takumi@hiroshima-u.ac.jp

Abstract

Autism spectrum disorders (ASDs) have garnered significant attention as an important grouping of developmental brain disorders. Recent genomic studies have revealed that inherited or *de novo* copy number variations (CNVs) are significantly involved in the pathophysiology of ASDs. In a previous report from our laboratory, we generated mice with CNVs as a model of ASDs, with a duplicated mouse chromosome 7C that is orthologous to human chromosome 15q11-13. Behavioral analyses revealed paternally duplicated (*patDp/+*) mice displayed abnormal behaviors resembling the symptoms of ASDs. In the present study, we extended these findings by performing various behavioral tests with C57BL/6J *patDp/+* mice, and comprehensively measuring brain monoamine levels with *ex vivo* high performance liquid chromatography. Compared with wild-type controls, *patDp/+* mice exhibited decreased locomotor and exploratory activities in the open field test, Y-maze test, and fear-conditioning test. Furthermore, their decreased activity levels overcame increased appetite induced by 24 hours of food deprivation in the novelty suppressed feeding test. Serotonin levels in several brain regions of adult *patDp/+* mice were lower than those of wild-type control, with no concurrent changes in brain levels of dopamine or norepinephrine. Moreover, analysis of monoamines in postnatal developmental stages demonstrated reduced brain levels of serotonin in young *patDp/+* mice. These findings suggest that a disrupted brain serotonergic system, especially during postnatal development, may generate the phenotypes of *patDp/+* mice.

Keywords: Autism, mouse model, behavior, serotonin

Introduction

Autism is a widely accepted neurodevelopmental disorder characterized by several major criteria, including impairments in social interaction, verbal and non-verbal communication difficulties, repetitive or rigid behavior, and restricted interest. Autism spectrum disorders (ASDs) comprise autistic disorder, Rett's disorder, Asperger's disorder, and pervasive developmental disorder not otherwise specified (PDD-NOS) in DSM-IV. The prevalence of ASDs was recently estimated to have increased to 1 in 166 births. According to previous studies of twins, these disorders are highly heritable because concordance rates for monozygotic twins (70–90%) are several fold higher than the corresponding rates for dizygotic twins (0–10%). Although there are many candidate genes for pathophysiology in ASDs, recent high-resolution genetic techniques revealed that a *de novo* copy number variation (CNV) is also a significant risk factor for ASDs, and is a more important risk

factor than previously recognized.

In several candidate chromosomal regions with relevance for ASDs, duplication of human chromosome 15q11-13 is the most frequent chromosome rearrangement, found in 1–4% of ASDs patients. Moreover, this region is an imprinting region where deletions or methylation abnormalities of paternal and maternal alleles leads to Prader-Willi syndrome and Angelman syndrome, respectively. In chromosomal duplication, these imprinting effects can also affect the resulting phenotypes. Maternal duplication of human chromosome 15q11-13 is believed to cause ASDs, whereas paternal duplication usually results in a normal behavioral phenotype. However, recent findings suggest that maternal interstitial duplications may be less prevalent than previously assumed, and indeed paternal duplication of this region may lead to autistic-like behavior.

Various neurotransmitters may be involved in the pathophysiology of ASDs. Notably, serotonin (5-HT) concentrations in platelets of patients with ASDs are higher and more widely distributed than those of controls. However, this abnormality may not result in abnormal brain 5-HT levels because 5-HT generally does not penetrate the blood brain barrier (BBB). Nevertheless, a recent report showed that 5-HT could cross the BBB in rats. Thus, the relationship between peripheral and central 5-HT in ASDs remains unclear, and might be more complex than established mechanisms would indicate. As further evidence for 5-HT abnormality in ASDs, administration of selective serotonin reuptake inhibitors (SSRIs) improved repetitive behavior which is a core symptom in ASDs.

Results

During the 120 min test period of the open field test, *patDp/+* mice exhibited less distance traveled (Fig. 1B; $F_{1,42}$=5.84; p=0.02), less time spent in the center area accompanied by thigmotaxis (Fig. 1A; averaged trace images of each genotype) (Fig. 1C; time spent in center area; $F_{1,42}$=11.61; p<0.01), and less vertical activity (Fig. 1D; $F_{1,42}$=10.12; p<0.01) compared with WT mice. The ratio of center time/total distance for the first 30 min was also calculated as "anxiety index". *patDp/+* mice significantly showed the higher ratio than WT mice (Fig. 1E; t_{42}=2.2, p<0.05, t-test). These results suggest that *patDp/+* mice exhibited increased anxiety-like behavior and/or decreased locomotor exploration in novel environments.

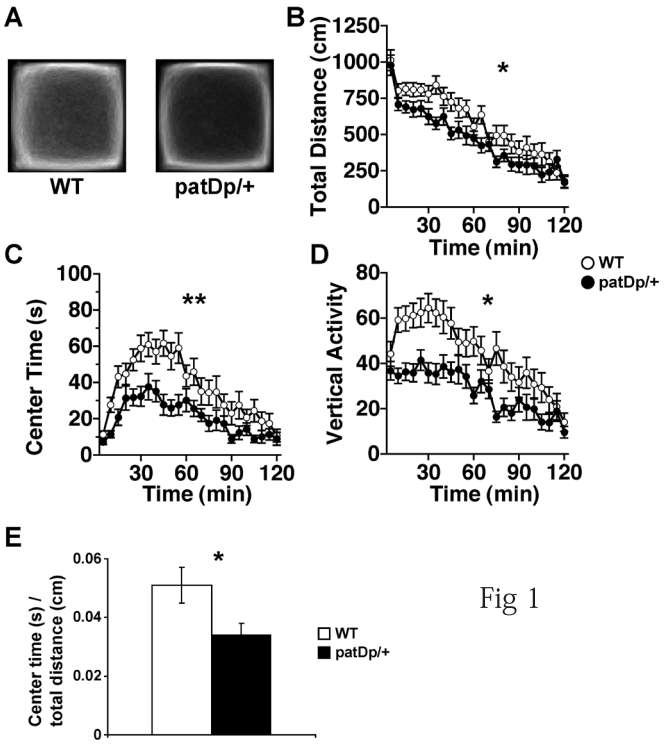

Fig 1

We used the novelty suppressed feeding test to determine whether *patDp/+* mice exhibit anxiety-like behaviors or

are the lowered motivation caused by reduced activity. In this test, *patDp/+* mice had longer latencies to feed than WT mice (Fig. 2B). Furthermore, most WT mice ate chow within 5 min, whereas approximately 60% of *patDp/+* mice did not (Fig. 2A). Kaplan-Meier survival analysis and the Mantel-Cox log-rank test revealed that this was a significant difference ($p<0.01$). The amount of food consumed in the home cage after the test and body weight decreased (%) by 24 h food deprivation were not significantly different between *patDp/+* and WT mice ($t_{25}=1.57$, $p=0.13$, *t*-test, for food consumed, $t_{25}=0.51$, $p=0.61$ for body weight, data not shown). These results indicate that *patDp/+* mice have increased anxiety-like behavior and/or decreased activity, even when food deprivation opposes these effects.

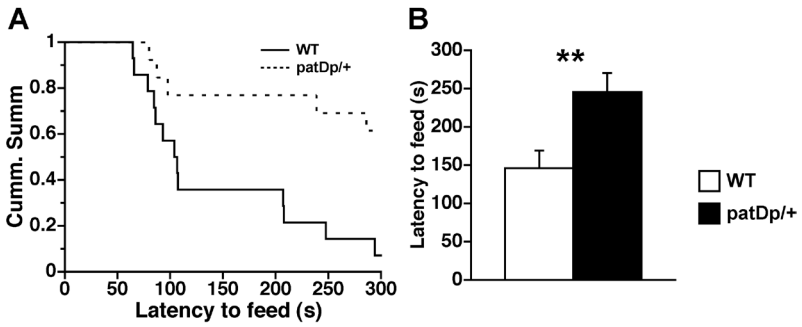

Fig 2

To establish the relationship between brain neurochemistry and behavioral disruptions in *patDp/+* mice, we quantified levels of biogenic monoamines *ex vivo*, including 5-HT and its major metabolite 5-hydroxyindoleacetic acid (5-HIAA), using HPLC in several adult brain regions. We specifically focused on 5-HT because it is one of the most notable molecules for the pathophysiology of ASDs. Levels of 5-HT and 5-HIAA were significantly decreased in several brain regions from *patDp/+* mice (5-HIAA; OB, Ce, Mid, $t_{18}=2.72$, 2.20, 2.99, $p<0.05$, 5-HT; OB, Mid, $t_{18}=2.23$, 2.67, $p<0.05$). In contrast, there was no change in levels of the other monoamines, dopamine (DA) and norepinephrine (NE), compared with WT mice in any brain region. These findings suggest that the neurochemical differences between *patDp/+* and WT mice are specific for the serotonergic system. However, metabolic rates of 5-HT turnover, determined from the ratio of 5-HIAA to 5-HT, in *patDp/+* mice were not altered compared with WT mice, suggesting that monoamine oxidase (MAO) functions at a similar rate in both WT and *patDp/+* adult mice. Collectively, these results demonstrate alterations in the serotonergic system of *patDp/+* mice that may contribute to their behavioral phenotypes.

ASDs are thought to be developmental disorders, and there are several neurodevelopmental disorders wherein subjects exhibit low brain levels of biogenic amines. Thus, we performed a comprehensive investigation of brain monoamine levels in several brain regions of mice from postnatal weeks 1 to 3. Two-way ANOVA revealed that 5-HT concentrations in *patDp/+* mice tended to decrease in all brain regions tested over these developmental stages (genotype effect) (Fig. 3). We also found that DA and its metabolites homovanillic acid (HVA) and 3,4-dihydroxyphenylacetic acid (DOPAC) tended to increase over these developmental stages in some brain regions of *patDp/+* mice, such as the pons and medulla (Fig. 3). Conversely, brain levels of NE and its metabolite 3-methoxy-4-hydroxyphenylglycol (MHPG) did not consistently increase or decrease over these developmental stages in *patDp/+* mice . These results suggest that 5-HT signaling in the brains of *patDp/+* mice is altered during these developmental stages.

Fig 3

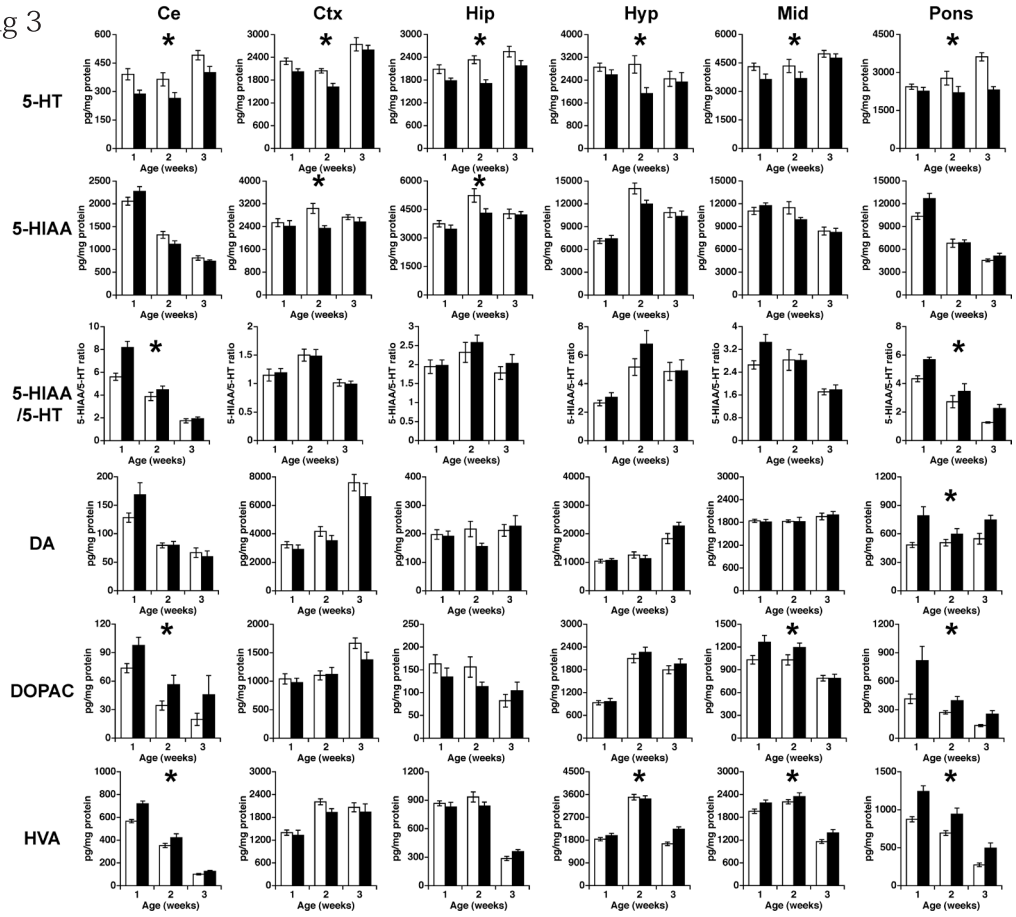

Discussion & Conclusion

Major autistic phenotypes such as impaired social interaction in the 3-chamber sociability test and perseverative responding in reversal learning tests have been reported in *patDp/+* mice from either the C57BL/6J or 129S6 strains. In the present study, we report additional behavioral abnormalities of C57BL/6J *patDp/+* mice. When conducting daily breeding procedures with these animals, we observed decreased movements and behavior. In support of this observation, *patDp/+* mice exhibited decreased exploratory activity in the open field test. Furthermore, this abnormal phenotype was observed in other behavioral tests, such as the Y-maze test. Collectively, these findings strongly suggest that *patDp/+* mice have decreased exploratory activity. In an evaluation of the underlying causes of decreased exploratory activity in *patDp/+* mice, motor tests showed that *patDp/+* mice possess normal motor coordination. This excludes the possibility that decreased exploratory activity in these animals resulted from dysfunctional motor coordination. Furthermore, lower exploratory activity in *patDp/+* mice overcame increased appetite induced by 24 hours of food deprivation. As another example, in the marble burying test, *patDp/+* mice buried significantly fewer marbles than WT mice, but no difference in locomotor activity between *patDp/+* and WT mice were observed. These results further suggest that decreased activity in *patDp/+* mice may be elicited by anxiety induced by novel environmental conditions. However, decreased activity in *patDp/+* mice was observed in their home cages and no significant differences were observed

in the elevated plus maze test. Regarding these discrepancies, it is important to note that these measures are not inherently correlated and may reflect unique aspects of anxiety-like behaviors. However, reduced locomotor activity in the open field test was not reported in 129S6 mice. This may be due to lower levels of spontaneous locomotor activity in 129S6 mice compared with C57BL/6J. Interestingly, longer latencies to approach food during either eight-arm radial maze or T-maze tests have been observed in 129S6 mice. Taken together, these findings indicate that the *patDp/+* phenotype includes decreased exploratory activity, increased fear, or decreased motivation. In addition, patients with paternally derived duplication of 15q11-13 display motor coordination problems. The mouse cerebellum is involved in exploratory behavior and motivational processes, and reduced exploration and stereotyped behavior in children with autism is linked with cerebellar hypoplasia. Thus, the cerebellum of *patDp/+* mice provides an intriguing target for further study.

The results of the present study demonstrate behavioral and neurochemical abnormalities in *patDp/+* mice backcrossed to the C57BL/6J strain. These animals displayed lower locomotor/exploratory activity in most of the activity-related behavioral tests studied, and showed decreased 5-HT levels in several brain regions during development and at adulthood. We also found that tissue levels of DA and its metabolites were increased during development. Based on these findings, we propose that alterations in the serotonergic system at an early stage may contribute to abnormal behavioral phenotypes in adult *patDp/+* mice.

References

1) Tamada, K., Tomonaga, S., Hatanaka, F., Nakai, N., Takao, K., Miyakawa, T., Nakatani, J. and Takumi, T. Decreased exploratory activity in a mouse model of 15q duplication syndrome; implications for disturbance of serotonin signaling. ***PLoS ONE*** 15, e15126, 2010.

2) Takumi, T. A humanoid mouse model of autism. ***Brain Dev.*** 32, 753-758, 2010.

3) Nakatani, J., Tamada, K., Hatanaka, F., Ise, S., Ohta, H., Inoue, K., Tomonaga, S., Watanabe, Y., Chung, Y. J., Banerjee, R., Iwamoto, K., Kato, T., Okazawa, M., Yamauchi, K., Tanda, K., Takao, K., Miyakawa, T., Bradley, A. and Takumi, T. Abnormal behavior in a chromosome-engineered mouse model for human 15q11-13 duplication seen in autism. ***Cell*** 137, 1235-1246, 2009. Cover Picture.

Novel signaling pathway from DNA damage repair to RNAi

Hitoshi Nakayashiki
Kobe University
hnakaya@kobe-u.ac.jp

Abstract

RNA silencing is thought to have evolved as a mechanism to defend the genome against invading viruses and endogenous transposable elements. However, exactly how genome defense against transposable elements is triggered remains largely unknown at the molecular level. Here we show that the conserved catalytic DD(35)E motif in integrase was crucial for inducing RNA silencing against the LTR-retrotransposn MAGGY in the fungus *Magnaporthe oryzae.*

Keywords: RNAi, RNA silencing, DNA damage, LTR-retrotransposon

Introduction

To date, the molecular mechanisms leading to transposon suppression by RNA silencing have been demonstrated in some cases. For example, fortuitous read-through transcription of dispersed Tc1 copies can lead to dsRNA formation as a result of a 'snap back' of the terminal inverted repeats (TIR), which serve as a trigger for RNA silencing against the element (1). In the case of the MuDR transposon in maize, a locus, called Mu killer (Muk), which resulted from the inverted duplication of a partially deleted autonomous MuDR element, produces a hairpin transcript that can form dsRNA, which is processed into small RNAs (2). It is not clear, however, how generally applicable these mechanisms are for triggering RNA silencing against various types of transposable elements. Relatively long TIRs, which could serve as a source for dsRNA triggers, are detectable only in certain groups of DNA transposons. A significantly large proportion of transposable elements, especially retroelements, do not carry inverted repeats that are any longer than the length of siRNAs (21-26 nt). In addition, if spontaneous generation of inverted duplication of transposable elements in the genome were a prerequisite for triggering RNA silencing, it would not be a potent genome defense mechanism.

To address molecular mechanisms that lead to the initiation of RNA silencing against retrotransposons, we made a series of deletion and site-directed mutants of the Ty3/Gypsy LTR-retrotransposon, MAGGY, identified in the phytopathogenic fungus, *Magnaporthe oryzae*, as a model. Previous studies showed that the MAGGY element was targeted for RNA silencing and DNA methylation in the original host *M. oryzae* strains, as well as in MAGGY-free strains when introduced by transformation (3,4).

Results

We first constructed deletion and frameshift mutants of MAGGY in the gag (Δgag), reverse transcriptase (ΔRT) and integrase (ΔINT) domains, and examined their ability to trigger RNA silencing. In addition, a site-directed mutant (T5244G) of the chromodomain-like module in the integrase domain was also examined.

The mutant and wild-type MAGGY constructs were introduced into the MAGGY-free *M. oryzae* strain, Br48. All the MAGGY mutants were severely impaired in transposition activity (data not shown). Northern analysis revealed that the level of MAGGY siRNA accumulation, a hallmark of RNA silencing, differed significantly among the mutants. No detectable siRNA accumulation was found in the Δgag and ΔRT transformants, except for a very faint signal in one of the ΔRT transformants. Some siRNA accumulation was detected in the ΔINT transformants while, surprisingly, the siRNA accumulation in the T5244G transformants was almost the same as that in the wild-type MAGGY transformants. The type of mutant, rather than the copy number integrated in the genome, appeared to account for the level of siRNA accumulation in the transformants (data not shown), suggesting that some biological activity of MAGGY was crucial for the induction of siRNA accumulation in *M. oryzae*.

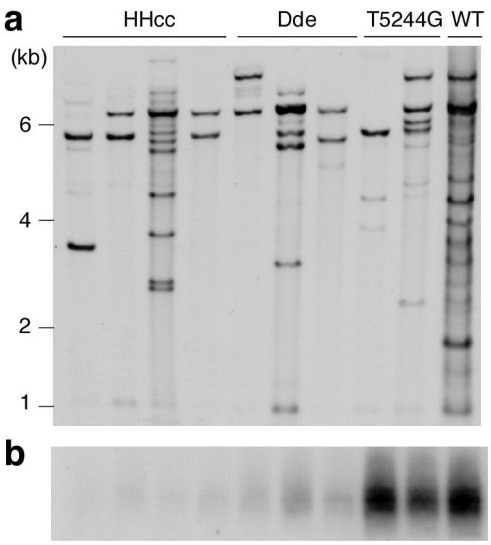

Figure 1. The levels of siRNA accumulation induced by transposition-deficient MAGGY integrase mutants were largely dependent on the type of mutation rather than on the copy number in the genome. Genomic Southern (a) and northern analysis (b) of Magnaporthe oryzae transformants with transposition-deficient MAGGY mutants. MAGGY siRNAs were detected in (b). Equal loading of total RNA was estimated by EtBr staining of predominant RNAs. HHcc, zinc finger mutant; Dde, catalytic core mutants; T5244G, chromodomain mutant; WT, wild-type. kb. kilo-basepairs.

Site-directed mutations were then generated in the N-terminus conserved signature, Zinc finger and DD(35)E motifs, which are widely conserved among integrases of retroviruses and retrotransposons. Intriguingly, northern analysis revealed that the level of siRNA accumulation was significantly reduced in the Zinc finger (HHcc) and DDE (Dde) mutants regardless of their genomic copy numbers, indicating a crucial role of active integrase in the induction of RNA silencing (Fig. 1a, b). We further examined which step of retrotransposition was blocked in the DDE mutants. The cDNA intermediate of MAGGY was formed in the DDE mutants as well as in wild-type MAGGY. Translocation of the cDNA intermediate to the nucleus was also not impaired in the DDE mutants (data not shown). There results suggested that the integrase-mediated reaction in the nucleus could be a key process for invoking RNA silencing against the element.

Discussion & Conclusion

Due to environmental factors and normal metabolic processes, hydrolytic DNA damage is estimated to occur at a rate of several 10^4 lesions per cell per day (5). To immediately detect and repair DNA damage on the huge molecular complex that is the chromosome, genome surveillance systems for DNA damage should be efficient and exhaustive. It would be highly effective if such surveillance systems participated in generating signals for RNA silencing against transposable elements when DNA damage caused by the elements is detected and repaired. This study indicated that such a connection between RNA silencing and DNA damage could indeed exist. Detailed molecular mechanisms generating signals from DNA damage to RNA silencing are intriguing points to address in the future as an extension from this work.

References

1) Sijen, T. & Plasterk, R. H. Transposon silencing in the *Caenorhabditis elegans* germ line by natural RNA. *Nature* **426**, 310-314 (2003).

2) Slotkin, R. K., Freeling, M. & Lisch, D. Heritable transposon silencing initiated by a naturally occurring transposon inverted duplication. *Nat. Genet.* **37**, 641-644 (2005).

3) Murata, T. *et al.* siRNA-dependent and -independent post-transcriptional cosuppression of the LTR-retrotransposon MAGGY in the phytopathogenic fungus *Magnaporthe oryzae*. *Nucleic Acids Res.* **35**, 5987-5994 (2007).

4) Nakayashiki, H., Ikeda, K., Hashimoto, Y., Tosa, Y. & Mayama, S. Methylation is not the main force repressing the retrotransposon MAGGY in *Magnaporthe grisea*. *Nucleic Acids Res.* **29**, 278-284 (2001).

5) Bernstein,C. & Bernstein,H. *Aging, Sex and DNA Repair* (Academic Press Inc., San Diego, 1991).

Identification of autoimmune susceptible genes using murine models of autoimmune diseases.

Taku Okazaki
Institute for Genome Research, The University of Tokushima
tokazaki@genome.tokushima-u.ac.jp

Abstract

Programmed cell death 1 (PD-1) belongs to the CD28/CTLA-4 co-receptor family and negatively regulates immune responses. PD-1KO mice serve as a useful model to analyze the influence of genetic background on autoimmune diseases because PD-1KO mice develop different types of autoimmune diseases when genetic background is replaced by backcrossing. To date, we have reported that PD-1KO mice develop autoimmune dilated cardiomyopathy and gastritis, myocarditis, polyneuropathy and sialadenitis, and accelerated type I diabetes on BALB/c, MRL, NOD-H2b, and NOD backgrounds, respectively. Based on these findings, we are trying to identify strain-specific genetic factors that determine the target organ or magnitude of the autoimmune response.

By genetic linkage analyses using PD-1KO mice, we have identified 2 to 7 loci each for type I diabetes, myocarditis, polyneuropathy, gastritis, and sialadenitis. We have been trying to generate congenic mice for these loci to analyze their effect and identify their causal genes. So far, we have succeeded in the genetic reconstitution of type I diabetes in C57BL/6 mice by introducing 4 NOD-derived chromosomal regions and PD-1 deficiency.

These results indicate that these 4 loci and PD-1 deficiency are sufficient for the development of type I diabetes in C57BL/6 mice. Further analyses are expected to identify their causal genes and unravel the complete molecular pathology of the disease.

Keywords: autoimmunity, linkage analysis, co-stimulation, type I diabetes

Introduction

Since most autoimmune diseases are polygenic, analysis of the synergistic involvement of various immune-regulators is essential for the full understanding of the molecular pathology of these diseases. Linkage analyses in animal models of autoimmune diseases have provided informative results on the polygenic regulation of autoimmune diseases. Many autoimmune susceptible loci have been identified in each animal model and the immunological function of each locus has been vigorously analyzed by generating various congenic animals. However, the mutual relationship of these loci has not been analyzed well because of the many possible combinations and rather limited number of congenic mice, which can be established only by repeated backcrossing. Moreover, the low resolution of the linkage analyses on polygenic diseases prevented identification of a single gene from each susceptibility locus. Taken together, our knowledge about the polygenic regulation of autoimmune diseases is very limited.

Programmed cell death 1 (PD-1), an immuno-receptor belonging to the CD28/CTLA-4 family provides negative co-stimulation to antigen stimulation by recruiting the protein tyrosine phosphatase, SHP-2 (src homology 2-domain containing tyrosine phosphatase 2).[1] PD-1 deficiency has been shown to accelerate autoimmune predisposition and to induce autoimmune diseases.[1-3] PD-1 knock out (PD-1KO) mice develop lupus-like glomerulonephritis and arthritis on the C57BL/6 background, autoimmune dilated cardiomyopathy and gastritis on the BALB/c background, lethal myocarditis on the MRL background, acute type I diabetes on the NOD background, and polyneuropathy, sialadenits, and gastritis on the NOD.H2b background (Figure 1). The development of different forms of autoimmune diseases on different genetic backgrounds of mice indicates that autoimmune phenotypes of PD-1KO mice are influenced by other genetic factors. Conversely, we may be able to identify strain specific autoimmune susceptible genes more efficiently by using PD-1KO mice.

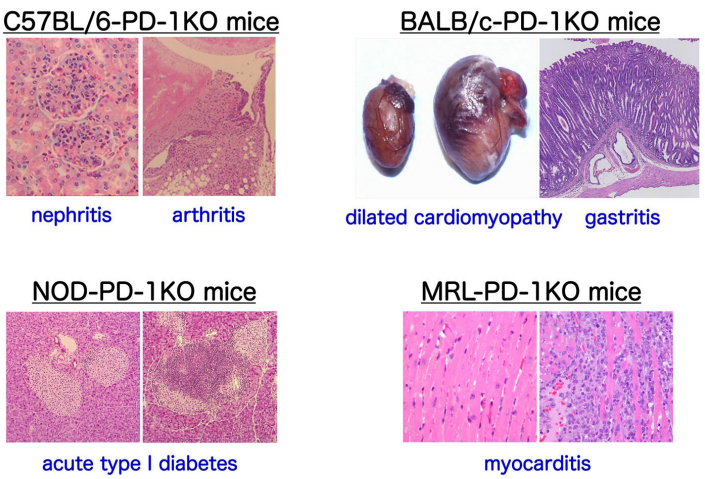

Figure 1. Autoimmune diseases in PD-1KO mice. PD-1KO mice develop lupus-like glomerulonephritis and arthritis on the C57BL/6 background, autoimmune dilated cardiomyopathy and gastritis on the BALB/c background, acute type I diabetes on the NOD background, and lethal myocarditis on the MRL background.

Results

We have performed genetic linkage analyses of type I diabetes using F2 and BC1 progenies of NOD-PD-1KO mice and C57BL/6-PD-1KO mice. Among more than 20 reported loci for type I diabetes (*Idd* loci), only 2 of them (*Idd1* and *Idd17*) showed significant association to type I diabetes in the BC1 experiment. In the F2 experiment, we identified two new susceptible loci for type I diabetes (*Iddp1* and *Iddp2*), which functioned in a dominant fashion.[4] Then, we started to generate congenic mice in which these 4 loci are derived from NOD mice but all the other chromosomal regions are derived from C57BL/6 mice (C57BL/6.*Idd1*/*17*/*p1*/*p2* mice). As expected C57BL/6.*Idd1*/*17*/*p1*/*p2*-PD-1KO mice developed type I diabetes, indicating that these 4 loci are sufficient for the development of type I diabetes in C57BL/6-PD-1KO mice. We have planed to generate 10 lines of sub-congenic mice that harbor shorter NOD-derived chromosomal regions. To date, 3 of them have been successfully generated and the other lines are under construction.

Because *Idd1*, which contains MHC genes showed very high association to type I diabetes in the linkage analysis, we have introduced NOD congenic mice carrying C57BL/10-derived MHC haplotype (NOD.H2b) from Jackson laboratory. NOD.H2b mice did not develop type I diabetes even in the absence of PD-1 gene as expected. However, NOD.H2b-PD-1KO mice developed

several autoimmune phenotypes including polyneuropathy, gastritis, and sialadenitis.[2] By genetic linkage analyses using BC1 progenies of NOD.H2b-PD-1KO mice and C57BL/6-PD-1KO mice, we have identified 7 loci for polyneuropathy. In addition, 2, 4, and 7 loci for sialadenitis, gastritis, and vasculitis, respectively were identified.[5] Based on these findings, we have started to generate various kinds of congenic mice that may either develop or escape from each phenotypes. To date, the backcrossing has been repeated for 3 to 5 generations.

Next, we have performed genetic linkage analyses of myocarditis using F2 progenies of MRL-PD-1KO mice and BALB/c-PD-1KO mice and identified 5 and 2 loci on MRL and BALB/c chromosomes, respectively. We have started to introduce 5 MRL loci into BALB/c mice by backcrossing. To date, the backcrossing has been repeated for 5 generations and we have started the intercross to generate homozygous mice.

Discussion & Conclusion

In the current project, we have been trying to identify genetic factors that function together with PD-1 deficiency to induce autoimmune diseases. It is noteworthy that type I diabetes was genetically reconstituted in diabetes-resistant strain, C57BL/6 mice by introducing 4 NOD-derived chromosomal regions and PD-1 deficiency. The successful reconstitution indicates that these 5 genetic factors are sufficient for the development of type I diabetes in C57BL/6 mice and that the clarification of these factors leads to the comprehensive understanding of the molecular mechanisms of type I diabetes.

The generation of congenic mice needs a long time and enormous efforts. For example, we are trying to introduce 5 MRL-derived chromosomal regions into BALB/c mice. The probability of a transmission of a 50 cM chromosomal region from a heterozygous parent to its progeny without internal recombination is 1 out of 4. Therefore, we have to generate more than 1,000 (4^5=1024) mice to make one generation forward. In addition, it is still hard to make these regions homozygous. The expectation value for the progeny that is homozygous for all 5 chromosomal regions (50 cM each) is 1 out of 1,048,576 (16^5). Although the actual frequencies are higher than these values because most of the regions are shorter than 50 cM and we can make 5 regions homozygous in a stepwise manner, the backcrossing took longer time than expected. Although we are aware that we have to improve our system, the generation of congenic mice is the only method that allows us to examine the sufficiency of identified loci for the disease development and congenic mice would be irreplaceable materials for further analyses when diseases are successfully reconstituted.

More and more practical studies are favored these days and grants for basic and time-consuming studies like us are limited. Therefore, we really appreciate the generous support by the Novartis Foundation (Japan) for the Promotion of Science.

References

1) Okazaki T and Honjo T. The PD-1-PD-L pathway and immunological tolerance. Trends. Immunol. 27:195-201 (2006)

2) Yoshida T, Jiang F, Honjo T, and Okazaki T. PD-1 deficiency reveals various tissue-specific autoimmunity by H-2^{b} and dose-dependent requirement of H-2^{g7} for diabetes on NOD background. Proc. Natl. Acad. Sci. USA. 105:3533-3538 (2008)

3) Wang J, Okazaki IM, Yoshida T, Chikuma S, Kato Y, Nakaki F, Hiai H, Honjo T, Okazaki T. PD-1 deficiency results in the development of fatal myocarditis in MRL mice. Int Immunol. 22:443-52 (2010)

4) Wang J, Yoshida T, Nakaki F, Hiai H, Okazaki T, and Honjo T. Establishment of NOD-*Pdcd1*$^{-/-}$ mice as an efficient animal model of type I diabetes. Proc. Natl. Acad. Sci. USA. 102:11823-11828 (2005)

5) Jiang F, Yoshida T, Nakaki F, Terawaki S, Chikuma S, Kato Y, Okazaki IM, Honjo T, and Okazaki T. Identification of QTLs that modify peripheral neuropathy in NOD.*H2*^{b}–*Pdcd1*$^{-/-}$ mice. Int. Immunol. 21:499-509 (2009)

The Mechanisms How Myocardial Ischemia-reperfusion Initiates Inflammatory Response in the Myocardium

Masafumi Takahashi
Division of Bioimaging Sciences,
Center for Molecular Medicine, Jichi Medical University
masafumi2@jichi.ac.jp

Abstract

Inflammation plays a key role in the pathophysiology of myocardial ischemia-reperfusion (I/R) injury; however, the mechanism by which myocardial I/R induces inflammation remains unclear. Recent evidence indicates that a sterile inflammatory response triggered by tissue damage is mediated through a multiple-protein complex called the inflammasome. In the present study, we investigated the role of inflammasome in myocardial I/R injury. Here, we have shown that inflammasomes are formed by I/R and that its subsequent activation of inflammasomes leads to interleukin-1β (IL-1β) production, resulting in inflammatory responses such as inflammatory cell infiltration and cytokine expression in the heart. In mice deficient for ASC (apoptosis-associated speck-like adaptor protein) and caspase-1, these inflammatory responses and subsequent injuries, including infarct development and myocardial fibrosis and dysfunction, were markedly diminished. Our results demonstrate the molecular basis for the initial inflammatory response after I/R and suggest that the inflammasome is a potential novel therapeutic target for preventing myocardial I/R injury.

Keywords: Cytokine, Heart, Inflammation, Interleukin, Leukocyte

Introduction

Increasing evidence indicates that inflammation is involved in the pathophysiology of myocardial I/R injury [1]. One prominent and early mediator for inflammation in I/R injury is IL-1β [2]. In the generation of IL-1β, pro-IL-1β, an inactive precursor, undergoes proteolysis by the converting enzyme caspase-1. Caspase-1 is activated within a cytosolic multiprotein complex—the inflammasome. The inflammasome contains adaptor protein ASC which in turn recruits and activates caspase-1 [3,4]. Therefore, we hypothesized that the inflammasome is an initial sensor for danger signal(s) in myocardial I/R injury. In the present study, we investigated the role of the inflammasome and ASC in the pathophysiology of myocardial I/R injury.

Results

We first investigated whether ASC was expressed in myocardial tissues obtained from patients who had died after an acute myocardial infarction and found that ASC was highly expressed in the infiltrated inflammatory cells and weakly expressed in cardiomyocytes and the interstitial

cells. Similarly, when experimental myocardial I/R was produced by occluding the left anterior descending followed by reperfusion in mice (C57BL/6), ASC were clearly expressed at the site of the injured myocardium. To determine whether ASC is critical for myocardial I/R injury, we used mice deficient for ASC. ASC deficiency clearly reduced myocardial infarct areas and improved function in a murine model of myocardial I/R injury. Furthermore, ASC deficiency attenuated inflammatory responses, such as the infiltration of macrophages and neutrophils and the expression of inflammatory cytokines, in the injured myocardium. However, the capillary density was not influenced by ASC deficiency. Supporting this finding, flow cytometry analysis showed no effect of ASC deficiency on the percentage of peripheral $CD34^{+}/Flk\text{-}1^{+}$ cells (an ordinary endothelial progenitor cell marker) after myocardial I/R injury.

Discussion & Conclusion

There is increasing evidence that indicates the importance of inflammation in the pathophysiology of myocardial I/R injury [1]. For instance, interventions targeted at leukocytes or inflammatory mediators substantially reduce myocardial I/R injury. In particular, the neutralization of IL-1□ reduces injury, suggesting that IL-1β is the key mediator in the pathophysiology of myocardial I/R injury [2,5]. This finding is supported by the observed reduction in injury after myocardial infarction in the absence of caspase-1 activity. However, recent evidence indicates that sterile inflammation is triggered by tissue damage, and endogenous danger signals are mediated by the inflammasome. Thus, we hypothesized that the inflammasome is an initial sensor in myocardial I/R injury and showed that ASC deficiency considerably improves inflammatory responses and subsequent injury after myocardial I/R [6]. These findings highlight the importance of the inflammasome in the initial inflammatory response to myocardial I/R injury.

Several limitations in this study should be noted. First, although the present study demonstrated that inhibition of initial inflammation improved cardiac function and remodeling after I/R, inflammation in myocardial I/R has been shown to be not only deleterious not also beneficial in the process of myocardial damage and remodeling. Second, although the inflammatory response after myocardial infarction in mice shares many common characteristics with higher mammalian species and is a excellent model for exploration of cellular and molecular mechanisms, we should understand the potential limitations of extrapolating data from mice to humans. Thus, further investigations are necessary to understand the precise role of inflammasome in myocardial I/R injury.

In summary, this study is the first to demonstrate the essential role of the inflammasome in the pathophysiology of myocardial I/R injury. Moreover, our results suggest that the inflammasome is a novel therapeutic target for preventing myocardial I/R injury.

References

1) D.M. Yellon, D.J. Hausenloy, Myocardial reperfusion injury, N Engl J Med 357 (2007) 1121-1135.

2) A.A. Wanderer, Ischemic-reperfusion syndromes: biochemical and immunologic rationale for IL-1 targeted therapy, Clin Immunol 128 (2008) 127-132.

3) F. Martinon, A. Mayor, J. Tschopp, The inflammasomes: guardians of the body, Annu Rev Immunol 27 (2009) 229-265.

4) N. Yajima, M. Takahashi, H. Morimoto, Y. Shiba, Y. Takahashi, J. Masumoto, H. Ise, J. Sagara, J. Nakayama, S. Taniguchi, U. Ikeda, Critical role of bone marrow apoptosis-associated speck-like protein, an inflammasome adaptor molecule, in neointimal formation after vascular injury in mice, Circulation 117 (2008) 3079-3087.

5) M.W. Hwang, A. Matsumori, Y. Furukawa, K. Ono, M. Okada, A. Iwasaki, M. Hara, T. Miyamoto, M. Touma, S. Sasayama, Neutralization of interleukin-1beta in the acute phase of myocardial infarction promotes the progression of left ventricular remodeling, J Am Coll Cardiol 38 (2001) 1546-1553.

6) M. Kawaguchi, M. Takahashi, T. Hata, Y. Kashima, F. Usui, H. Morimoto, A. Izawa, Y. Takahashi, J. Masumoto, J. Koyama, M. Hongo, T. Noda, J. Nakayama, J. Sagara, S. Taniguchi, U. Ikeda, Inflammasome activation of cardiac fibroblasts is essential for myocardial ischemia/reperfusion injury, Circulation 123 (2011) 594-604.

Novel strategy towards therapeutic approach for lissencephaly using calpain inhibition.

Hirotsune Shinji
Osaka City University Graduate School of Medicine
shinjih@med.osaka-cu.ac.jp

Abstract

Lissencephaly is a devastating neurological disorder characterized by smooth cerebral surface, thick cortex and dilated ventricules due to defective neuronal migration. *LIS1* was identified as the gene mutated in lissencephaly patients, and was found to be a regulator of cytoplasmic dynein. Interestingly, more than half of LIS1 protein is degraded at the cell cortex after transport to the plus-end of MTs via calpain-dependent proteolysis. We demonstrated that an inhibition or knockdown of calpain protected LIS1 from proteolysis resulting in the augmentation of LIS1 levels in *Lis1*+/- mouse embryonic fibroblast (MEF) cells, which lead to rescue of the aberrant distribution of cytoplasmic dynein and intracellular components including mitochondria. We also show that presence of calpain inhibitors improves neuronal migration of *Lis1*+/- cerebellar granular neurons. Strikingly, intra-peritoneal injection of ALLN to pregnant *Lis1*+/- dams rescued apoptotic neuronal cell death, reduction of brain weight and neuronal migration defects in *Lis1*+/- offspring. Furthermore, knockdown of calpain during neuronal migration by *in utero* injection of stRNA against calpain rescued cortical layering in *Lis1*+/- mice. Thus, our findings suggest that the inhibition of calpain is a potential therapeutic intervention for the devastating human disorder lissencephaly.

Keywords: Lissencephaly, Calpain inhibitor, Haploinsufficiency

Introduction

Lissencephaly is a severe human neuronal migration defect characterized by a smooth cerebral surface, mental retardation and seizures. LIS1 was the first gene cloned in any organism important for neuronal migration, as it was deleted or mutated in humans with lissencephaly in a heterozygous fashion. LIS1 and its binding protein, NDEL1 regulate cytoplasmic dynein. We recently reported that LIS1 and NDEL1 cooperatively regulate anterograde transport of cytoplasmic dynein in a kinesin dependent fashion. In addition, NDEL1 also regulates microtubule organization with Aurora-A, which is essential for neurite extension. In the series of experiments, we found that half of LIS1 is degraded via calpain-dependent proteolysis, and that inhibition or knockdown of calpains protects LIS1 from proteolysis, which suggests that calpain inhibitor will be applicable towards therapeutic intervention for lissencephaly.

Results

1. We first examined the response of LIS1 protein levels to the inhibition of calpain by ALLN using mouse embryonic fibroblast (MEF) cells established from Lis1+/+ or Lis1+/- embryos. We explored time course of the response. LIS1 protein gradually increased in the Lis1+/- MEF cells, and reached to plateau two hours after the start of ALLN treatment (Fig. 1). After two hours of administration of ALLN, LIS1 protein was increased from 0.5 (where 1.0 is equivalent to wild-types levels of LIS1) to 1.1. To address the effect of other calpain inhibitors, we also examined the effect E64d and obtained similar results (Fig. 1).

Fig. 1

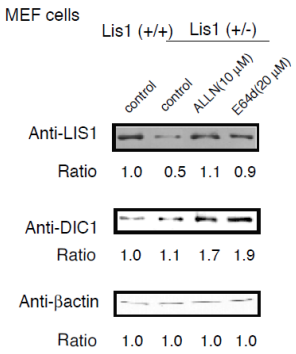

2. We previously demonstrated that LIS1 is required for plus-end directed transport of cytoplasmic dynein[5]. When Lis1 is mutated, the centrosomal accumulation of LIS1 is reduced, resulting in the impairment of plus-end directed transport of cytoplasmic dynein. As a result, cytoplasmic dynein is abnormally accumulated around the centrosome. Therefore, we determined whether preventing the degradation of LIS1 rescued the distribution of LIS1 and cytoplasmic dynein within the Lis1+/- MEF cells. Treatment of Lis1+/- MEF cells by ALLN or E64d clearly improved the reduction of centrosomal concentration of LIS1 after 2 hours of the treatment.

   In addition, the abnormal accumulation of cytoplasmic dynein around the centrosome was rescued by ALLN or E64d treatment (Fig. 2).

Fig. 2

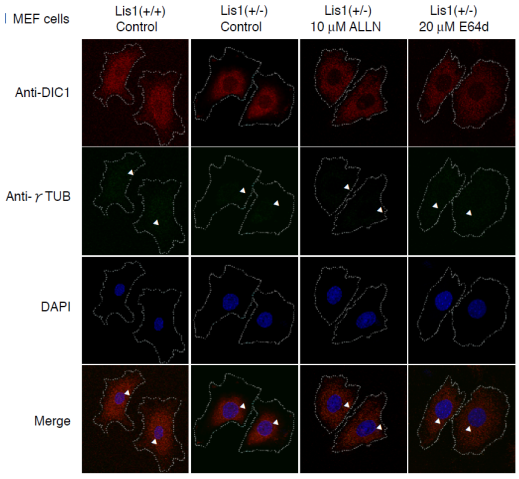

3. To define the effect of calpain inhibitors on mammalian neuronal migration, we used mouse cerebellar granule neurons in an in vitro migration assay combined with ALLN or E64d treatment. We previously showed that Lis1+/– cerebellar granule neurons displayed defective migration compared with Lis1+/+ cerebellar granule neurons. We confirmed that Lis1+/– cerebellar granule neurons displayed a leftward shift of the bin distribution of migration distance, and the mean distance decreased by 50% from the WT level. We next tested whether

Fig. 3

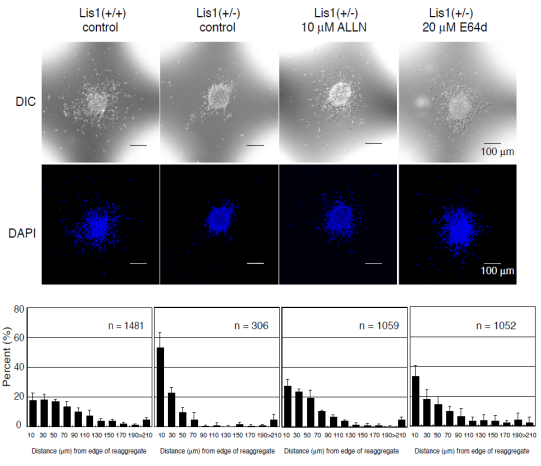

ALLN or E64d treatment was sufficient to rescue the migration defect in Lis1+/– cerebellar granule neurons. Lis1+/– cerebellar granule neurons in the presence of ALLN or E64d displayed a shift in migration distance bins back toward the right, with a similar distribution to that of WT neurons (Fig. 3).

4. We next examine whether the administration of ALLN to pregnant Lis1+/- dams rescued defective neuronal migration in vivo. In Lis1+/- mice, apoptotic cell death was clearly increased as the previous report. In contrast, administration of ALLN suppressed apoptotic cell death in Lis1+/- mice. We next examined the effect of ALLN on the cortical and hippocampal layering of neurons. Lis1+/- mice exhibited laminar splitting and discontinuities of pyramidal cells in the CA3 and CA2 region of the hippocampus. After administration of ALLN in utero, Lis1+/- mice also displayed splitting and diffuse pyramidal cells of the hippocampus, but these defects were markedly improved (Fig. 4). To examine cortical lamination, we analyzed Brn-1 immunoreactivity, to label interneurons of layer 2 and 3. In Lis1+/- mice, Brn-1 positive cells (which migrate at a later stages) exhibited a broader distribution compared to Lis1+/+ mice. Administration of ALLN resulted in more packed lamination in Lis1+/- mice.

Fig. 4

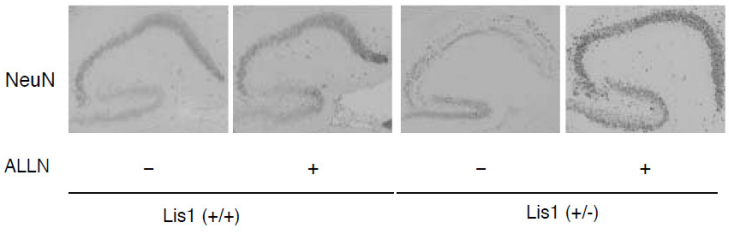

Discussion & Conclusion

LIS1 levels correlate with in vivo phenotypes in mice and humans. Reductions of LIS1 protein result in progressively more severe phenotypes in mice in a dose-dependent fashion. Recently, it was shown that increased LIS1 expression affects human and mouse brain development. In our case, inhibition of calpain activity results in normalization close to the wild type levels rather than accumulation of LIS1 in excess. We believe that the restoration of more normal LIS1 levels was one among others that calpain inhibition resulted in phenotypic improvement of Lis1+/- mice.

In spite of this encouraging first step in a preclinical model, several problems remain and must be overcome if this promising avenue of therapy can be eventually tested in human lissencephaly. It will probably be necessary to further refine the use of calpain inhibitors or select other drugs for the effective inhibition of LIS1 degradation. In addition, the safe and effective delivery of such drugs at early enough time points to achieve effective blood concentration will be essential for clinically effective treatment of human lissencephaly. Although it will not treat lissencephaly, there may be some benefits to restore LIS1 to more normal levels even after birth, since this may improve the often difficult to treat epilepsy displayed by patients with lissencephaly. To treat postnatal patients, delivering therapeutic agents across blood-brain barrier (BBB) will be essential. In spite of the challenges, our work provides a potential avenue to consider therapeutic strategies for early brain developmental defects such as lissencephaly due to LIS1 mutations, or any other disorder that results from haploinsufficiency.

References

1) Torisawa, T., Nakayama, A., Furuta, K., Yamada, M., Hirotsune, S., Toyoshima, YY. (2010) Functional dissection of LIS1 and NDEL1 towards understanding the molecular mechanism of cytoplasmic dynein regulation. **J Biol Chem** (in press)

2) Pramparo, T., Youn, YH., Yingling, J., Hirotsune, S., Wynshaw-Boris A. (2010) Novel embryonic neuronal migration and proliferation defects in Dcx mutant mice are exacerbated by Lis1 reduction. **J Neurosci** 30: 3002-3012.

3) Yamada, M., Toba, S., Takitoh, T., Yoshida, Y., Mori, D., Nakamura, T., Iwane, A. H., Yanagida, T., Imai, H., Yu-Lee, L. Y., Schroer, T., Wynshaw-Boris, A., and Hirotsune, S. (2010) mNUDC is required for plus-end-directed transport of cytoplasmic dynein and dynactins by kinesin-1, **EMBO J.** 29: 517-531.

4) Youn, Y. H., Pramparo, T., Hirotsune, S., and Wynshaw-Boris, A. (2009) Distinct dose-dependent cortical neuronal migration and neurite extension defects in Lis1 and Ndel1 mutant mice, **J Neurosci** 29, 15520-15530.

5) Yamada, M., Yoshida, Y., Mori, D., Takitoh, T., Kengaku, M., Umeshima, H., Takao, K., Miyakawa, T., Sato, M., Sorimachi, H., Wynshaw-Boris, A., and Hirotsune, S. (2009) Inhibition of calpain increases LIS1 expression and partially rescues in vivo phenotypes in a mouse model of lissencephaly, **Nat Med** 15, 1202-1207.

6) Mori, D., Yamada, M., Mimori-Kiyosue, Y., Shirai, Y., Suzuki, A., Ohno, S., Saya, H., Wynshaw-Boris, A., and Hirotsune, S. (2009) An essential role of the aPKC-Aurora A-NDEL1 pathway in neurite elongation by modulation of microtubule dynamics, **Nat Cell Biol** 11, 1057-1068.

III.

Reports from the Recipients of Grants for International Meetings

The 5th International Symposium on Filoviruses (Filo2010)

1. Representative
   Yoshihiro Kawaoka, D.V.M., Ph.D.
   Institute of Medical Science, The University of Tokyo

2. Opening period and Place
   April 18 (Sun) - 21 (Wed), 2010
   Sheraton Miyako Hotel Tokyo (Daigo, Saga, Ise, Magnolia)

3. Number of participants / Number of participating countries and areas
   107 participants from 15 countries

4. Total cost
   ¥23,702,085 JPY

5. Main use of subsidy
   Travel expenses for invited speakers

6. Result and Impression
   Due to the volcanic eruption in Iceland, many of the registrants and speakers could not fly to Tokyo. It caused program change and great decrease of the number of participants. Still meeting itself was a great success and closed with standing ovation to the organizers from the audience.

7. Additional description
   There was a great accomplishment in the filoviruses research, the organizers and the participants are now planning to publish the original work on filoviruses as a supplement to the Journal of Infectious Diseases.

The International Symposium on Protein Community

1. Representative
   Toshiya Endo (Nagoya University)

2. Opening period and Place
   Sept. 13-16, 2010

3. Number of participants / Number of participating countries and areas
   270/8（Japan, USA, UK, Germany, Netherland, Sweden, Korea, Taiwan）

4. Total cost
   ¥14,716,000 JPY

5. Main use of subsidy
   Travel expenses for a foreign invited speaker

6. Result and Impression

   The International Conference on Protein Community brought together nearly 300 scientists in Japan to exchange ideas on how proteins are expressed, folded, translocated, assembled, and disassembled in health, and the events that can go awry leading to a myriad of protein conformational diseases. The meeting, held in September, 2010, coincided with the 1,300th birthday of Nara, Japan's ancient capital, and provided a meditative setting for reflection on the impact of this field in biology and medicine and the success of this program in Japan since this group's first meeting in Kyoto on the Stress Response (1989) and in Awaji Island on the Life of Proteins (2005). The highlight was, without question, the social periods held after the long days of talks and posters at which graduate students, postdocs, and all of the speakers were together sitting on tatami-mats at low tables enjoying each others company in a relaxing and open forum. (Reported by Rick Morimoto)

7. Additional description

   The meeting report "The life of proteins: the good, the mostly good, and the ugly" (written by Richard I. Morimoto, Arnold J. M. Driessen, Ramanujan S. Hegde, and Thomas Langer) will appear in January 2011 issue of *Nature Structural and Molecular Biology*.

The 17th International RUNX Workshop

1. Representative
   Ichiro Taniuchi,
   President of the organizing committee for the 17th International RUNX Workshop , Team Leader, Laboratory for Transcriptional Regulation, RIKEN, RCAI

2. Opening period and Place
   From 11th July 2010 to 14th July 2010 at the Oriental Hotel Hiroshima, Hiroshima, JAPAN

3. Number of participants / Number of participating countries and areas
   102 participants including 61 participants from 13 oversea countries including Israel, France, Germany, United Kingdom, Scotland, USA, India, Thailand, Singapore, China, Taiwan, and Korea.

4. Total cost
   ¥6,730,347 JPY

5. Main use of subsidy
   The cost of the conference room (screen, projector, microphones, partitions, signs)

6. Result and Impression
   The meeting was very successful with total 52 oral presentations in 6 sessions and 10 poster presentations. Most participants had very nice impression on the organization of the meeting, in particular on the very smooth and on-time regulation of scientific program. All participants also enjoyed food and culture in Japan.

7. Additional description
   The Runx family genes were identified at the same time in 1993 from several fields such as virology, oncology and development. This history of discovery of Runx genes already represented multiple biological functions of Runx family genes, stimulating the researchers to set up the joint meeting to promote research of Runx genes. Then the 1st Runx workshop has started in 1994 just with a few laboratories and has been followed up annually. Because of a rapid growth of this research area and several epoch-making presentation with a meeting split of sharing unpublished results, the International RUNX Workshop became well recognized all over the world.
   The International RUNX Workshop came back to Japan this year since Dr. Yoshiakai Ito, Kyoto University at that time organized the 7th Runx workshop at Kyoto in 2000. Dr. Ichiro Taniuchi at RIKEN, Research Center for Allergy and Immunology, who is a present of the 17th International RUNX Workshop, selected Hiroshima as a meeting venue. Hiroshima had a disaster by Atomic Bomb attack and peoples in Hiroshima have been suffering from diseases mainly leukemia. Considering that one of the major topics in the Runx workshop is a leukemogensis by

Runx1/AML1 dysfunction as well as an international movement for an abolition of nuclear weapons, Dr. Taniuchi decided to have the meeting at Hiroshima. Indeed almost all participants visited the Hiroshima Peace Memorial Museum during the meeting.

The 18th international RUNX Workshop will be held next at San Diego in USA.

2010 International Polyamine Conference: Progress in Medicine and Life Sciences

1. Representative
   Senya Matsufuji, MD, PhD
   Professor, The Jikei University School of Medicine

2. Opening period and Place
   June 14 - 18, 2010
   Gotemba Kogen Resort (Gotemba-shi, Shizuoka, Japan)

3. Number of participants / Number of participating countries and areas
   Number of participants: 115 (26 from abroad and 86 domestic)
   Number of participating countries 13 (Finland, Ireland, Israel, Italy, Portugal, South Africa, South Korea, Spain, Sweden, UK, USA, Vietnam, and Japan)

4. Total cost
   ¥9,813,050

5. Main use of subsidy
   Travel and accommodation costs for invited speakers from abroad.

6. Result and Impression

   The conference consisted of 8 sessions with total of 33 oral presentations, including 18 invited lectures. They covered function, regulation, molecular evolution and structure of polyamines, polyamines in plants and microorganisms, polyamines in medicine, and polyamines as the target of drug discovery. In addition, 34 posters were presented and 4 of them were selected for short oral presentations in an extra session. The presentations clearly showed the progress in molecular-level understanding for the function and regulation of polyamines. Analyses of genetically altered model organisms revealed biological significance of the regulatory system of polyamines. Topics related to clinical medicine, such as diagnosis of early cancer with polyamine derivatives in urine and large-scale clinical trials for polyamine-related drugs drew much attention. In particular, lectures on drug discovery that targets polyamine function to control epigenetic gene regulation were impressive. Overall, the conference was a good blend of basic, applied, and clinical sciences. The extra-academic settings such as the venue in a resort with hot spring, fine food and drinks, and a view of Mt. Fuji also helped the success of the conference. The conference has greatly contributed to an advance of the research field both in Japan and the world.

7. Additional description

   The organizing committee greatly appreciates the NOVARTIS Foundation for the support.

The 16th International Conference of the International Society of Differentiation

1. Representative
   Naoto Ueno, Professor, National Institute for Basic Biology

2. Opening period and Place
   Nov. 14 – 18, 2010
   Nara-Ken New Public Hall, Kasugano-cho 101, Nara 630-8212, Japan

3. Number of participants / Number of participating countries and areas
   250 / 22 countries (Australia, Canada, China, Czech, Denmark, Finland, France, Germany, Hong Kong, Iran, Korea, Malaysia, Netherlands, Saudi Arabia, Singapore, Sweden, Switzerland, Taiwan, UK, USA & Japan)

4. Total cost
   ¥18,836,443 JPY (Subsidy from The Novartis Foundation for the Promotion Sciences: 400,000 JPY)

5. Main use of subsidy
   Invited speakers' travel expenses (Airfare & Accommodation fee)

6. Result and Impression
   The three and half day conference in which 250 attendants representing 22 countries got together turned out to be very successful in terms of richness in science as well as of deepness of interaction among attendants and speakers. Seamless stream of excellent presentations by oral speakers in addition to poster presentations from basic cell and developmental biology to stem cell and cancer biology stimulated all the attendants.

7. Additional description
   In this conference, we had students' session and offered platform presentation opportunity to 6 students from poster presentations. We also awarded three excellent students with Beverly McKinnell Award to encourage them.

第 24 期（2010 年度）助成事業報告

当財団は、1987 年 9 月 4 日文部大臣の認可のもとに設立されて以来、寄附行為に定めた研究助成を中心とした公益事業を行ってきました。2010 年度は、下記に示した総額 4,000 万円の助成事業を行っております。

ノバルティス研究奨励金	38 件（1 件	100 万円）	3,800 万円
研究集会助成	5 件（1 件	40 万円）	200 万円
		総額	4,000 万円

2010 年度ノバルティス研究奨励金贈呈者

この事業は、生物・生命科学およびそれに関連する化学の領域において、我が国で行われる創造的な研究の助成を目的としています。

（受付順、敬称略、所属・職位は申請時。助成金額：1 件 100 万円）

番号	氏　名	研究機関名	役職	研究テーマ
1	齊藤　峰輝	琉球大学大学院 医学研究科	准教授	HTLV-1 関連脊髄症発症における HBZ 遺伝子の作用機構の解明
2	大西　暁士	大阪バイオサイエンス研究所	研究員	光情報伝達における翻訳後修飾 SUMO 化の生理機能と作用機序の解明
3	渡辺　賢二	静岡県立大学薬学部	准教授	創薬を目的とした有用天然物の生合成遺伝子発現によるシンセティックバイオロジーの確立
4	大澤　春彦	愛媛大学大学院 医学系研究科	教授	レジスチンを標的とした 2 型糖尿病遺伝子・環境因子相互作用の分子機構解明へのエピジェネティクスの応用
5	藤田　恭之	北海道大学 遺伝子病制御研究所	教授	正常上皮細胞と癌細胞の相互作用－新規な癌治療法の開発を目指して－
6	永田　浩一	愛知県心身障害者コロニー発達障害研究所	部長	統合失調症の神経発達障害仮説の実験的検証
7	岩田　仲生	藤田保健衛生大学 医学部	教授	ゲノムとマウスを用いた精神疾患感受性の同定
8	合田　亘人	早稲田大学 理工学術院	教授	低酸素応答性転写因子による肝臓内代謝制御機構とその破綻に起因した代謝性疾患の発症機構の解明
9	高田　健介	徳島大学疾患ゲノム 研究センター	講師	末梢 T 細胞の恒常性を制御する自己認識のメカニズム
10	河村　和弘	秋田大学 医学部附属病院	講師	体外培養下でのヒト休眠原始卵胞の人為的活性化による成熟卵の作出
11	小曽戸　陽一	川崎医科大学	准教授	脳サイズ・神経細胞数を決定する分子メカニズムの解明
12	佐々木　誠	東北大学大学院 生命科学研究科	教授	海洋天然物の実用的合成を基盤とする革新的抗がん剤リード化合物の創製
13	青野　重利	自然科学研究機構岡崎統合 バイオサイエンスセンター	教授	ガス分子により駆動される生体内シグナル伝達の分子機構解明
14	加納　純子	大阪大学 蛋白質研究所	特任独立 准教授	染色体末端テロメアによる細胞分裂期制御メカニズム
15	南野　徹	千葉大学大学院 医学研究院	講師	次世代の血管新生治療の開発

番号	氏　名	研究機関名	役職	研究テーマ
16	河崎　洋志	東京大学大学院 医学系研究科	特任 准教授	感覚神経回路の時空間的な形成制御メカニズムの解明
17	南嶋　洋司	慶應義塾大学 医学部	特別研究 助教	HIF の水酸化酵素 PHD2 をターゲットとした新たな虚血再還流障害治療法の可能性
18	小迫　英尊	徳島大学疾患酵素学 研究センター	准教授	細胞内情報伝達によるリン酸化を介した核ー細胞質間輸送装置の機能制御の解明
19	秦　猛志	東京工業大学大学院 生命理工学研究科	助教	テトラヒドロピラン骨格を有する生物活性化合物の触媒的不斉合成及び構造活性相関研究
20	田中　実	自然科学研究機構 基礎生物学研究所	准教授	エネルギー代謝による幹細胞・性分化制御機構の解析
21	來生　知	横浜市立大学大学院 医学研究科	講師	がん再発に関わる CD11b+ 骨髄単球細胞の腫瘍血管再形成における役割
22	日比野　浩	新潟大学大学院 医歯学総合研究科	教授	内耳内リンパ液の特異環境の破綻に立脚する難聴の病態生理の解明
23	齋藤　望	北海道大学大学院 薬学研究院	准教授	アレンインの触媒的環化付加反応を機軸とする Welwitindolinone A isonitrile 及びその類縁体の合成
24	黒河　博文	東北大学大学院 医学系研究科	講師	Keap1-Nrf2 生体防御系による酸化ストレス感知の構造基盤
25	北村　浩	名古屋市立大学 大学院医学研究科	准教授	新しいマクロファージ機能制御分子 M-mod の肥満性糖尿病における病理学的役割の解析
26	西田　元彦	理化学研究所 生命分子システム基盤研究領域	研究員	内向き整流性カリウムチャンネルの研究
27	花房　洋	名古屋大学大学院 理学研究科	助教	ROCO ファミリーキナーゼ LRRK1 による EGFR メンブレントラフィック制御
28	松尾　拓哉	名古屋大学 遺伝子実験施設	助教	植物時計の進化の解明に向けた緑藻の生物時計の解析
29	河野　肇	帝京大学医学部	講師	動脈硬化における自然免疫炎症の関与とその制御
30	竹本　大吾	名古屋大学大学院 生命農学研究科	助教	植物共生糸状菌の共生確立における活性酸素生成酵素複合体の役割の解明
31	高橋　智聡	金沢大学がん研究所	教授	Retinoblastoma がん抑制遺伝子不活性化による蛋白質ファルネシル化亢進の薬理学的・臨床的意義
32	中村　卓郎	財団法人癌研究会 癌研究所	部長	Trib1 による白血病発症機構の解析
33	西城　忍	東京大学医科学研究所	助教	C 型レクチンによる免疫系制御機構の解明
34	小室　一成	大阪大学大学院 医学系研究科	教授	p53 を標的とした新規心不全治療法の開発
35	江本　憲昭	神戸薬科大学 臨床薬学研究室	教授	腎糸球体における血管内皮－上皮細胞間シグナルを介した慢性腎臓病の病態解明
36	金城　雄樹	国立感染症研究所 生物活性物質部	室長	播種性カンジダ症に対する免疫療法の開発
37	脇本　敏幸	東京大学大学院 薬学系研究科	講師	タンパク質脱リン酸化酵素阻害剤 Calyculin A に基づくサブタイプ選択的阻害剤の開発
38	新明　洋平	熊本大学大学院 生命科学研究部	助教	脳梁形成における軸索ガイダンス分子 draxin の役割

2010 年度研究集会助成金贈呈集会

この事業は、生物・生命化学およびそれに関連する化学の領域において、我が国で開催される国際色豊かな研究集会の助成を目的としています。

（受付順、敬称略、所属・職位は申請時。助成金額：1 件 40 万円）

番号	研究集会名	開催期日（開催地）	助成先代表者	
			所属・職位	氏名
1	第 5 回国際フィロウイルスシンポジウム	2010.4.18 ～ 4.21（東京）	東京大学 医科学研究所 教授	河岡　義裕
2	タンパク質社会に関する国際会議	2010.9.12 ～ 9.16（奈良）	名古屋大学 大学院理学研究科 教授	遠藤 斗志也
3	第 17 回国際RUNXワークショップ 2010	2010.7.11 ～ 7.14（神奈川）	独）理化学研究所 免疫・アレルギー科学総合研究センター チームリーダー	谷内　一郎
4	2010 国際ポリアミン会議 －医学・生命科学への展開－	2010.6.14 ～ 6.18（静岡）	東京慈恵会医科大学 教授	松藤　千弥
5	第 16 回国際分化学会国際会議	2010.11.14 ～ 11.18（奈良）	自然科学研究機構 基礎生物学研究所 教授	上野　直人

第 24 期（2010 年度）財務報告

貸借対照表

2011 年 3 月 31 日現在

（単位：円）

科　　目	金　額
Ⅰ資産の部	
1．流動資産	
流動資産合計	46,845,925
2．固定資産	
(1) 基本財産	
投資有価証券（指定）	1,000,000,000
投資有価証券（一般）	100,000,000
基本財産合計	1,100,000,000
(2) その他固定資産	
その他固定資産合計	40,092,646
固定資産合計	1,140,092,646
資産合計	1,186,938,571
Ⅱ負債の部	
1．流動負債	
流動負債合計	38,061,430
負債合計	38,061,430
Ⅲ正味財産の部	
1．指定正味財産	
指定正味財産合計	1,000,000,000
(うち基本財産への充当額)	(1,000,000,000)
2．一般正味財産	148,877,141
(うち基本財産への充当額)	(100,000,000)
正味財産合計	1,148,877,141
負債及び正味財産合計	1,186,938,571

収支計算書

2010 年 4 月 1 日から 2011 年 3 月 31 日まで

（単位：円）

科　　目	決算額
Ⅰ事業活動収支の部	
1．事業活動収入	
寄付金収入	40,038,000
事業活動収入計	68,622,359
2．事業活動支出	
事業費支出	50,720,917
助成金支出	40,000,000
管理費支出	4,522,946
事業活動支出計	55,243,863
事業活動収支差額	13,378,496
Ⅱ投資活動収支の部	
1．投資活動収入	
投資活動収入計	200,000,000
2．投資活動支出	
投資活動支出計	200,000,000
投資活動収支差額	0
Ⅲ財務活動収支の部	
1．財務活動収入	0
2．財務活動支出	0
財務活動収支差額	0
当期収支差額	13,378,496
前期繰越収支差額	△ 4,594,001
次期繰越収支差額	8,784,495

役員名簿（理事・評議員・選考委員）

理　事　会

2011 年 10 月 1 日現在（順不同、敬称略）

職　名	氏　名	現　　職	就任年月日	常勤･非常勤
理事長	金 子　章 道	畿央大学大学院健康科学研究科教授 慶應義塾大学名誉教授	2003 年 6 月 10 日	非常勤
理　事	浅 野　茂 隆	早稲田大学先端科学･健康医療融合研究機構長 東京大学名誉教授	1999 年 6 月 4 日	非常勤
	石 川　裕 子	ノバルティス ファーマ株式会社 常務取締役 人事･コミュニケーション本部長	2004 年 6 月 7 日	非常勤
	大 島　泰 郎	共和化工株式会社 環境微生物学研究所長 東京工業大学名誉教授	1997 年 6 月 8 日	非常勤
	黒　川　　清	政策研究大学院大学教授 東京大学名誉教授	1999 年 6 月 4 日	非常勤
	眞 崎　知 生	筑波大学名誉教授 京都大学名誉教授	1999 年 6 月 4 日	非常勤
	マックス・ ブルガー	ノバルティス　サイエンスボード議長 バーゼル大学教授	1987 年 9 月 16 日	非常勤
	眞 弓　忠 範	大阪大学名誉教授	2004 年 6 月 7 日	非常勤
	三 谷　宏 幸	ノバルティス ファーマ株式会社 代表取締役社長	2007 年 9 月 5 日	非常勤
	村 崎　光 邦	CNS薬理研究所長 北里大学名誉教授	2001 年 6 月 1 日	非常勤
	森　美 和 子	北海道医療大学客員教授 北海道大学名誉教授	2005 年 6 月 13 日	非常勤
監　事	中 嶋　徳 三	中嶋徳三公認会計士事務所 公認会計士	2006 年 6 月 5 日	非常勤
	松本　秀三郎	元ノバルティス ファーマ株式会社 常勤監査役	1998 年 2 月 10 日	非常勤

評 議 員 会

2011 年 10 月 1 日現在（順不同、敬称略）

職 名	氏 名	現 職	就任年月日	常勤・非常勤
評議員会議長	黒岩 常祥	立教大学極限生命情報センター長 東京大学名誉教授	2002年2月7日	非常勤
評議員	赤池 紀扶	熊本保健科学大学リハビリテーション学科教授 銀杏学園理事・副学長 九州大学名誉教授	1999年6月4日	非常勤
	赤沼 安夫	財団法人朝日生命成人病研究所名誉所長	2001年6月1日	非常勤
	浅島 誠	東京大学大学院総合文化研究科客員教授 東京大学名誉教授	1999年6月4日	非常勤
	遠藤 政夫	山形大学名誉教授	1997年6月8日	非常勤
	小川 聡	国際医療福祉大学三田病院長 慶應義塾大学名誉教授	2001年6月1日	非常勤
	川嵜 敏祐	立命館大学糖鎖工学研究センター長 京都大学名誉教授	1999年6月4日	非常勤
	川島 博行	元新潟大学大学院医歯学総合研究科教授	2001年6月1日	非常勤
	北 徹	神戸市立医療センター中央市民病院 病院長	1999年6月4日	非常勤
	後藤 勝年	JST サテライト茨城センター長	2001年6月1日	非常勤
	榊 佳之	豊橋技術科学大学学長 東京大学名誉教授	2001年6月1日	非常勤
	柴崎 正勝	財団法人微生物化学研究会 微生物化学研究所長	2005年6月13日	非常勤
	冨永 健	昭和大学附属豊洲病院乳癌検診・治療センター 元センター長・教授	1998年6月5日	非常勤
	中西 重忠	財団法人大阪バイオサイエンス研究所所長 京都大学名誉教授	1999年6月4日	非常勤
	長田 敏行	法政大学生命科学部学部長 東京大学名誉教授	2005年6月13日	非常勤
	西川 武二	慶應義塾大学名誉教授 日本ワックスマン財団常務理事	2001年6月1日	非常勤
	西宗 義武	大阪大学微生物病研究所特任教授	1999年6月4日	非常勤
	水野 美邦	順天堂大学医学部教授	1999年6月4日	非常勤

選 考 委 員 会

2011 年 10 月 1 日現在（順不同、敬称略）

職 名	氏 名	現 職	就任年月日	常勤･非常勤
選考委員長	村田 道雄	大阪大学大学院理学研究科教授	2008年6月20日	非常勤
選考委員	一條 秀憲	東京大学大学院薬学系研究科教授	2011年6月17日	非常勤
	岡 慎一	国立国際医療センター エイズ治療・研究開発センター長	2011年6月17日	非常勤
	岡 芳知	東北大学大学院医学系研究科教授	2008年6月20日	非常勤
	貝淵 弘三	名古屋大学大学院医学研究科教授	2009年6月19日	非常勤
	狩野 方伸	東京大学大学院医学系研究科教授	2009年6月19日	非常勤
	岸本 健雄	東京工業大学大学院生命理工学研究科教授	2011年6月17日	非常勤
	笹井 芳樹	理化学研究所発生・再生総合研究センター グループディレクター	2008年6月20日	非常勤
	笹井 宏明	大阪大学産業科学研究所教授	2010年6月18日	非常勤
	佐田 政隆	徳島大学大学院ヘルスバイオサイエンス 研究部教授	2009年6月19日	非常勤
	鹿内 利治	京都大学大学院理学研究科教授	2011年6月17日	非常勤
	高柳 広	東京医科歯科大学大学 大学院医歯学総合研究科教授	2011年6月17日	非常勤
	竹内 勤	慶應義塾大学医学部教授	2009年6月19日	非常勤
	西田 篤司	千葉大学大学院薬学研究科教授	2009年6月19日	非常勤
	長谷部 光泰	自然科学研究機構 基礎生物学研究所教授	2009年6月19日	非常勤
	福田 恵一	慶応義塾大学医学部教授	2008年6月20日	非常勤
	南 雅文	北海道大学大学院薬学研究院教授	2011年6月17日	非常勤
	峯岸 敬	群馬大学大学院医学系研究科教授	2010年6月18日	非常勤
	宮園 浩平	東京大学大学院医学系研究科教授	2009年6月19日	非常勤
	室原 豊明	名古屋大学大学院医学系研究科教授	2011年6月17日	非常勤

事務局便り

ご寄附のお願い

当財団は、生物・生命科学および関連する化学の領域において、創造的な研究等を支援することにより、学術の進展と福祉の向上に寄与することを目的にしております。

これらの公益事業は、寄附金および基本財産の運用益にて行われており、当財団は事業の趣旨にご賛同いただける方々からのご寄附を募っております。

なお、当財団は特定公益増進法人の認定を受けております。

特定公益増進法人とは、公益法人等のうち教育または科学の振興、文化の向上、社会福祉への貢献その他公益の増進に著しく寄与するものとして認定された法人をいいます。

これらの法人に対して、個人または法人が寄附を行った場合は、下記の税法上の優遇措置を受けることができます。

優遇措置の概略

個人：支出した寄附金（その年の総所得額の40％を限度とする）のうち、5千円を超える部分について寄附金控除が認められます。また、上記の寄附金控除の対象になっている寄附金は、個人住民税の寄附金控除が受けられます。

法人：支出した寄附金は、通常一般の寄附金の損金算入限度額と同額まで、別枠で損金に算入できます。

ご寄附は、随時受付けております。
詳しくは、財団事務局までお問合せ下さい。
（電話：03-5464-1460、Eメール：novartisfound.japan@novartis.com）

事務局より

東日本大震災で被災された皆様に、心よりお見舞いを申し上げます。

本年度も財団年報を発行できますことは、助成を受けられた皆様および財団関係者のご尽力の賜物と厚く御礼申し上げます。

さて、公益法人制度の改制に伴いまして、当財団は引き続き税制の優遇措置が受けられる公益財団法人への移行を目指し、本年度に申請を行いました。現在審査が進行中ですが、来年度には移行のご報告ができるものと考えております。

なお、助成事業は財団の設立以来1,413件、総額17億2千7百万円余りに達しました。今後も事務局は、学術の進展に寄与できる喜びを胸に助成事業に邁進する所存です。

今後ともご指導、ご支援の程よろしくお願い申し上げます。

事務局長　松田光陽

財団法人　ノバルティス科学振興財団
〒106-0031 東京都港区西麻布4-16-13
西麻布28森ビル2F
Tel:03-5464-1460　Fax:03-5467-3055
E-メール：novartisfound.japan@novartis.com
ホームページ :http://www.novartisfound.or.jp